

Numerical assessment of effective width method in plated box girders with stocky stiffened flanges in pure bending

Tamizi, Z.



Master's Thesis

Numerical assessment of effective width method in plated box girders with stocky stiffened flanges in pure bending

Zahra Tamizi

to obtain the degree of Master of Science
at the Delft University of Technology,
in Civil Engineering.

Delft, University of Technology
Faculty of Civil Engineering and Geoscience
Structural Engineering - Steel and Timber Construction

Student number:	5618282	
Project duration:	March,2023-December,2023	
Thesis committee:	Prof. Dr. M.(Milan) Veljkovic, Dr. T. (Trayana) Tankova, Dr. Ir. P.C.J. (Pierre) Hoogenboom, Ing.B.S.(Björn) Hylkema MSEng.RC, R.(Remco) de Bruijn MSc.	TU Delft, Chair TU Delft, Daily supervisor TU Delft Witteveen en Bos, Daily supervisor Witteveen en Bos, Daily supervisor

Preface

This thesis report marks the culmination of my academic journey leading to the degree of Master of Science in Civil Engineering at Delft University of Technology. It signifies the completion of my studies within the Structural Engineering master's program, with a specialization in Steel and Timber Construction.

I would like to express my sincere appreciation to those who have consistently motivated me and provided guidance throughout the process of writing this thesis. My gratitude goes to the members of my graduation committee, comprising experts from TU Delft and Witteveen en Bos. Firstly, I want to thank the chair of the committee Prof. Dr. Milan Veljkovic, for his feedback and guidance during the research process. I am deeply grateful to Dr. Trayana Tankova, for her assistance and unwavering motivation during challenging periods of the thesis journey. I extend my appreciation to Dr. Ir. Pierre Hoogenboom, for his contributions as a thesis committee member and suggestions he provided for improving the work. A special thanks goes to my daily supervisors from Witteveen en Bos, Björn Hylkema and Remco de Bruijn for creating a friendly sphere to ask questions, sharing their expertise, and providing valuable feedback.

Acknowledging the support and interest in my education, credit goes to my friends, family, and loved ones. Their unwavering encouragement and constant presence have been a source of inspiration, fueling my determination to overcome challenges in my academic journey.

Zahra Tamizi
Utrecht, December 2023

Abstract

Plated girders have been extensively used in steel bridge construction since the 19th century. Over the past century, the effective width method was developed to take the nonlinearities resulting from shear lag and plate buckling into account. This method leads to having a cross-section with a reduced area in which the stress can linear be considered. The section properties of the reduced cross-section can be used for determining the resistance and the longitudinal stress in the plated girder. The reduction of the cross-section area takes place in two steps. First, the section area is reduced in local scale for subpanels that have class 4, and local effective section properties will be determined. Second, the local effective cross-section is reduced to consider the overall buckling, which can be plate-like buckling, column-like buckling, or their interaction.

The longitudinal compressive stress that can be determined from effective section properties in a box girder with pure bending moment will be higher since the effective section includes a reduced second moment of inertia and an increased distance between the neutral line and the compression flange. This master thesis aims to assess whether effective section properties accurately determine the compression stress magnitude in box sections with pure bending moment that remain unaffected by local buckling and experience overall buckling in the form of pure column-like buckling in the compression flange.

The findings indicate that if the subpanels of the isolated compression plate are stocky, and the overall buckling failure has the form of pure column-like buckling, the stress, and behavior remain within the elastic region up to column-like buckling failure. There does not exist any sudden increase in compression stress magnitude in the plate. The analytical method that can address the maximum magnitude of the compression stress in the plate has contribution of the gross section area of the plate.

If such a stiffened plate with pure column-like buckling failure and stocky subpanels serves as the compression flange of a box girder, the same conclusion was reached regarding determining the first moment of inertia. However, in the presence of the slender web in the cross-section, the effective area of the web, in combination with the gross section area of compression flange should be considered for determining the section properties with which the maximum longitudinal stress can be determined.

Table of contents

Preface	ii
Abstract	iii
Table of contents	iv
List of figures	vi
List of the tables	vii
Nomenclature	viii
1. Introduction	1
1.1 Background information	1
1.2 Problem definition	2
1.3 Research objectives	2
1.4 Methodology	3
1.5 Application	5
1.6 Report outline	6
2 State of the art	7
2.1 Previous work	7
2.2 Slender elements	7
2.2.1 Buckling of unstiffened plate	8
2.2.1.1 Panel in compression	9
2.2.1.2 Panel with gradient stress	9
2.2.2 Buckling of stiffened Plate	10
2.2.2.1 Stiffened Panel in pure compression	10
2.3 Elastic-plastic behavior of stiffened panels	12
2.3.1 Failure modes of plates	12
2.3.1.1 The effect of Initial imperfection	14
2.3.1.2 The effect of residual stress	15
2.3.1.3 The effect of loading type and boundary conditions	15
2.4 Eurocode effective width method	15
2.4.1 Eurocode method for unstiffened plate	16
2.4.2 Eurocode method for stiffened plate	16
2.4.3 Effective width from shear lag nonlinearity	19
2.4.4 Effective width method in bending	19
3 Definition of finite element model of the stiffened plate	21
3.1 Material properties	21
3.2 Imperfection	22
3.2.1 Equivalent geometrical imperfection	22
3.2.2 Applied Imperfection on the plates	23
3.2.3 Analysis type and evaluation strategy	27
3.3 Solving method	27
3.4 Boundary condition	27
3.5 Validation of the model	28
3.6 Mesh	30
3.7 Verification of the model	30
4 Elastoplastic behavior of stiffened panels with pure column-like buckling failure	31
4.1 Parametric study of the elastic-plastic behavior of wide stiffened panels.	31
4.2 Result of the GMNIA analysis	33
4.2.1 Failure behavior	33
4.2.2 Resistance	34

4.2.3	Initial imperfection	35
4.2.4	Stress	35
4.3	Comparing resistance with criteria of a new draft of EN1993-1-5:.....	38
4.3.1	Alternative interaction formula:.....	38
4.3.2	Resistance	38
4.4	Summary of the result	39
5	Definition of the FEM model of steel box girders	41
5.1	Box girders configurations.....	41
5.2	Imperfection	42
5.3	Definition of boundary conditions	43
5.4	Transverse stiffeners.....	43
5.1	Solving method	44
5.2	Mesh	44
5.2.1	Validation	44
5.2.2	Verification	45
5.3	Shear-lag effect.....	45
5.4	Point for monitoring the stress	46
6	Behavior of box girders.....	47
6.1	Model A.....	47
6.1.1	Detecting failure	48
6.1.2	Resistance of the girder	50
6.1.3	Development of the stress in the flange of the girder.....	51
6.1.4	Development of stress in the web of the girder.....	53
6.1.5	Section properties representative of the stress.....	54
6.1.6	Single plate versus plate as the compression flange of the girder in bending	55
6.1.7	Effect of gradient stress introduction.....	56
6.2	Model B.....	58
6.2.1	Resistance of the girder	58
6.2.2	Development of stress in the web of the girder.....	59
6.2.3	Section properties representative of the stress.....	61
6.1	Model C.....	62
6.1.1	Resistance of the girder	63
6.1.2	Development of the stress in the web	64
6.1.3	Section properties presentative of the stresses	65
6.2	Summary of the results.	65
6.3	Discussion.....	66
7	Conclusion.....	68
7.1	Conclusions.....	68
7.2	Future research.....	69
	References.....	70
	ANNEX I	72
	ANNEX II	78
	Annex III.....	83

List of figures

Figure 1:1 Left: reduced cross section by local buckling of the subpanels. Right: reducing local effective cross section for overall buckling.	1
Figure 1:2 Effective section area with reduced compression flange and shift in the neutral line towards tension side [1].....	2
Figure 1:3 Column-like behavior of an unstiffened plate with a small aspect ratio α [1].....	3
Figure 1:4 Sets analysis A and B with compression failure, set analysis C with tension failure.....	4
Figure 1:5 Cross section of Haringvliet bridge.....	5
Figure 2:1 Definition of b_c and b_e	9
Figure 2:2 Stiffened plate scheme b) overall buckling c) nodal buckling d)global interactive buckling [10].....	11
Figure 2:3 Peak stress in panels with $30 < b/t_p < 50$ and $30 < L/R < 90$ [18].....	12
Figure 2:4 Direct stress distribution for slender subpanel in plate loading [18].....	13
Figure 2:5 Direct stress distribution for stocky subpanel in plate loading [18].....	13
Figure 2:6 Direct stress distribution for stocky subpanel in plate loading, low flexural rigidity of the stiffener [18].....	13
Figure 2:7 Direct stress distribution for slender subpanel in plate loading, low flexural rigidity of the stiffeners [18].....	13
Figure 2:8 Development of yielding in test set up 1 and stress distribution in half of the top flange test [20].....	14
Figure 2:9 Development of yielding in test set up 2 and stress distribution in half of the top flange test [20].....	14
Figure 2:10: Plate buckling reduction factor [1].....	16
Figure 2:11 Effective area of a stiffened plate under uniform compression [1].....	17
Figure 2:12 Column-like and plate-like buckling interaction [1].....	17
Figure 2:13 Plate with two stiffeners in compression [1].....	18
Figure 2:14 Definition of e_1 and e_2	18
Figure 2:15 Development of the strength and eccentricity versus compression strain in the compression flange [9].....	19
Figure 2:16 Distribution of stress caused by local buckling w of plate elements subject to compression strain [9].....	20
Figure 2:17 Equivalent effective width [9].....	20
Figure 3:1 Stress strain curve [1].....	21
Figure 3:2 Engineering and true stress-strain curve.....	21
Figure 3:3 Left: Imperfection in one stiffener [26] Right: imperfection in all stiffeners.....	23
Figure 3:4 Stiffeners imperfection in transverse direction.....	24
Figure 3:5 Stiffeners imperfection in longitudinal direction.....	23
Figure 3:6 Global imperfection mode in panels [26].....	23
Figure 3:7 A)Pure column- like buckling behavior, B) plate- like buckling behavior, C) Interaction behavior, D) Dominant column-like behavior [30].....	24
Figure 3:8 Dominant column-like buckling plate side.....	24
Figure 3:9 Dominant column-like buckling stiffeners side.....	24
Figure 3:10 Global imperfection node file transverse direction.....	25
Figure 3:11 Global deflection node file in longitudinal direction.....	25
Figure 3:12 Local imperfection in subpanels.....	25
Figure 3:13 Local imperfection node file in the transverse direction.....	25
Figure 3:14 Local imperfection node file in the longitudinal direction with 10 half-sine waves.....	26
Figure 3:15 Local imperfection node file in the longitudinal direction with 9 half-sine waves.....	26
Figure 3:16 Evaluation strategy for ultimate resistance [28].....	27
Figure 3:17 Boundary condition for plate with support in all direction.....	28
Figure 3:18 Configuration of the stiffened plate for validation of the model.....	29
Figure 3:19 FEM mesh in model number 3.....	30
Figure 4:1 Load deflection diagram model 1 at failure.....	33
Figure 4:2 Longitudinal stress at point A.....	33
Figure 4:3 Longitudinal stress at point B.....	33
Figure 4:4 Aspect ratio 0.8 $a=2760$	34
Figure 4:5 Aspect ratio 0.6 $a=207$	34
Figure 4:6 Aspect ratio 0.4 $a=2760$	35
Figure 4:7 Aspect ratio 0.3 $a=2070$	35
Figure 4:8 Aspect ratio 0.2 $a=2192$	35
Figure 4:9 Stress in the middle strut having initial imperfection towards stiffeners.....	35
Figure 4:10 Stress in the middle strut having initial imperfection towards plate.....	36
Figure 4:11 Development of the longitudinal stress from GMNIA analysis on the plate A) aspect ratio 0.8, B) aspect ratio 0.6, C) aspect ratio 0.4, D) aspect ratio 0.3 E) aspect ratio 0.2.....	36
Figure 4:12 Stress from GMNIA analysis compared to stress from gross section properties A) aspect ratio 0.8, B) aspect ratio 0.6, C) aspect ratio 0.4, D) aspect ratio 0.3 E) aspect ratio 0.2.....	37
Figure 4:13 Stress at the edges.....	38
Figure 4:14 $p_{c, numerical}$ and $p_{c, analytical}$	38
Figure 5:1 Definition of combination of positive initial imperfection.....	42
Figure 5:2 Scheme of the model.....	43
Figure 5:3 Defining the reference point and the boundary conditions defined on the reference point.....	43
Figure 5:4 Rotation rigidity from the connecting to the transverse elements in the longitudinal stiffeners.....	44
Figure 5:5 Mesh definition on the box girder.....	44
Figure 5:6 Mesh sensitivity analysis of the box girder.....	45
Figure 5:7 Stress distribution from LEA of the model.....	45
Figure 5:8 Longitudinal stress a) negative global imperfection b) positive global imperfection.....	46
Figure 6:1 Plastic strain at failure of the box number 1 left) global deflection in the middle panel towards plate right) global deflection in the middle panel towards stiffeners.....	49
Figure 6:2 Plastic strain at failure of the box number 2 left) global deflection in the middle panel towards plate right) global deflection in the middle panel towards stiffeners.....	49

Figure 6:3 Plastic strain at failure of the box number 3 left) global deflection in the middle panel towards plate right) global deflection in the middle panel towards stiffeners	49
Figure 6:4 Plastic strain at failure of the box number 4 left) global deflection in the middle panel towards plate right) global deflection in the middle panel towards stiffeners	49
Figure 6:5 Moment deflection diagram from GMNIA analysis A) Model 1a, B) model2a, C) model3 a, D) model4a	51
Figure 6:6 Development of the stress in the compression flange GMNIA analysis A) Model 1a, B) model2a, C) model3 a, D) model4a	52
Figure 6:7 Development of the stress in the girder A) Model 1a, B) model2a, C) model3 a, D) model4-a	53
Figure 6:8 Development of the stress in the web of girder GMNIA analysis A) Model 1a, B) Model2a, C) Model3a, D) Model4-a	54
Figure 6:9 Section properties representative of the longitudinal stresses versus GMNIA stress A) Model 1a, B) model2a, C) model3 a, D) model4-a	55
Figure 6:10 Resistance behavior difference in a single plate comparing top late as the compression element of the box girder analysis A) Model 1a, B) Model2a, C) Model3 a, D) Model4-a	56
Figure 6:11 Effect of gradient loading on the resistance A) Model 1a, B) Model2a, C) Model3 a, D) Model4a	57
Figure 6:12 A) Stress in the strut of the plate with uniform compression stress b) stress in the strut of the plate with gradient compression stress	57
Figure 6:13 Moment deflection diagram from GMNIA analysis A) Model 1b, B) model2b, C) model3 b, D) model4b	59
Figure 6:14 Development of the stress in the web of the girder from GMNIA set analysis b. A) Model 1b, B) Model2b, C) Model3 b, D) Model4-b	60
Figure 6:15 Section properties representative of the maximum stress GMNIA set analysis. A) Model 1b, B) Model2b, C) Model3 b, D) Model4-b	61
Figure 6:16 Classification of the part with gradient stress	62
Figure 6:17 Resistance of the girder type c. A) Model 1c, B) Model2c, C) Model3 c, D) Model4c	63
Figure 6:18 Type C analysis stress in the web of the girder A) Model 1c, B) Model2c, C) Model3 c, D) Model4c	64
Figure 6:19 type C analysis compression and tension in the flange of the box girder A) Model 1c, B) Model2c, C) Model3 c, D) Model4c	65

List of the tables

Table 3-1 Initial imperfection magnitude [1]	22
Table 3-2 Combination of the initial imperfection	26
Table 3-3 Validation of the model for unstiffened plate	28
Table 3-4 Validation of the model for stiffened plate	29
Table 3-5 Results of LBA, LEA and GMNIA analysis	29
Table 3-6 Mesh sensitivity analysis	30
Table 4-1 The equivalent stiffener dimension	31
Table 4-2 Dimension of stiffened plate	32
Table 4-3 Critical buckling stress based on EN1993-1-5	32
Table 4-4 Internal compression part classification [33]	32
Table 4-5 GMNIA analysis and ultimate resistance	34
Table 4-6 Stiffened plate resistance based on the criteria of minimum rigidity of the stiffener	39
Table 5-1 Dimension of the girders	42
Table 5-2 Mesh sensitivity analysis	45
Table 6-1 Box girder with the unstiffened web model 1 and 2 category A	47
Table 6-2 Box girder with stiffened web model 3 and 4 category A	47
Table 6-3 Resistance of the girders set A	50
Table 6-4 Box girder with the unstiffened web model 1 and 2 category B	58
Table 6-5 Box girder with the stiffened web model 3 and 4 category B	58
Table 6-6 Box girder resistance type B	58
Table 6-7 Box girder with the unstiffened web model 1 and 2 category C	62
Table 6-8 Box girder with the unstiffened web model 3 and 4 category C	62

Nomenclature

Abbreviations

LEA	Linear elastic analysis
LBA	Linear buckling analysis
GMNIA	Geometrically and materially nonlinear analysis with imperfections included
FEM	Finite element method

List of symbols

$A_{c,eff}$	The effective area of the plate in compression
A_g	Gross area of the compression zone
A_s	Area of the stiffeners
$A_{s,1}$	Area of one stiffener with adjacent part of plate
a	Length of a stiffened or unstiffened plate
b	Width of a stiffened or unstiffened plate
b_c	Width of compression part of stiffened or unstiffened plate
b_e	Effective area of the compressed part of plate
b_i	Distance between stiffeners
E	Module of elasticity
D	Bending stiffness of the plate defined by: $D = \frac{E.t^3}{12(1-\nu^2)}$
h_s	Height of stiffeners
$I_{gross\ section}$	Second moment of inertia of the gross section
$I_{effective\ section}$	Second moment of inertia of the effective section
I_s	Second moment of inertia of stiffener
$I_{s,1}$	Second moment of inertia of one stiffener with adjacent part of plate
f_y	Yields stress
M_{el}	Elastic bending moment resistance from gross section properties
M_{GMNIA}	Bending moment from Geometrical and material nonlinear analysis with initial
M_{Ed}	The design bending moment
N_{Ed}	The design axial force
t_p	Plate thickness
t_s	Thickness of stiffeners
$y_{effective\ section}$	Distance between compression flange and the neutral line in effective section
$y_{gross\ section}$	Distance between compression flange and the neutral line in gross section
W_{eff}	Effective elastic section modulus
W_g	Gross elastic section modulus
α	Aspect ratio $\frac{a}{b}$: a: unloaded width, b: loaded length
$\sigma_{com,Ed}$	The maximum design compressive stress
$\sigma_{cr,c}$	Column-like buckling stress
$\sigma_{cr,p}$	Plate-like buckling stress
$\bar{\lambda}_c$	Column slenderness
$\bar{\lambda}_p$	Plate slenderness
$\bar{\lambda}_{p,red}$	Reduced plate slenderness
ν	Poisson ratio
χ_c	Buckling reduction factor of a compressed column
ψ	The ratio between the maximum and the minimum compression stress in the plate
$\gamma_{sl,i}$	Relative bending stiffness
ν	Poisson's coefficient
ξ	Interaction ratio between plate and column buckling
ψ	Stress ratio between maximum and minimum compression stress
ρ	The reduction factor for plate buckling
ρ_i	The local reduction factor for subpanels buckling
ρ_c	The reduction factor for interaction of column-like and plate-like buckling

1

Introduction

Box girders have wide thin plates that are mainly stiffened by open or closed stiffeners to deal with the stability problem of the thin plates.

The verification of the slender steel structures is covered in EN 1993-1-5 by the effective width method. The Eurocode's effective width method offers a practical approach for assessing the resistance of the slender structures by considering all instability phenomena, which introduce nonlinear stress distribution, as a reduction in the panel width. In EN1993-1-5, part 4-3-(1), it is also mentioned that effective cross-section properties should also be used for determining the internal stresses. This master thesis will investigate the implementation of column buckling in this method for determining the internal longitudinal stress using geometrically and materially nonlinear analysis with imperfections through finite element program Abaqus.

1.1 Background information

Effective width method is introduced to deal with stability problem of the slender parts of the sections in compression. Effective area of the compressed part of the section should be determined based on the slenderness of each plate elements (flange and the web) separately. The reductions that need to be considered for determining the effective section area of the compressed part of the cross-section by plate buckling takes place in two stages.

First, the local reduction factor for the slender parts of the cross-section (parts with class 4) will be determined. The local reduction factor will be applied on the subpanels including, distance between longitudinal stiffeners in the plate sheet and on each part of the longitudinal stiffeners (web and flange) separately as shown in Figure 1-1 left.

In the second stage, as depicted in Figure 1-1 on the right, the reduced cross-section with all the local reductions will again be reduced to consider overall buckling. The overall buckling can have the form of pure column-like buckling, interaction of column-like buckling and plate-like buckling or pure plate-like buckling.

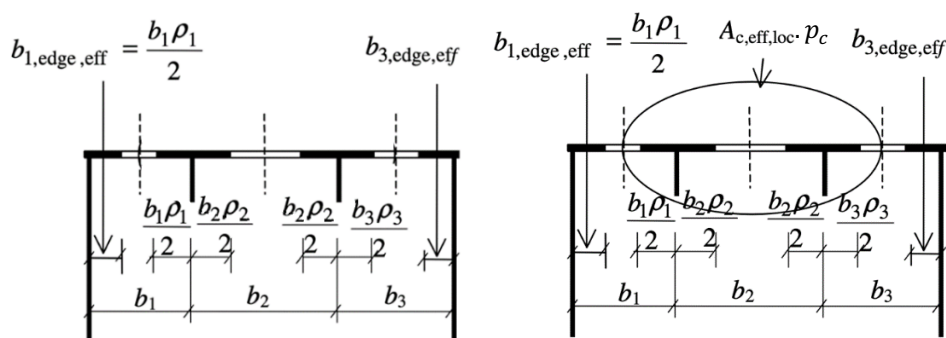


Figure 1.1 Left: reduced cross section by local buckling of the subpanels. Right: reducing local effective cross section for overall buckling.

By using effective section properties, an elevated longitudinal stress will be determined in the box girder with pure bending moment. The increased magnitude of the stress at the compression flange level, determined from effective section properties, is the result of shifting in the position of the neutral towards the tension side in the effective cross section and reduction of second moment of inertia in the effective cross-section as shown in Figure 1-2.

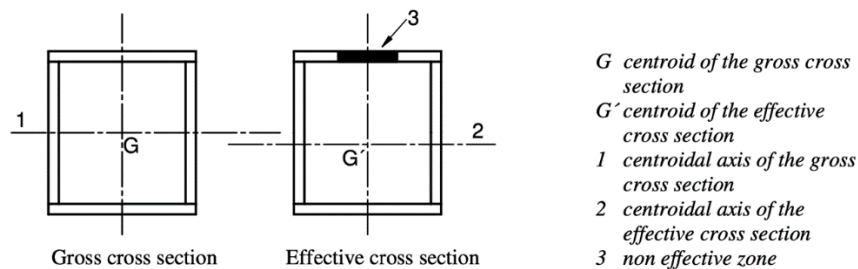


Figure 1:2 Effective section area with reduced compression flange and shift of the neutral line towards tension side [1]

$$\sigma_{longitudinal} = \frac{M_{Ed} \cdot y_{effective\ section}}{I_{effective\ section}} \gg \frac{M_{Ed} \cdot y_{gross\ section}}{I_{gross\ section}} \quad (1-1)$$

The elevated magnitude of the compression stress should be considered in design, following part 4-3-(1) of N 1993-1-5, which mentions, "In calculating longitudinal stresses, account should be taken of the combined effect of shear lag and plate buckling using the effective areas" [1].

1.2 Problem definition

In bridge application, the overall buckling in the form of pure column-like buckling is a common buckling failure mode. Moreover, the longitudinal stiffeners are relatively dense and close to each other in the compression deck. The deck of the steel box girders in the bridge application has common configurations defined below.

- 1) Subpanels in the compression flange of the cross-section have class 3, meaning there is not any instability due to local buckling in the subpanels.
- 2) The compression flange's buckling failure takes the form of pure column-like buckling, meaning the post buckling reserve of the plate is not considered.

The purpose is to address the question whether effective section properties can be used for the accurate determination of absolute maximum longitudinal stress in the compression flange of the box girders with pure bending moment in this case. Ultimately, finding the analytical method for determining longitudinal stresses that can more accurately assess the longitudinal stress in the compression flange.

The focus in this study is on evaluation of the plates with only pure column like buckling failure. This study will not cover the interaction of the column-like and plate-like buckling. It also does not cover combination of the local buckling and plate buckling in the compression flange of the girder.

1.3 Research objectives

The aim is to obtain a more accurate assessment of the stress in the compression flange of the box girders loaded by pure bending moment.

The main research question is:

- In the box girder with compression flange featuring class 3 subpanels and overall buckling in the form of pure column-like buckling loaded by pure bending moment; can the longitudinal stress be determined accurate from effective section properties?

The main research question will be answered with the following sub-questions:

1. Which section properties represent the stresses resulting from the applied compression force on the single stiffened plate with stocky plates and overall buckling in the form of pure column-like buckling? Is it the gross section area or the effective section area of the plate? Also, Can the

reduction factor for column-like buckling be accurately determined when a stiffened plate is vertically supported along the unloaded edges?

2. In the case of a box girder with pure bending moment, does the neutral line shift towards the tension side, leading to an increased compression zone in the cross-section. In other words, should $y_{\text{effective-section}}$ be used in the analytical formula $M.y/I$ for determining the longitudinal stresses?
3. When dealing with box girder with a compression flange consist of subpanels of class 3 and global buckling in the form of pure column-like buckling combined with a web of class 3, which section properties are representative of the compression stresses resulting from bending moment? Is it the gross section properties or the effective section properties of the box girder?
4. What impact does a class 4 web (in girder) and its buckling have on the longitudinal stresses in the compression flange of a box girder, and how can this effect be taken into the account?
5. Are effective section properties applicable when a box girder experiences tension failure?

1.4 Methodology

The effective width method is based on the ultimate resistance models. To be able to accurately address the problem, determining the minimum resistance is of major concern.

The methodology employed is a two-stage approach.

In the first stage, finite element analysis will be performed on individual single stiffened panels to ensure that their behavior remain in pure column-like buckling region. Additionally, finding the imperfections leading to the lowest resistance. These imperfections will subsequently be applied to the compression flange of the girder in the final stage.

In the second stage, the behavior of the stiffened plate, as the compression flange of the box girder, will be studied. The finite element analysis will be perform using Abaqus, considering material nonlinearity and geometrical nonlinearity with initial imperfection. The obtained results will then be compared with the analytical method which is effective cross-section criteria outlined in the EN1993-1-5.

Phase 1: Analytical method

In the initial step, two Python script (presented in Annex II and III) were developed to compute the effective cross-section properties, of a single plat with pure compression and box girder with pure bending moment following EN1993-1-5 criteria. These Python scripts were subsequently used to identify suitable plate and box girders configurations.

The configurations of interest are:

In the compressed plate

- Local buckling is prevented by the application of class 3 subpanels.
- Global instability failure of the compression plates takes place as pure column-like buckling with the ρ_c reduction factor below 0.85.
- The aspect ratio(a/b) in the plate is lower than 1.
- Stiffeners are defined as T shape open stiffeners representative of the stiffeners in the reference bridge (Haringvliet)

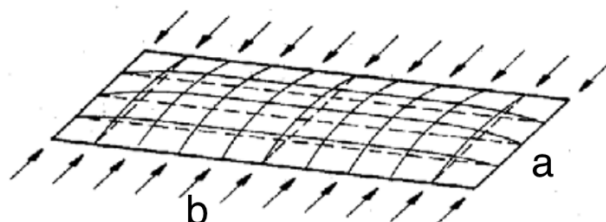


Figure 1:3 Column-like behavior of an unstiffened plate with a small aspect ratio a [1]

In the Box girder

In defining the configurations of the box girders, the predefined single plates were used as the compression flange of the girders.

In defining the web and tension flange of the box girder, the purpose was to determine a configuration in which the following conditions are met:

- In group A of the box girders, local buckling in the web is prevented by using class 3 subpanels. Furthermore, by having overall buckling reduction factor equal to one in the web, it has been ensured that it is active with its full area. In this set of analyses, studying only one stability problem which is column-like buckling of the compression flange is of concern.
- In group B of the box girders, the webs or subpanels of the webs have class 4, so that column-like buckling of the compression flange in combination with the buckling of the web is studied.
- In group C of the box girders, the failure will be as the result of the tension flange failure.

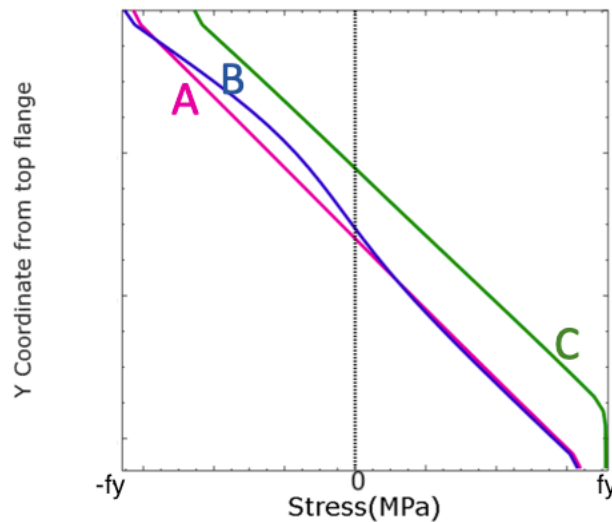


Figure 1:4 Sets analysis A and B with compression failure, set analysis C with tension failure.

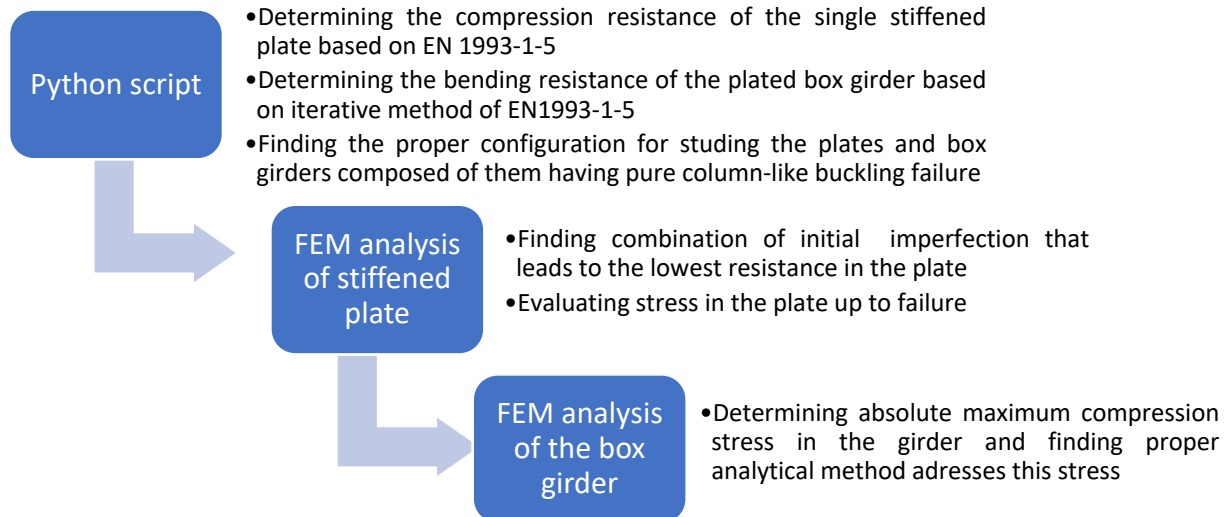
Phase 2: Analysis of the single plates

In this phase, the load-bearing capacity of the five plates is monitored up to failure, the purpose is to control the development of stress in the panels in pure compression up to failure. Column-like buckling for plates with an aspect ratio of 0.19, 0.3, 0.4, 0.6, and 0.8 were studied, and the derived reduction factor related to column-like buckling from GMNIA analysis was compared to the analytical method. Different initial imperfections are applied on these five plates to find the imperfection that leads to the lowest compression resistance. The absolute maximum compression stress in the plate is determined from GMNIA analysis, and the proper analytical method for determining this stress is introduced.

Phase 3: Analysis of the box girders

In this phase of the thesis, the whole cross-section of box girders was modeled and GMNIA analysis was performed. The position of the neutral line was derived and compared to the EN1993-1-5 criteria regarding the effective width method. The indication from previous calculations regarding the combination of the initial geometrical imperfection that leads to the lowest resistance is used for applying initial imperfection on the compression flange of the girder. These imperfections are combined with global initial imperfection in the web of the girder.

Two sets of models for stiffened and unstiffened webs were considered. Smaller cross-sections are defined without longitudinal stiffeners in the web and the larger cross-sections are defined with longitudinal stiffeners in the web.



1.5 Application

The investigation centers on the Haringvliet bridge specifications, and the thesis question arises from the verification of connections between prefabricated steel elements at the deck level in this bridge.

In the verification of the existing structure of Haringvliet bridge, effective section property is applied to assess stresses at the deck level. It becomes evident that the connections between prefabricated steel elements at the deck level will suffer elevated normal stresses magnitude comparing to the linear elastic analysis by considering the stresses determined from effective section properties. This will lead to the conclusion that major part of the connection at the deck level need strengthening.

Haringvliet bridge is made of plated panels stiffened with bulb-open stiffeners. A significant aspect of the bridge that raises questions about the applicability of Eurocode design criteria for determining the longitudinal stresses in this structure are class 3 subpanels in the compression deck and buckling in the form of pure column-like buckling.

In the FEM analysis of large structures, the material is usually modeled as elastic. Result of this study will reveal whether the stress from linear elastic analysis adequate for further verification of the connection or they should be increased by considering the effective section properties. Having a simple model that can help to determine the actual stress in the cross-section will save the time-consuming and error-sensitive nonlinear calculations.

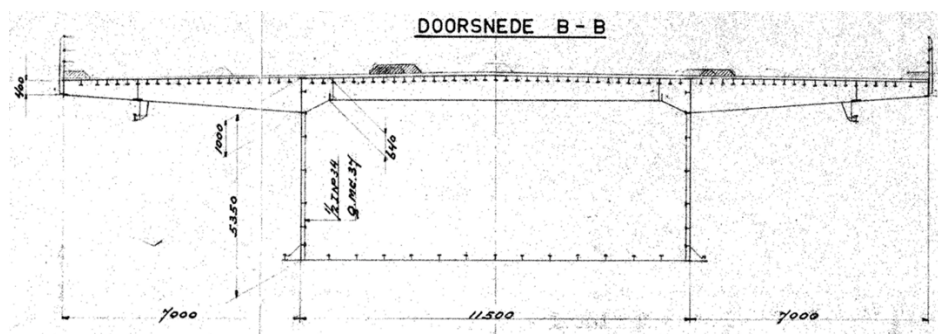


Figure 1:5 Cross section of Haringvliet bridge

1.6 Report outline

The report is structured into several chapters. The contents of the chapters are outlined below.

Chapter 1: Introduction

This chapter introduces the master thesis, outlining its purpose and significance.

Chapter 2: Literature review

In this chapter, a literature study is outlined providing relevant background information and summarizing previous research. The types of failures in stiffened plates under pure compression and the methodology for defining effective section properties based on EN1993-1-5 were studied.

Chapter 3: Finite element model for single plates

This chapter describes the definition of the finite element model used to analyzed single plates subjected to pure compression.

Chapter 4: Analysis of single plate

The results of the analysis on single plates are discussed in this chapter. In the end the first research objective is addressed.

Chapter 5: Finite element model for box girders

This chapter outlines the definition of the finite element model used in the analysis of box girders with pure bending moment.

Chapter 6: Analysis of Box Girders

Results from the analysis of box girders are presented in three distinct sections, corresponding to the outcomes of set analyses A, B, and C. Set analysis A addresses the second and third research objectives. Set analysis B addresses the fourth objective and set analysis C provides insights into the fifth objective.

Chapter 7: Conclusions

In this chapter the answer to the final research is presented. Suggestions for future research are introduced in the end.

2

State of the art

Box girders have wide thin plates that are mainly stiffened by open or closed stiffeners to deal with the stability problem of the thin plates.

Effective width approach in Eurocode is developed based on the ultimate state models of single plates and therefore can predict the ultimate resistance properly, However, the question is to what extent effective width can predict the position of the neutral line and actual stress distribution in the ultimate state and before the ultimate state in the box girders.

2.1 Previous work

The first work in the field of buckling theory was performed by Euler [2], who derived the linear elastic buckling value for an ideal, axially compressed column. The Perry-Robertson [3] approach is based on the column model with an initial imperfection, and the first yielding in the extreme fiber is taken as the elastic limit load. Their model has been widely used in design codes.

Caldwell [4] proposed the effective width method as a method for accounting for local plate deflection when using the column model on a stiffened plate. Following this, much work has been devoted to finding appropriate expressions for the effective width of plating.

Navier [5] derived the differential equation for the bending of rectangular plates and used trigonometric functions to obtain linear elastic buckling values for certain problems.

Pioneering work on large deflection of plates was performed by Kirchhoff [6], who discovered the importance of nonlinear terms for large deflections. The final form of the plate differential equation for large deformations was derived by von Karman [7].

2.2 Slender elements

Structural cross-sections containing slender elements are referred to as class 4 or slender cross-sections. These cross-sections are characterized by failure due to local buckling. The concept of cross-section classification as a means of codified treatment for local buckling of cross-sections that are partly or fully in compression is developed for an idealized bilinear stress-strain response. Each plate element is classified according to its width-to-thickness ratio and will be compared to the limits given in the code which are based on boundary conditions (internal, outstand), manufacturing method, and stress distribution in the element. In the class 4 cross-section, the failure will occur before reaching yield stress, meaning there is no benefit from the spread of plasticity and strain hardening. Cross-sectiona response is assumed to be related to the behavior of its most slender plate element, thereby the interaction of constituent plate elements i.e., the ability of the less slender elements to provide some resistance against local buckling in the slenderer elements is neglected. [8]

The classification criteria are not explicitly defined for stiffened plate elements. In general classification of the stiffened panel will be performed on the sub-elements, but the behavior on a global scale is more complex.

Eurocode introduced two approaches to account for the effects of local buckling in the design of stiffened plates. The more conservative method is to determine cross-section resistance by limiting the stress to critical buckling stress of the weakest element. In this limit, the stress strain stays linear and elastic along the cross-section. A less conservative modified version of the reduced stress method is to take into account further straining of the cross-section after buckling of the weakest part up to attaining the critical stress limit of the strongest plate element or even the yield strain. This modified approach is not dealt with in Eurocode [9]. Another method is named the effective width method in which the reduction of the strength and stiffness is reflected in reducing the width of the compression parts. For the tension part, only reduction from the shear lag effect is considered.

The effective width method is developed to account for all possible phenomena causing nonlinear stress distribution in the cross-section including shear lag, local buckling, and global buckling. The reference stress equal to yield stress is chosen and real stress distribution is smeared over an equivalent width having the reference stress equal to the yield stress.

The concept of linear strain stress distribution is generally not applicable in the elements when the elastic stress or elastic strain exceeds. By effective width concept, nonlinear effects from shear lag and plate buckling can be modeled keeping the hypothesis of linear strain distribution and having an easy way to determine the cross-section properties, resistance, and the longitudinal stresses [10].

2.2.1 Buckling of unstiffened plate

Compression in the plate causes out-of-plane deformation, however, the plate supported in four edges is still capable of carrying load after elastic buckling. The region after elastic buckling is named post-critical buckling resistance. In this region, the stiffness is significantly decreased.

In general, the nonlinear post-buckling problem for a plate with constant thickness is governed by the Von Karman [7] differential equation.

Equilibrium equation:

$$\frac{\partial^4 w}{\partial x^4} + 2 \frac{\partial^4 w}{\partial x^2 \partial y^2} + \frac{\partial^4 w}{\partial y^4} = \frac{1}{D} \left[q + \frac{\partial^2 \phi}{\partial y^2} \frac{\partial^2 w}{\partial x^2} + \frac{\partial^2 \phi}{\partial x^2} \frac{\partial^2 w}{\partial y^2} - 2 \frac{\partial^2 \phi}{\partial x \partial y} \frac{\partial^2 w}{\partial x \partial y} \right] \quad (2-1)$$

Compatibility equation:

$$\frac{\partial^4 \phi}{\partial x^4} + 2 \frac{\partial^4 \phi}{\partial x^2 \partial y^2} + \frac{\partial^4 \phi}{\partial y^4} = Et \left[\left(\frac{\partial^2 w}{\partial x \partial y} \right)^2 - \frac{\partial^2 w}{\partial y^2} \frac{\partial^2 w}{\partial x^2} \right] \quad (2-2)$$

Solutions for plates in the post-critical range fall into two categories. The first category deals with some form of solution for the differential equation like the FEM method or folded plate theory. The second category deals with some simple solution forms for the equation which are mainly derived from the ultimate state models [10].

Folded plate

In this theory, the whole element is as an assemble of compenence rectangular plate considered. In-plane effects are analyzed by plane stress theory and bending of each element normal to its plane is analyzed by flexural theory. This method is applicable on any cross section whether open or close and can deal with various kinds of stresses. This method is advantageous for the analysis of box girder bridges [10].

FEM method:

the study domain is divided into the elements that are connected in the boundary at discrete nodes. The displacement field is expressed by the local values at the nodes which are supposed to be the representative of the real field. To model the post-critical behavior of the plates in FEM properly, the material should be defined with plastic behavior with an elastic unloading pattern. It also should contain the residual stress and the initial imperfections. The FEM model can include shear lag, torsional and restrained effects also cross-sectional distortional effects can be included [10].

Ultimate state models

The failure of the panel occurs either by plastic yield or by sudden instability. Plastic yield is a progressive collapse failure in the plate. The membrane stresses redistribute over the panel and due to the development of the second order effect plastic deformation occurs and exceeds over major parts of the plate. Part of the forces is transfer to the boundary elements which maintain their stability. The in-stability

failures occur suddenly and correspond to the development of the plastic hinges in the plate or related boundary element. The disadvantage of the ultimate state models is that they are specified for elementary load modes. The solution for these elementary load cases is presented below [10].

2.2.1.1 Panel in compression

In panels with pure compression, only part of the plate close to the longitudinal edges can attain yield stress in the post-critical stage. Due to the bowing effect in the central zone of the panel, the stress will be lower. For the design purpose, the non-uniform stress distribution can be replaced by a uniform distribution over reduced plate width. The concept of effective width is used for such simplification. The reference stress for determining the effective width is equal to the edge stress which is yield stress in the collapse limit [10]. Standards also allow to replacement of the effective width by effective plate thickness.

$$\text{Winter [11]: } \frac{b_e}{b} = \frac{1}{\lambda_p} \left(1 - \frac{0.22}{\lambda_p} \right) \quad \bar{\lambda}_p \geq 0.67 \quad (2-3)$$

$$\text{Faulkner [12]: } \frac{b_e}{b} = \frac{1.05}{\lambda_p} \left(1 - \frac{0.226}{\lambda_p} \right) \cdot \bar{\lambda}_p \geq 0.55 \quad (2-4)$$

$$\text{Gerard [13]: } \frac{b_e}{b} = \frac{0.82}{\lambda_p^{0.85}} \quad (2-5)$$

2.2.1.2 Panel with gradient stress

For combined bending and compression generally, the effective width is calculated as a ratio of the compressed part. In comparison to uniform compression, two problems arise in the general case.

$$\frac{b_e}{b_c} = \frac{1}{\lambda_p} \left[1 - \frac{0.05(3+\psi)}{\lambda_p} \right] \quad (2-6)$$

a) Definition of value for b_c

The width of the compression zone (Figure 2-1) will generally vary during loading. As a simplification, b_c measured from the neutral axis of the full section of the plate. This assumption is modified in the effective width calculation of the girders and b_c measured from the neutral axis of the effective section for panels.

b) Distribution of b_e

The part of the effective width adjacent to the maximum compression close to the edge will be less than $0.5 b_e$ it also depends on the ψ value (σ_2/σ_1) [10].

$$0 < \psi < 1$$

$$\text{For the part close to the edge: } b'_e = b_e [0.5 - 0.1(1 - \psi)] \quad (2-7)$$

$$\text{For the part close to the neutral line: } b''_e = b_e [0.5 + 0.1(1 - \psi)] \quad (2-8)$$

$$\psi < 0$$

$$\text{For the part close to the edge: } b_{e1} = 0.4 b_e \quad (2-9)$$

$$\text{For the part close to the neutral line: } b_{e2} = 0.6 b_e \quad (2-10)$$

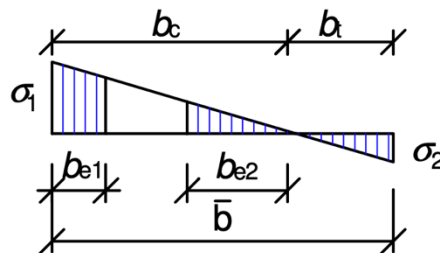


Figure 2:1 Definition of b_c and b_e

2.2.2 Buckling of stiffened Plate

The behavior of the stiffened plate is very complex therefore there are no extensive parametric studies performed on stiffened plates compared to the unstiffened plate. The general problem was considered an elastic bifurcation problem and was treated as the linear theory of buckling.

The general theory of stiffened plate was developed by Klopper and Scheer [14] for the stiffeners with zero torsional rigidity, his method was limited to one or two longitudinal stiffeners. It was based on the representation of the transverse displacement by double Fourier sine series.

$$w(x, y) = \sum_{m=1}^{\infty} \sum_{n=1}^{\infty} a_{mn} A. \sin\left(m. \frac{\pi x}{a}\right). \sin\left(n. \frac{\pi y}{b}\right) \quad (2-11)$$

The expression was introduced to the condition of neutral equilibrium developed by Rayleigh-Ritz for gaining the dimensionless unknown buckling coefficient. Massonnet gives a mathematical solution for more general plates with rigid and simple support edges. Usually, plates are stiffened by several stiffeners. In plates with more than two stiffeners, the developed mathematical expression by Massonnet and Klopper-Scheer will become too complicated to find the buckling coefficient [10]. In that case, these stiffeners are smeared over the width of the plate. Therefore, the plate is transformed into a fictitious orthotropic plate.

$$\text{Relative flexural rigidity: } \gamma = \frac{E.I_s}{b.D} \quad (2-12)$$

$$\text{Relative torsional rigidity: } \nu = \frac{c}{b.D} \quad (2-13)$$

$$\text{Relative extensional rigidity: } \delta = \frac{A_s}{b.t} \quad (2-14)$$

Klopper, Scheer, and Moller give some typical results and diagrams for these types of plates for different aspect ratios and relative rigidities. One assumption in developing the orthotropic plate theory is having equally spaced stiffeners and simple supported edges. The differential equation governing the buckling of orthotropic plates is:

$$\frac{\partial V_x}{\partial x} + \frac{\partial V_y}{\partial y} + \left(q - N_x \frac{\partial^2 w}{\partial x^2} - N_y \frac{\partial^2 w}{\partial y^2} + 2N_{xy} \frac{\partial^2 w}{\partial y. \partial x} \right) = 0. \quad (2-15)$$

Most of the previous research was performed on the stiffened plate with zero torsional rigidity (mainly stiffeners with open cross-section). In the new research about the stiffened plate, more focus is conducted on the stiffeners with close cross sections with higher torsional rigidity.

2.2.2.1 Stiffened Panel in pure compression

For uniformly compressed stiffened plate disregarding the restrains from boundary connected elements and shear stress the first approximation for the buckling mode of the structure is:

$$w_1(x, y) = A. \sin\left(\frac{\pi x}{a}\right). \sin\left(\frac{\pi y}{b}\right) + (1 - A). \sin\left(\frac{m\pi x}{a}\right). \sin\left(\frac{n\pi y}{b}\right) \quad (2-16)$$

m: is the number of half-waves in the longitudinal direction that develop between the longitudinal ribs

n: is the number of panels between the stiffeners.

The buckling surface consists of a combination of

- 1) the overall buckling mode of the orthotropic plate with smeared stiffeners,
- 2) the nodal buckling of plate panels between the longitudinal stiffeners which depends on the rigidity of the longitudinal stiffeners (Figure 2-2).

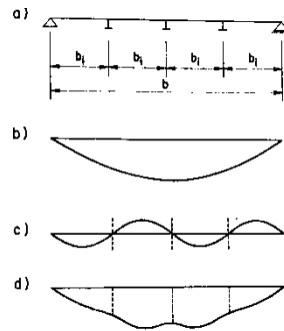


Figure 2:2 Stiffened plate scheme b) overall buckling c) nodal buckling d) global interactive buckling [10]

Different approaches exist for analyzing the uniformly compressed stiffened plate including modified linear plate buckling theory, strut approach, and orthotropic plate approach.

Linear plate buckling theory

This theory indicates that buckling behavior depends on the relative stiffness of the plate and stiffeners. The equation describing the critical stress has the same format as the unstiffened plate with different buckling coefficients (k) depending on the flexural stiffness of the stiffeners [10].

$$\sigma_{cr} = k \cdot \frac{\pi^2 \cdot E}{12(1-\nu^2)} \cdot \left(\frac{t_p}{b}\right)^2 \quad (2-17)$$

This method is simple to apply, however, it does not include imperfections, residual stress, and modes of failure.

Strut approach

In this method stiffened plate is replaced by a series of unconnected columns. Provided that the longitudinal stiffeners do not collapse by local instability, three modes of failure for struts may be considered. This method is basic of the design in many codes and is more realistic if the plate has large longitudinal stiffeners [10].

In a stiffened plate, providing that the stiffeners do not suffer from local instability, three failure modes may be considered:

- 1) Failure of the compression plate by plate buckling and yielding of the stiffeners.
- 2) Failure of stiffeners by yielding in compression
- 3) Tensile yielding on the stiffener outstands.

The load carrying capacity is then calculated as the sum of the ultimate loads of the struts.

Orthotropic plate approach

In this method, the stiffness of the stiffeners is smeared over the width of the plate. Maquoi and Massonnet [15] were the first to develop a design method that considers the post-critical resistance produced by membrane stresses in stiffened panels. The main assumptions in this model are:

- 1) flexural and extensional rigidity of the stiffeners can be continuously smeared to obtain an orthotropic plate that can be analyzed by the non-linear large displacement theory of Von Karman.
- 2) The stiffened plate has sinusoidal initial imperfection and displacement develops in the same mode. This assumption is shown by Volmir to be accurate if the ratio of the average ultimate stress to critical stress does not exceed the value of 1.5.
- 3) Collapse is reached when the mean longitudinal membrane stress along the unloaded edge of the panel reaches yield stress.
- 4) The plate buckling reduction factor between the stiffeners is allowed by using an effective width approach [10].

The result of their analysis was a global efficiency factor equal to the ultimate load at collapse divided by the squash load of a fully effective stiffened plate (ρ_g), the local efficiency of the panel between stiffeners is taken into account by an effective width concept developed for unstiffened plates (ρ_1).

The total efficiency factor is calculated by multiplying these two reduction factors.

The stiffened plate is safe when mean compression stress does not exceed the value of $\rho_g \cdot \rho_1 \cdot f_y$.

Critic of this model is that it does not take into the account reduction in the rigidity of the stiffened plate.

Panel partly in bending stress.

There is no exact solution for this type of loading in the stiffened plate, practical design approaches are proposed to calculate the effective width of the compression part of the panel. Neglecting the tensile part of the panel can be a conservative assumption [16].

2.3 Elastic-plastic behavior of stiffened panels

The behavior of plates can be classified by slenderness. In general, a structure can be roughly divided into stocky and slender structure which behaves differently to stability phenomena.

Stocky plates are normally not susceptible to stability failure and the effect of imperfection is in most cases negligible. The out-of-plane deformation when reaching the elastic-plastic resistance is normally small. Therefore, a geometric linear analysis can be sufficient. Such a structure can reach elastic or elastic-plastic resistance.

Slender plates that are subjected to compression stress fail before reaching the elastic resistance of the perfect system. This happens because, due to imperfection, the compression produces out-of-plane deformations and leads to additional bending moments in the system. By increasing the load, the out-of-plane deformation of the plate increases in a nonlinear manner.

Classification of the elements for determining their behavior can be found in EN1993-1-5 or EN1993-1-1. These criteria are not defined for stiffened plate elements. In general, when a plate becomes slender additional stiffeners can be considered. Due to these stiffeners, the local behavior of the part of the panel between stiffeners can become stocky if the stiffeners are stiff enough.

2.3.1 Failure modes of plates

Depending on the relative sizes of the plate and stiffeners, failure may occur by panel buckling, by overall buckling, or as a complex interaction of the two, and in some cases, this may also be combined with lateral-torsional instability of the stiffeners.

Stiffened plates are often slender and local failure is likely to occur. Local buckling does not imply immediate collapse since, in many cases, a reserve of strength will exist. This arises from the ability of a section to redistribute loads and the significance of this will depend upon the geometrical properties. If the plate dimensions are such that bifurcation occurs in the elastic-plastic range, the capacity for redistribution will be small, and rapid unloading will follow.

However, if the panels are slenderer and buckling occurs in the elastic range, stresses will redistribute to stiffer sections of the plate and stability will be maintained. In this case, the ultimate load will not be reached until either the rate of unloading exceeds the rate of redistribution, or yielding has occurred in the remaining effective areas of the plate. This type of failure represents the collapse pattern when the stiffeners are relatively weak.

The other type of failure in compression panels may happen when both the plate and the stiffeners are stocky. In such cases, the plate will reach full yield stress in compression and with increasing the load it will squash at constant stress. The stiffeners will develop higher tensile stresses to resist additional applied moments and the capacity of the total section will thus decrease [17].

Webb and Dowling performed an extensive test on various configurations for plates. They also developed a finite element program for predicting the resistance and elastoplastic stress distribution in the stiffened panel [18]. They derived the averaged peak stress at the edges of the stiffened panel in pure compression and categorized behavior into three zones.

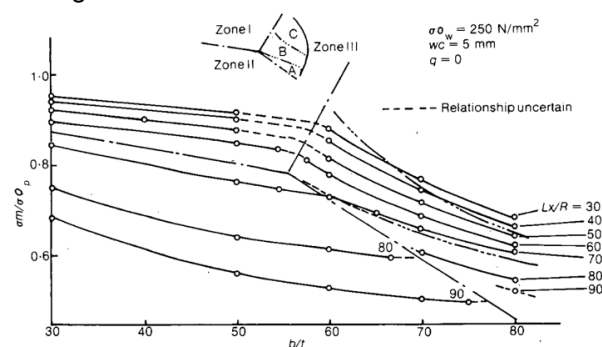


Figure 2:3 Peak stress in panels with $30 < b/t_p < 50$ and $30 < L/R < 90$ [18]

Zone 1) Failure occurs by yielding across the plating before extensive buckling occurs.

In this type of failure, for the case of stocky subpanels (low ratio of $\frac{b_i}{t_p}$) a linear stress-strain relationship is seen. The ultimate load is reached soon after first yielding in the plate. Out-of-plane deformations remain small and direct stresses are distributed almost uniformly across the plate. At the ultimate state, almost full yielding compression is sustained by the plate and additional applied load leads to increased deformation with straining of the plate at constant stress. For the cases with higher slenderness (high ratio of $\frac{b_i}{t_p}$), Before the peak load, behavior is similar to that described for stocky subpanels. Beyond this point, panel deformations increase rapidly. The small depressions are seen in the stress curves across the web are the result of high transverse moments which develop as the panels buckle [18].

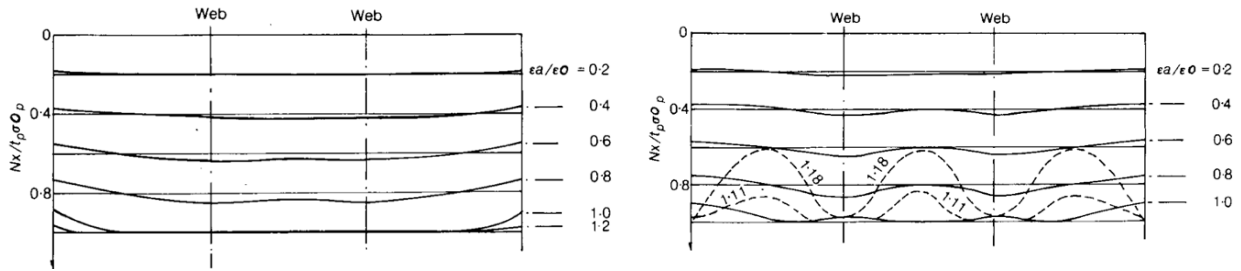


Figure 2:5 Direct stress distribution for stocky subpanel in plate loading [18] Figure 2:4 Direct stress distribution for slender subpanel in plate loading [18]

Zone 2) Failure occurs in an overall mode following the flexural failure of the stiffeners.

This type of failure occurs in geometries with low flexural rigidity of the stiffeners. The consequence is that the behavior of the panel is the same as that of an unstiffened section with three times the basic panel slenderness [18].

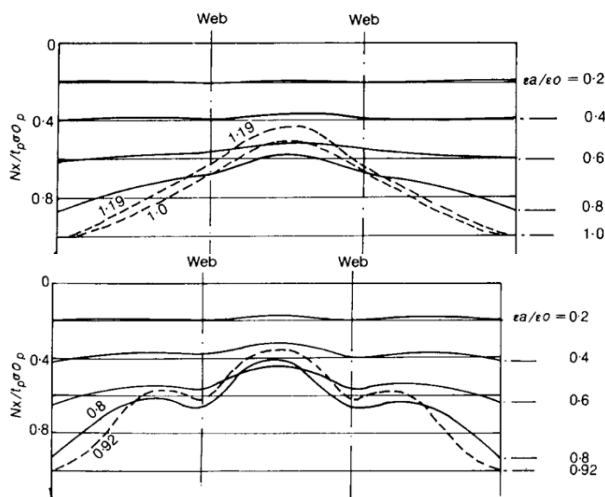


Figure 2:6 Direct stress distribution for stocky subpanel in plate loading, low flexural rigidity of the stiffener [18]

Figure 2:7 Direct stress distribution for slender subpanel in plate loading, low flexural rigidity of the stiffeners [18]

Zone 3) Failure happened by local panel buckling in a half-wave mode in subpanels.

For all geometries within this zone, the critical panel buckling stress is less than the yield stress. Close to the theoretical buckling stress panels, snap-through will occur and a three-half-wave mode develop (the panel has two stiffeners).

The number of half-waves that develop along the span will depend upon the aspect ratio of the panels and the degree of clamping afforded by the stiffeners. In the absence of residual stress plasticity developed over the stiffeners and hinges will be formed along the panels [17].

Other possible types of failure in a stiffened plate are:

Yielding along the plate-stiffener intersection

This type of failure normally takes place when the stiffeners are relatively strong so that the stiffeners remain straight until the plating between stiffeners buckles or even collapses locally. The stiffened panel will eventually reach the ultimate limit state by the failure of stiffeners together with some associated plating [19].

Local buckling of stiffener web

This type of failure happens when the ratio of the height to the thickness of the stiffener's web is inadequate to remain straight so that the stiffener web buckles or twists sideways [19].

2.3.1.1 The effect of Initial imperfection

Significant difference in load carrying capacity can exist depending on whether an overall mode of failure occurs towards the plating or the stiffeners. The direction of collapse in a compressed panel will depend upon the net eccentricity of the applied load and will therefore be a function of the direction and magnitude of an initial bow [17].

In stiffened panels, the overall bow will be influenced by the flexural rigidity of the stiffeners. In cases where failure is likely to occur by yielding in members, an overall bow towards plating will accelerate this process [17].

2.3.1.1.1 Effect of stiffened plate initial imperfection on the bending resistance

Test in the bending resistance and stress pattern in the stiffened box girder is performed by Massonnet et. al. Two of their test's set ups are the pure bending test and they monitor stresses until failure. In these test setups, the shear lag effect was driven out of the results. Both tests have the same dimensions and boundary conditions. The only difference between this test is the direction of initial imperfection. in test number 2, the stiffened plate had initial curvature toward the stiffeners and in test number 1 this curvature was towards the plate side [20].

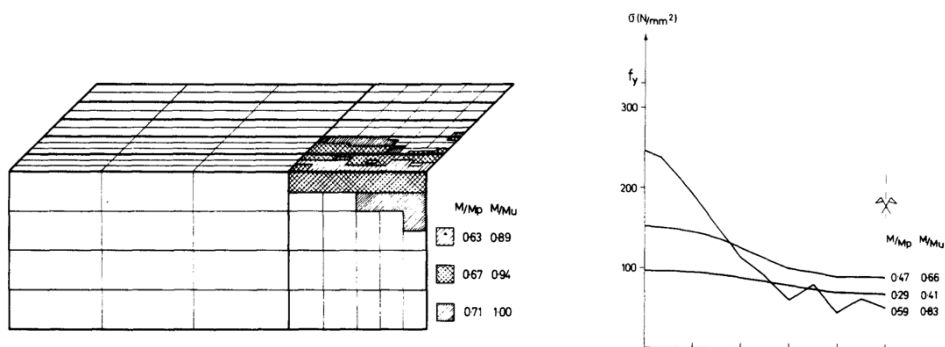


Figure 2:8 Development of yielding in test set up 1 and stress distribution in half of the top flange test [20]

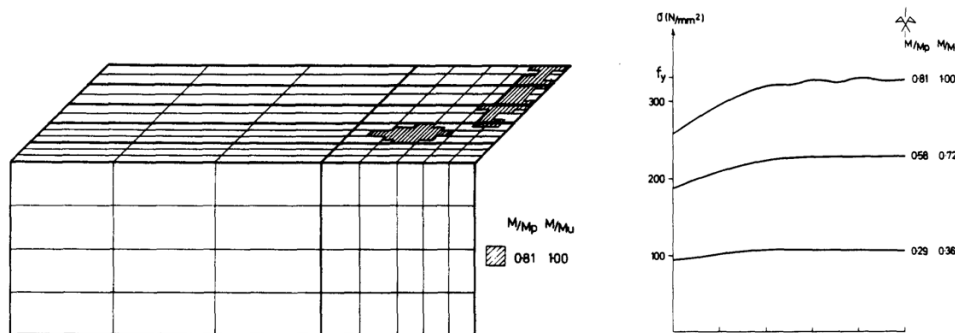


Figure 2:9 Development of yielding in test set up 2 and stress distribution in half of the top flange test [20]

Their test results prove that the assumed stress in obtaining the effective width is valid when the initial imperfection is toward the plate side. In other words, the stress considered in calculating the effective width and the resistance will be obtained by imperfection that causes extra tension in the plate and extra compression in the stiffeners.

2.3.1.2 The effect of residual stress

Residual stresses resulting from the welding process can have a significant effect on the load-bearing capacity of plated structures.

The influence of residual stress on the load-bearing capacity and buckling stress will largely depend upon the geometrical properties. Investigations carried out by Moxham [21] into unstiffened plate behavior showed that the effect of residual stress is most severe for panels of intermediate slenderness where interaction between local buckling and yielding occurs. Whereas, for plate panels of low slenderness, where failure occurs by squashing, residual stresses have a negligible effect, and the ultimate load capacity will be similar in magnitude to the residual stress-free case.

For panels of high slenderness, the presence of residual compression will lower the buckling load, but since the edges are initially stressed to yield in tension a larger post-buckling reserve is likely to exist than in the equivalent stress-free case. Therefore, the reduction in ultimate strength is likely to be less severe than the reduction in buckling strength.

In stiffened panels, residual stresses will be present in the stiffeners as well as in the plate, and investigations by Hasegawa et al [22] show that the smaller the flexural rigidity of the stiffeners, the greater the drop in strength as the result of the residual stress.

2.3.1.3 The effect of loading type and boundary conditions

Loading types can be divided into two categories, those applied in the plane of the plate and those acting normal to it. In the first group, forces may be tensile, compressive, or shear and may arise directly from application, or indirectly from the overall distortion of a structure. The second category is related to the pressure load out of the plate of the panel. The degree of restraint applied to the panel out-of-plane will affect the shape of deformation and structure of a given type of loading. In this study, the in-plane loading of the panels will be studied, mainly as the result of the pure bending on the box girders.

2.4 Eurocode effective width method

The design rules for unstiffened and stiffened flat plates, based on the effective width method, are introduced in section 4 of EN 1993-1-5. The Eurocode method for determining the cross-section properties and the ultimate resistance is to consider elements as a component of separate panels. For each panel, plate-like and column-like buckling and relevant critical stress $\sigma_{cr,p}$, $\sigma_{cr,c}$ will be determined. From the critical stress the relative slenderness is calculated, then a relevance reduction factor separately to platelike buckling (ρ) and column-like buckling (χ_c) will be determined. Having ρ and χ_c the final reduction factor will be interpolated by the weighting factor from the plate and column critical stresses ratio.

The Eurocode method in determining the effective width in the elements with stiffened panels is to consider the plate in two separate conditions. The reduction can take place in the stiffened plate in the format of pure orthotropic plate named plate-like buckling, pure buckling of the most compressed strut named column-like buckling. Interaction of them can also happen depending on the ratio of the critical stresses for both types of instability.

Although the stress distribution is non-linear, this method adopted a linear (i.e., uniform) stress distribution acting only on the effective parts of the cross-section, whereas the contribution of the buckled central parts is completely neglected in the cross-section resistance. Finally, assuming that the stresses along the effective parts of the plate (b_{eff}) at the ultimate limit state are equal to the yielding stress (f_y).

2.4.1 Eurocode method for unstiffened plate

In the case of an unstiffened plate depending on the aspect ratio of the panel pure plate-like or pure column-like buckling may happen. In the case of plate buckling ($\alpha > 1$), The reduction factor depends on the slenderness and stress pattern in the section derived from LEA.

$$\rho = \begin{cases} 1.0 & \text{if } \bar{\lambda} < 0.5 + \sqrt{0.085 - 0.055\psi} \\ \frac{\bar{\lambda} - 0.55(3 + \psi)}{\bar{\lambda}^2} & \text{if } \bar{\lambda} < 0.5 + \sqrt{0.085 - 0.055\psi} \end{cases} \quad (2-18)$$

$$\bar{\lambda} = \frac{\frac{b}{t}}{28.4 \varepsilon \sqrt{k_{\sigma, pl} \sigma}} \quad , \quad \varepsilon = \sqrt{\frac{235}{f_y}} \quad (2-19)$$

where $k_{\sigma, pl}$ is the elastic buckling coefficient for flat plates which depends on the stress pattern in the panel.

Stress distribution (compression positive)		Effective ^e width b_{eff}			
	$1 > \psi \geq 0$	$b_{eff} = \rho c$			
	$\psi < 0$	$b_{eff} = \rho b_c = \rho c / (1 - \psi)$			
$\psi = \sigma_2 / \sigma_1$	1	0	-1	$1 \geq \psi \geq -3$	
Buckling factor k_{σ}	0.43	0.57	0.85	$0.57 - 0.21\psi + 0.07\psi^2$	
	$1 > \psi \geq 0$	$b_{eff} = \rho c$			
	$\psi < 0$	$b_{eff} = \rho b_c = \rho c / (1 - \psi)$			
$\psi = \sigma_2 / \sigma_1$	1	$1 > \psi > 0$	0	$0 > \psi > -1$	-1
Buckling factor k_{σ}	0.43	$0.578 / (\psi + 0.34)$	1.70	$1.7 - 5\psi + 17.1\psi^2$	23.8

Stress distribution (compression positive)		Effective ^e width b_{eff}			
	$\psi = 1$	$b_{eff} = \rho \bar{b}$			
	$1 > \psi \geq 0$	$b_{c1} = 0.5 b_{eff} \quad b_{c2} = 0.5 b_{eff}$			
	$\psi < 0$	$b_{c1} = \frac{2}{5 - \psi} b_{eff} \quad b_{c2} = b_{eff} - b_{c1}$			
	$\psi = 1$	$b_{eff} = \rho \bar{b} = \rho \bar{b} / (1 - \psi)$			
	$0 > \psi > -1$	$b_{c1} = 0.4 b_{eff} \quad b_{c2} = 0.6 b_{eff}$			
$\psi = \sigma_2 / \sigma_1$	1	$1 > \psi > 0$	0	$0 > \psi > -1$	-1
Buckling factor k_{σ}	4.0	$8.2 / (1.05 + \psi)$	7.81	$7.81 - 6.29\psi + 9.78\psi^2$	$23.9 \quad 5.98(1 - \psi)^2$

Figure 2:10: Plate buckling reduction factor [1]

for aspect ratios $\alpha < 1$ column type of buckling may occur, and the check should be performed using the reduction factor ρ_c .

$$\sigma_{cr,c} = \frac{\pi^2 E t^2}{12(1 - \nu^2)} \quad , \quad \bar{\lambda}_c = \sqrt{\frac{f_y}{\sigma_{cr,c}}} \quad (2-20)$$

The reduction factor χ_c should be obtained from 6.3.1.2 of EN 1993-1-1. For unstiffened plates buckling curve a is applicable.

2.4.2 Eurocode method for stiffened plate

For stiffened panels, the conventional method of classification of the element is not simply applicable. The buckling behavior is the complex interaction of the local buckling in the subpanels between longitudinal stiffeners and global buckling in the format of plate-buckle, column-buckling, or their interaction.

The local effective width in the stiffened panel is calculated from the local reduction in the subpanels based on their slenderness. For determining local reduction factors in the subpanels and stiffeners they would be considered as an unstiffened plate.

First, the effective cross-section would be calculated considering all local reductions. $A_{c,eff,loc}$ presents the effective section areas of all the subpanels and stiffeners that are fully or partially in the compression, excluding the parts supported by an adjacent plate element with the width $b_{edge,eff}$.

$$A_{c,eff,loc} = A_{st,eff} + \sum_c \rho_{loc} \cdot b_{c,loc} \cdot t \quad (2-21)$$

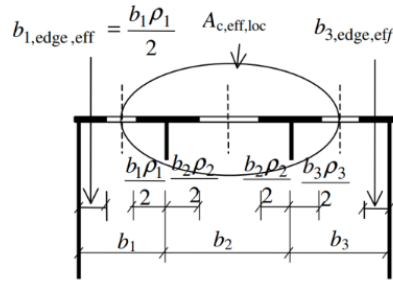


Figure 2:11 Effective area of a stiffened plate under uniform compression [1]

To consider the global buckling effects, the final reduction factor ρ_c will be calculated by interpolation between χ_c and ρ for column like buckling and plate like buckling respectively. The interaction coefficient ξ depends on the column like buckling stress and plate like buckling stress.

$$\xi = \frac{\sigma_{cr,p}}{\sigma_{cr,c}} - 1, \quad 0 \leq \xi \leq 1. \quad (2-22)$$

$$\rho_c = (\rho - \chi_c)\xi(1 - \xi) + \chi_c \quad (2-23)$$

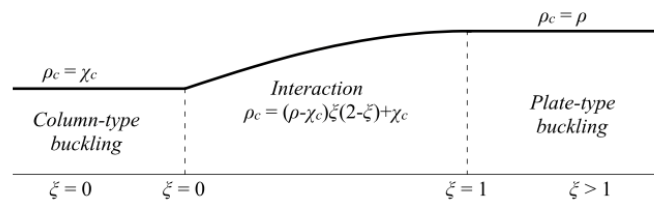


Figure 2:12 Column-like and plate-like buckling interaction [1]

plate-like buckling:

The detailed formula is introduced in the annex A1 of the EN1993-1-5. In part A1, based on the equivalent orthotropic plate theory the plate critical buckling stress for the stiffened plate with three or more stiffeners can be calculated. Through this method critical buckling coefficient will be calculated. The final critical buckling stress is the multiplication of the obtained buckling factor to the linear buckling stress. It is worth mentioning the validation criteria for the orthotropic plate theory in annex A 1 of EN1993-1-5, is having aspect ratio larger than 0.5. for the lower aspect ratio common procedure is to assume aspect ratio to be equal to 0.5.

$$\sigma_{cr,p} = k_{\sigma,p} \cdot \sigma_E \quad (2-24)$$

$$\sigma_E = \frac{\pi^2 E t^2}{12(1-\nu^2)} \quad (2-25)$$

$$k_{\sigma,p} = \begin{cases} \frac{2[(1+\alpha^2)^2 + \gamma - 1]}{\alpha^2(1+\psi)(1+\delta)} & \text{if } \alpha < \sqrt[4]{\gamma} \\ \frac{4(1+\sqrt{\gamma})}{(1+\psi)(1+\delta)} & \text{if } \alpha < \sqrt[4]{\gamma} \end{cases} \quad (2-26)$$

γ is the ratio between the flexural stiffness of the entire stiffened plate and that of the sheet plate alone.

$$\gamma = \frac{I_{sl}}{I_p}, \quad I_p = \frac{b \cdot t^3}{12(1-\nu^2)} \quad (2-27)$$

δ the ratio between the gross area of the stiffeners and that of the sheet plate alone.

The method in part A2 of EN1993-1-5 is for panels with less than three stiffeners, which cover the exact solution for buckling of such plates. This solution has been driven by considering a fictitious isolated strut supported on an elastic foundation reflecting the plate effect in the direction perpendicular to this strut. Critical plate buckling stress is the lowest value of the calculated critical stress for the three configurations shown in Figure 2-13.

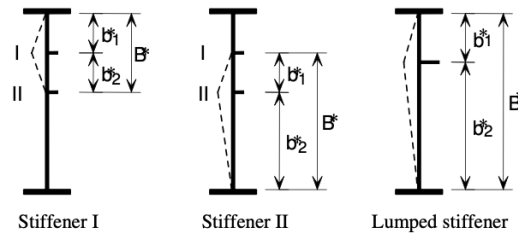


Figure 2:13 Plate with two stiffeners in compression [1]

By having the equivalent plate buckling stress the equivalent slenderness can be calculated for the plate,

$$\bar{\lambda}_p = \sqrt{\frac{\beta_{A,c} f_y}{\sigma_{cr,p}}}, \quad \beta_{A,c} = \frac{A_{c,eff,loc}}{A_c} \quad (2-28)$$

The final plate-like buckling reduction factor can be now calculated using the criteria defined for the unstiffened plate.

It should be noticed that this buckling stress corresponds to the occurrence of a global mode in the stiffened plate. EN1993-1-5 also indicates that appropriate charts or relevant computer simulations could be used as an alternative. Attention should be paid to the fact that the first mode is not necessarily the same as the global buckling mode of the stiffened plate [23].

Column-like buckling:

The column-type behavior is based on a simple assumption that the longitudinal (unloaded) edges are not supported so that the critical stress of a plate corresponds to the buckling stress of a column.

Column-like buckling dealt with the global failure mode of the plate. Column-like buckling will take place in the plates with a low aspect ratio or in the plate with large orthotropy. A more severe reduction factor than plate buckling (ρ) relates to column buckling (χ_c) is required.

For determining column-like buckling stress, criteria of EN1993-1-1 are used with a special imperfection factor (α) related to the type of stiffeners.

For a stiffened plate $\sigma_{cr,c}$ may be determined from the elastic critical column buckling stress $\sigma_{cr,sl}$ of the stiffener closest to the panel edge with the highest compressive stress.

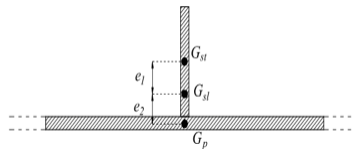
$$\sigma_{cr,sl} = \frac{\pi^2 E I_{sl,1}}{A_{sl,1} a^2} \quad (2-29)$$

In the EN1993-1-5, it is mentioned that for the stiffened plate with gradual stress distribution critical column-like buckling of the plate may be determined by extrapolation with respect to the width of the compression part.

$$\sigma_{cr,c} = \sigma_{cr,sl} \frac{b_c}{b_{sl,1}} \quad \bar{\lambda}_c = \sqrt{\frac{\beta_{A,c} f_y}{\sigma_{cr,c}}} \quad (2-30)$$

To determine the final column-like reduction factor, the imperfection is adjusted by equation 2-31.

$$\alpha_e = \alpha + \frac{0.09}{i/e}, \quad i = \sqrt{\frac{I_{sl,1}}{A_{sl,1}}} \quad (2-31)$$

Figure 2:14 Definition of e_1 and e_2

where α is the imperfection factor ($\alpha = 0.34$ for closed cross-section stiffeners and $\alpha = 0.49$ for open cross-section stiffeners), and e is the larger of distances e_1 (between the center of gravity of the stiffener alone G_{st} and the entire stiffener with the adjacent plate G_{sl}) and e_2 (between the adjacent plating alone G_p and the entire stiffener with the adjacent plate G_{sl}).

The final reduction factor χ_c for this instability mode can be calculated as a function of slenderness.

$$\phi = 0,5 \left(1 + \alpha_e (\bar{\lambda}_c - 0,2) + \bar{\lambda}_c^2 \right) \quad (2-32)$$

$$\chi_c = \frac{1}{\phi + \sqrt{\phi^2 - \bar{\lambda}_c^2}} \tag{2-33}$$

2.4.3 Effective width from shear lag nonlinearity

Although normal stress in the longitudinal direction caused by bending deformation is assumed to be uniform across flange width in the elementary beam theory, in the case of a beam cross-section with a wide flange the stress distribution will not be uniform. The longitudinal displacements in the parts of the flanges far from the web lag behind those near the web due to the action of in-plane shear strain. In the web flange interaction zone, longitudinal stress is much higher and Euler Bernoulli beam theory underestimates the stress in that part of the flange. By using an effective width method, the nonlinear stress distribution of the flange will be modeled as a linear stress distribution over the effective width with the stress equal to the highest normal stress [24].

$$B_e = \frac{1}{\sigma_{x,0}} \cdot \int_0^B \sigma_x(y) \cdot dy \tag{2-34}$$

Solution for this equation leads to definition of a reduction factor β outlined in part 3 of EN1993-1-5 [1].

$$b_{\text{eff}} = \beta b_0 \tag{2-35}$$

2.4.4 Effective width method in bending

The behavior of the class 4 cross-section can be explained in bending by following Figure 2-15. Euro code indicates that the development of plate buckling starts with the stress distribution obtained on the gross cross-section.

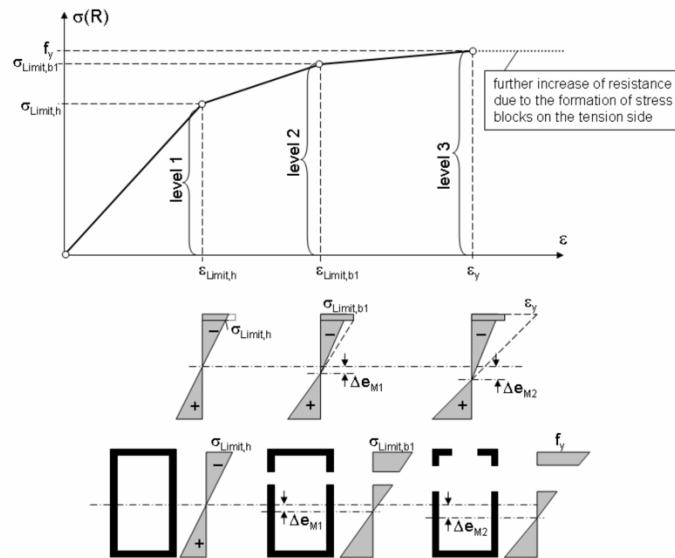


Figure 2:15 Development of the strength and eccentricity versus compression strain in the compression flange [9]

Cross-sections of prismatic members are remodeled as a set of separate plate elements that can be subjected to uniform or gradient compression. Each plate element has a buckling strength.

Level 1 is the end of the elastic stage and coincides with the buckling of the slenderest plate. Effective width method allows the benefit of higher resistance, by considering the resistance of the cross section after the buckling of the weakest part. Therefore, the resistance still increases even after buckling of the slender element. The ultimate bending resistance is defined at the time that the plate gets the yield stress at the most compressed fiber. To gain the effective width reduction of the flange can be done in one iteration, however, reduction in the web is an iterative process that depends on the maximum and minimum stress ratio. The eccentricity Δe_M for girder in bending resulting from the equilibrium of stress distributions in the cross-section leads to this iterative procedure for determining the final neutral axis of the cross-section. The point of attention is that this eccentricity does not cause any additional moment from N . Δe_M and the additional moment should be calculated based on the shifted position of the neutral line in the effective section reduced having pure compression $\Delta M = N \cdot \Delta e_N$.

The code suggests using a stress pattern from $\sigma = M_{Ed}/W_{eff}$ and keep doing iteration until having a constant stress pattern on the web of the reduced cross-section.

$$\sigma_{Limit} = \rho \cdot f_y$$

σ_{Limit} : is the mean value of a stress distribution resulting from buckling of the plate element.

ρ : is the plate buckling reduction factor depending on the plate's slenderness $\bar{\lambda}_p = \sqrt{\frac{f_y}{\sigma_{crit}}}$

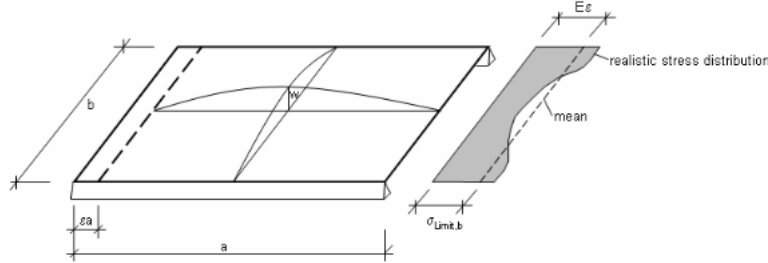


Figure 2:16 Distribution of stress caused by local buckling of plate elements subject to compression strain [9].

For the plate element in pure compression, there is an equivalence between the resistance calculated with the reduced stress σ_{limit} or calculated with the reduced section b_{eff} .

$$R_{ult} = f_y \cdot b_{eff} \cdot t = b \cdot t \cdot \sigma_{Limit} \quad (2-36)$$

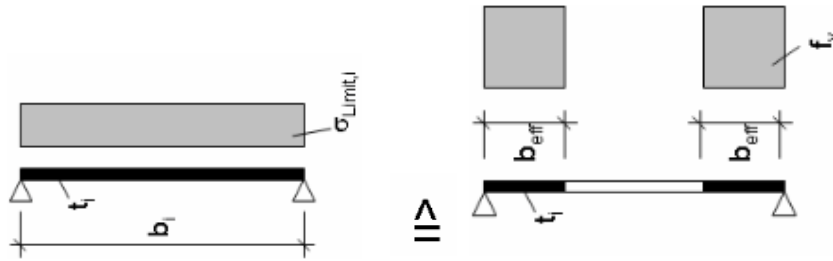


Figure 2:17 Equivalent effective width [9]

If the verification of the cross-section is going to be performed based on the criteria of the EN1993-1-5, The code allows for the reduction of the slenderness based on the maximum design compressive stress when it is lower than yield stress and therefore increases the buckling reduction factor.

$$\bar{\lambda}_{p,red} = \bar{\lambda}_p \cdot \sqrt{\frac{\sigma_{com,Ed}}{f_y}} \cdot \sqrt{\gamma_{M0}} \quad (2-37)$$

However, this reduction is mentioned to be conservative in the design. An alternative approach to consider the effective width for stress levels lower than yield stress is introduced in annex E of EN1993-1-5.

for internal compression elements:

$$\rho = \frac{1 - \frac{0.055(3+\psi)}{\bar{\lambda}_{p,red}}}{\bar{\lambda}_{p,red}} + 0.18 \frac{(\bar{\lambda}_p - \bar{\lambda}_{p,red})}{(\bar{\lambda}_p - 0.6)} < 1 \quad (2-38)$$

for outstand compression elements:

$$\rho = \frac{1 - \frac{0.188(3+\psi)}{\bar{\lambda}_{p,red}}}{\bar{\lambda}_{p,red}} + 0.18 \frac{(\bar{\lambda}_p - \bar{\lambda}_{p,red})}{(\bar{\lambda}_p - 0.6)} < 1 \quad (2-39)$$

3

Definition of finite element model of the stiffened plate

Within an isolated stiffened panel interaction may take place between adjacent plate and stiffener elements. The degree of interaction will depend upon the geometrical properties and instability within one element that may accelerate the collapse of another plate.

A stiffened panel is usually part of a larger structure, and it is therefore not obvious how to define the boundary conditions of an isolated panel. A common assumption is to consider the edges as simply supported, and free to move in-plane but forced to remain straight [25] [26].

The analysis of the understudied panels is performed through geometrical and material nonlinear analysis using Abaqus. Details of the model including the definition of the material, boundary conditions and loading, definition of mesh, and solving method are illustrated in this part of the report.

3.1 Material properties

Material is modeled elastic-plastic with strain hardening according to EN1993-1-1. The hardening is equal to $E/100$ and the yield stress is equal to 355 N/mm^2 . True stress-logarithmic strain material property is defined in numerical simulations. Young's modulus is equal to 210000 MPa and the Poisson ratio is equal to 0.3 for steel.

When defining plasticity data in Abaqus, true stress, and true strain must be used. ABAQUS requires these values to interpret the data in the input file correctly. However, quite often material test data are supplied using values of nominal stress and strain. In such situations, the plastic material data from nominal stress and strain to true stress and strain must be converted [27].

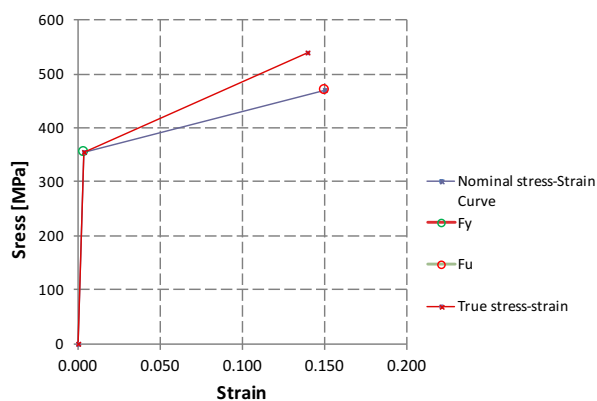


Figure 3:2 Engineering and true stress-strain curve

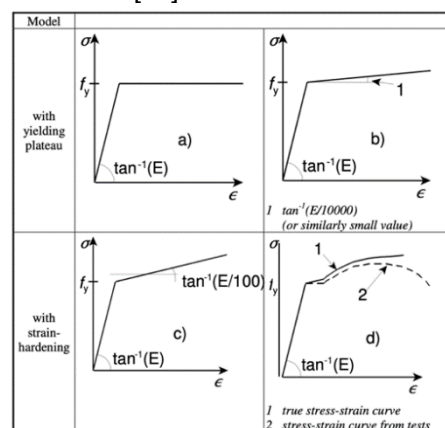


Figure 3:1 Stress strain curve [1]

The relationship between true strain and nominal strain is established by expressing the nominal strain from equation 3-1.

$$\varepsilon_{True} = Ln(1 + \varepsilon) \quad \sigma_{True} = \sigma(1 + \varepsilon) \quad (3-1)$$

3.2 Imperfection

Where imperfections need to be included in the finite element model to account for the geometrical deviation from the perfect shape. These imperfections should include both geometric and structural imperfections.

Imperfection can be applied in two different ways:

- 1) Measuring the geometrical imperfection and residual stress due to the fabrication process.
- 2) Using equivalent imperfection which will also allow to introduce residual stress in the section as an equivalent imperfection. There are two ways to define the equivalent initial imperfection. One method is to apply imperfection based on a predefined standardized function, and the other method is to modify the imperfection shape of the structural element by taking displacement driven from linear buckling analysis. The manually defined imperfection is more complex, but it usually leads to more robust and reliable models. Application of the eigenmode imperfection usually leads to a safe design [28].

In the case of large structures like box sections of the bridge structure with numbers of the longitudinal and transverse stiffeners measuring the imperfection and residual stress is not a realistic approach. In the case of applying equivalent initial imperfection in nonlinear analysis, different directions of imperfection should be chosen to identify the lowest resistance. If more than one equivalent imperfection is used, a combination of those should additionally be considered.

3.2.1 Equivalent geometrical imperfection

Equivalent geometrical imperfection can be categorized into four subgroups [29].

- 1) Equivalent geometrical imperfection for global structures(frame)
- 2) Equivalent geometrical imperfection for structural members
- 3) Equivalent geometrical imperfection for cross sections(plates)
- 4) Equivalent geometrical imperfection for shell structures

When equivalent geometrical imperfection is a combination of the imperfection from different subgroups, each imperfection should have its maximum value and they should be linearly added [28]. For equivalent cross-section imperfection in plated structures, considering the combination of imperfection is necessary. First, the leading imperfection should be chosen with the accompanying imperfection at an amplitude reduced to 70% [1]. The direction of the applied imperfection should be such that the lowest resistance is obtained.

Geometric imperfections amplitudes are given in the National Annex of EN1993-1-5, and shown in Table3-1. These standardized imperfections represent the most observed imperfections during the manufacturing process.

Type of imperfection	Component	Shape	Magnitude
global	member with length ℓ	bow	see EN 1993-1-1, Table 5.1
global	longitudinal stiffener with length a	bow	min ($a/400, b/400$)
local	panel or subpanel with short span a or b	buckling shape	min ($a/200, b/200$)
local	stiffener or flange subject to twist	bow twist	1 / 50

Table 3-1 Initial imperfection magnitude [1]

One of the most used hypotheses is to assume this pattern given by the eigenmodes of a perfect element obtained by a linear buckling analysis (LBA) as initial imperfection. These imperfections must cover the effects of other imperfections like load eccentricities, residual stresses, etc. It is known that multiple eigenmodes and different interactions corresponding to the desired deformation for local and global panel imperfection and stiffener imperfection should be considered. This is because the first buckling mode is not necessarily always the most disadvantageous one.

In wide stiffened panels, the global buckling mode appears sometimes only after tens of eigenmodes. Moreover, in the eigenmodes, the deformation of the stiffeners is combined with the deformation of the

panel, in most cases, which makes it impossible to define the correct amplitude for each type of imperfection separately. For this reason, the imperfections are introduced to the model as the external file.

3.2.2 Applied Imperfection on the plates

For dense stiffened panels, local buckling effects are important when the relative rigidity of the stiffeners is high. In the case of having stiffeners with low relative stiffness, the global imperfection is going to be the leading initial imperfection. Global deflection must be accounted for with the interaction with local buckling mode. In this study local initial imperfection between subpanel and bow imperfection in the stiffeners and their combinations are defined for analysis of each plate and the imperfection is applied as the external file to the FEM model. The applied initial imperfection is visualized below by plotting the deflection in the nodes for the case that the initial imperfection is towards the stiffeners (negative initial imperfection) for model number 1.

- **Stiffener imperfections**

The amplitude for stiffener imperfections has its shape represented in Figure 3-3 and is defined by equation 3-2. The direction of the initial imperfection in the longitudinal stiffeners is defined compatible with the global initial imperfection shape.

$$e_x(y, z) = e_{0s} \times \cos\left(\frac{n \cdot \pi \cdot z}{b}\right), \quad e_{0s} = \frac{y}{50} \tag{3-2}$$

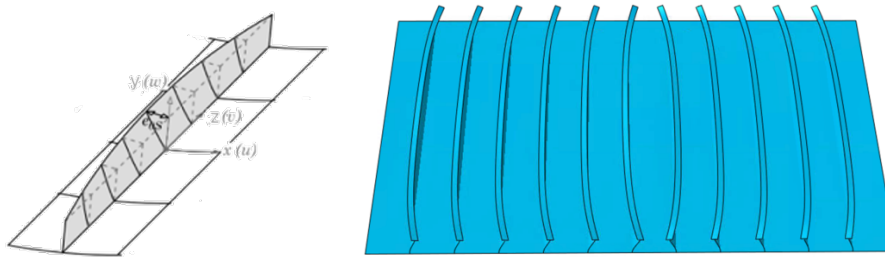


Figure 3:3 Left: Imperfection in one stiffener [26] Right: imperfection in all stiffeners

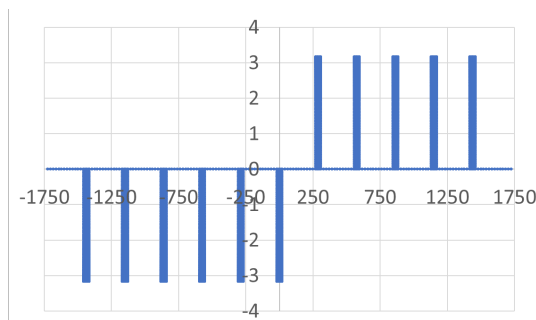


Figure 3:4 Stiffeners imperfection in transverse direction

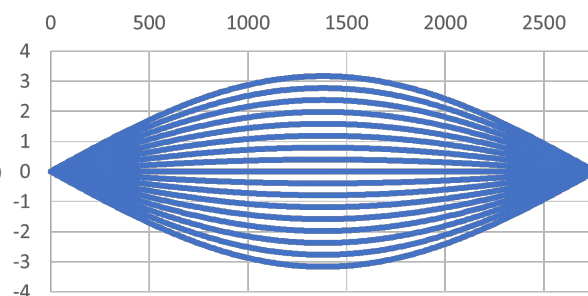


Figure 3:5 Stiffeners imperfection in longitudinal direction

- **Global Imperfection**

This type of deformation occurs generally when the stiffeners have low inertia (overall buckling mode). The modeling of global imperfections is given by:

$$e_x(y, z) = e_{0s} \times \cos\left(\frac{m \cdot \pi \cdot x}{b}\right) \times \cos\left(\frac{n \cdot \pi \cdot y}{a}\right), \quad e_{0s} = \min\left(\frac{a}{400}, \frac{b}{400}\right) \tag{3-3}$$

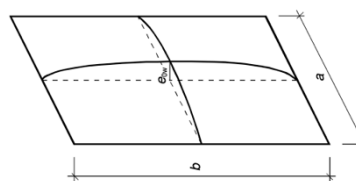


Figure 3:6 Global imperfection mode in panels [26]

In the design of stiffened plates, the current EN1993-1-5 considers that for certain geometries the behavior is column-like, for certain other geometries, the behavior is plate-like, while for the remaining geometries, the behavior is in between the plate-like and column-like behavior modes. The behavior is to be called pure column-like when the whole model behaves as a compressed column. The given criteria as initial global imperfection in the annex C5 of EN1993-1-5 is more representative of the plate-like buckling Figure 3-7 B. However, for the case of the column-like behavior of the plates, deformation is more like a half sin wave in the longitudinal direction [30].

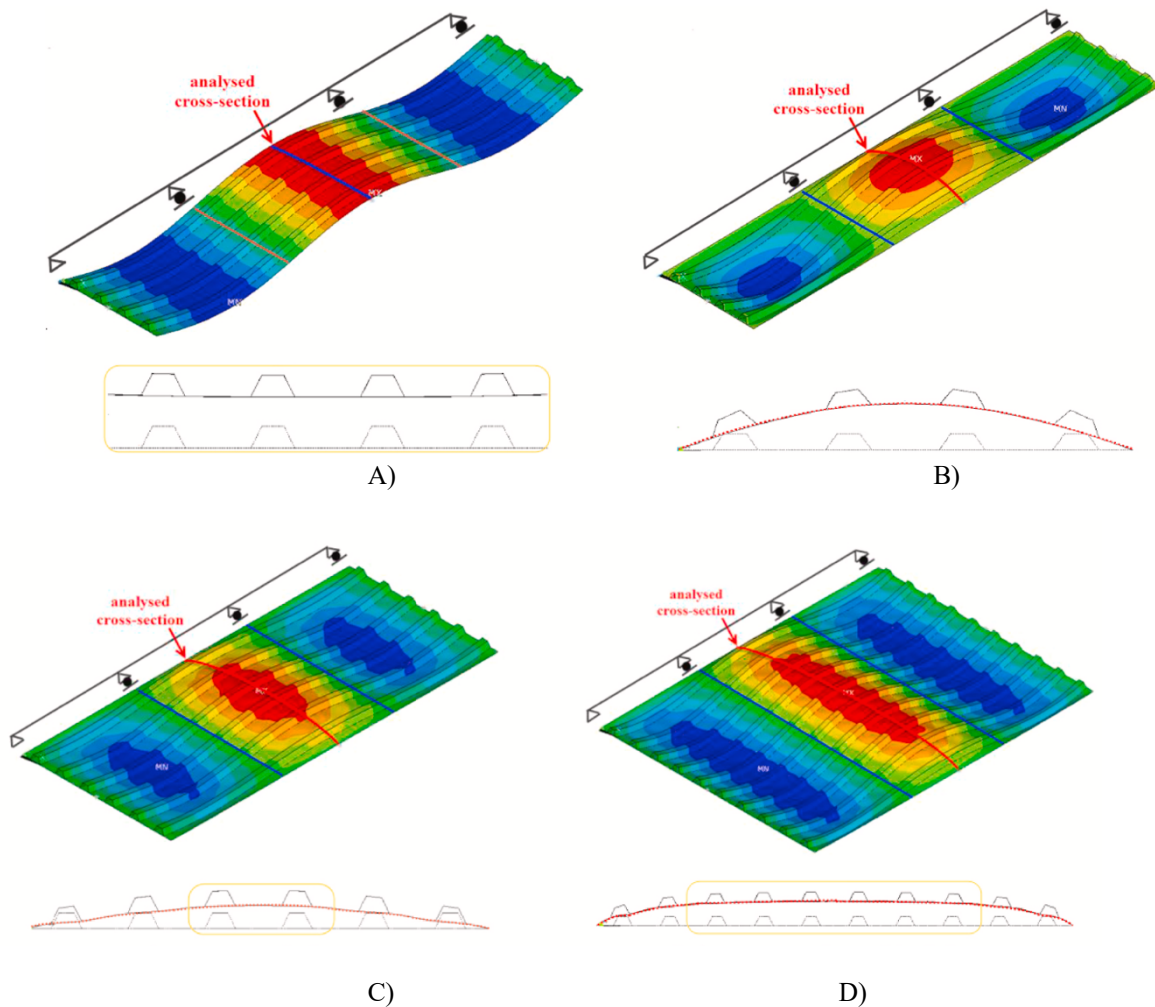


Figure 3:7 A) Pure column-like buckling behavior, B) plate-like buckling behavior, C) Interaction behavior, D) Dominant column-like behavior [30]

With the supports at the longitudinal edges, the behavior can never exactly reach the pure column-like behavior, thus, this behavior could be called dominantly column-like behavior Figure 3-7 D. In practice, the pure column-like buckling will be observed after a certain transition length along the width of the plate.

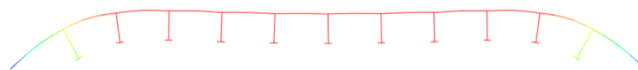


Figure 3:8 Dominant column-like buckling plate side.



Figure 3:9 Dominant column-like buckling stiffeners side.

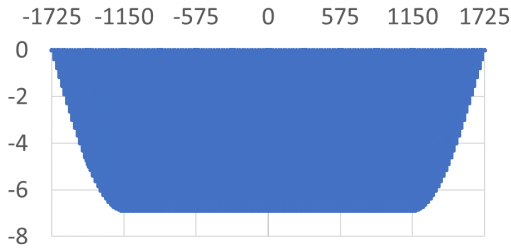


Figure 3:10 Global imperfection node file transverse direction longitudinal direction

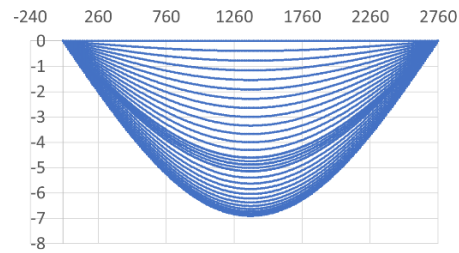


Figure 3:11 Global deflection node file in longitudinal direction

Since the failure behavior of the studied stiffened plates is pure column-like buckling (dominant column-like buckling), the global initial imperfection is defined as only a half-sine wave in the longitudinal direction. Allowance has been made for the transition length, and this has been equal to the width of two subpanels. In the transition length, imperfection increases from zero at the longitudinal edges to the maximum initial imperfection of $\min(a, b)/400$ at the second side stiffeners.

• **Local imperfections**

Local imperfection is defined on a subpanel that corresponds to the part of the panel between stiffeners as represented in Figure 3-12. The local initial imperfections which are a function of the number of stiffeners are given by equations 3-4.

$$e_x(y, z) = e_{0s} \times \cos\left(\frac{m \cdot \pi \cdot z}{b_i}\right) \times \cos\left(\frac{m \cdot \pi \cdot y}{a_i}\right), \quad e_{0s} = \min\left(\frac{a}{200}, \frac{b_i}{200}\right) \tag{3-4}$$

$$b_i = \frac{b}{n_s + 1}$$

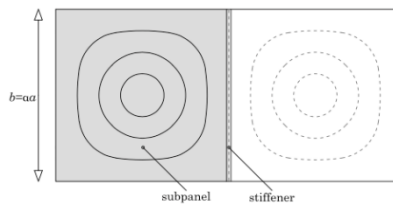


Figure 3:12 Local imperfection in subpanels

The number of half-waves is different for each panel, and it depends on the number of longitudinal stiffeners. The methodology for defining the number of half-sine waves in the longitudinal direction involves having local half-sin waves close to the number of local half-sin waves in the transverse direction. When the number of half-sin waves in the longitudinal direction includes a fraction, the two closest integer number of longitudinal half sin-waves are considered.

$$n_i = \text{int}\left(\frac{a}{b_i}\right) - 1 \quad n_j = \text{int}\left(\frac{a}{b_i}\right) + 1 \tag{3-5}$$

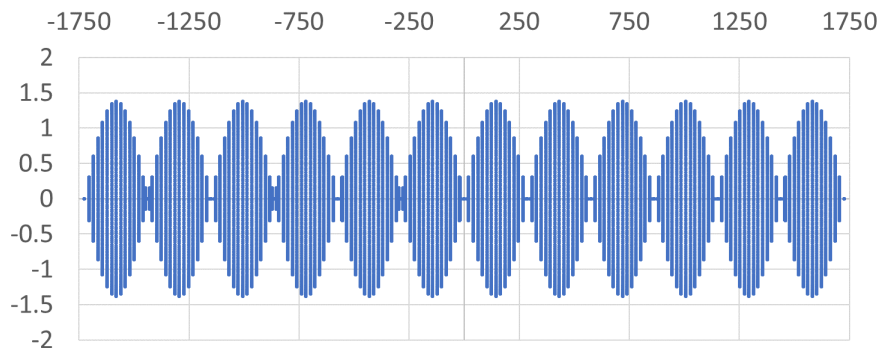


Figure 3:13 Local imperfection node file in the transverse direction

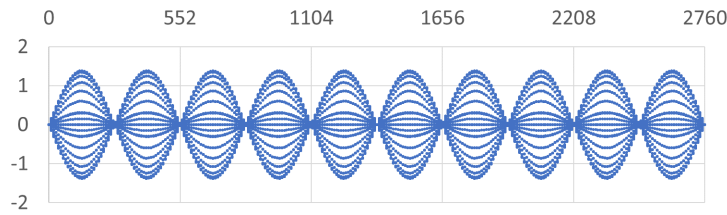


Figure 3:14 Local imperfection node file in the longitudinal direction with 10 half-sine waves

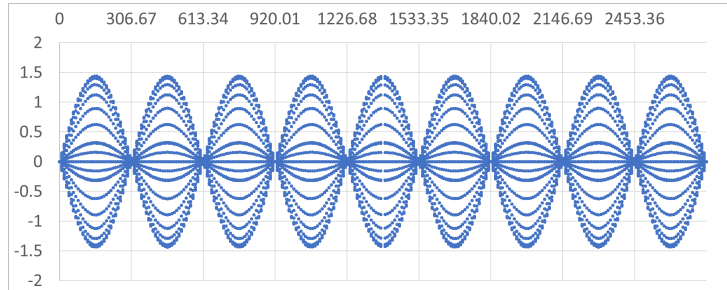


Figure 3:15 Local imperfection node file in the longitudinal direction with 9 half-sine waves

For each plate twenty-three different types of imperfection and combination are defined, including the global imperfection and local imperfection with different lengths of the half sin waves in the longitudinal direction. The combinations of initial imperfections is shown in Table3-2 . Results of the analysis of each plate is presented for each combination of initial imperfections is presented in the annex I of the report.

Imperfection code	Imperfection type
combination1	global mode with magnitude of $-\min(a,b)/400$. (IP_g)
combination2	global mode with magnitude of $\min(a,b)/400$. (IP_g)
combination3	local i longitudinal sin waves with a magnitude of $\min(a_i,b_i)/200$. (IP_{i-i})
combination4	local i longitudinal sin waves with a magnitude of $-\min(a_i,b_i)/200$. (IP_{i-i})
combination5	local j longitudinal sin waves with a magnitude of $\min(a,b)/200$. (IP_{i-j})
combination6	local j longitudinal sin waves with a magnitude of $-\min(a,b)/200$. (IP_{i-j})
combination7	longitudinal stiffeners with a magnitude of $h/50$ following the form of global imperfection (IP_s)
combination8	$-IP_g + 0.7 IP_s + 0.7 IP_{i-j}$
combination9	$-IP_g + 0.7 IP_{i-j}$
combination10	$-IP_g + 0.7 IP_s - 0.7 IP_{i-j}$
combination11	$-IP_g - 0.7 IP_{i-j}$
combination12	$-IP_g + 0.7 IP_s + 0.7 IP_{i-i}$
combination13	$-IP_g + 0.7 IP_{i-i}$
combination14	$-IP_g + 0.7 IP_s - 0.7 IP_{i-i}$
combination15	$-IP_g - 0.7 IP_{i-i}$
combination16	$IP_g - 0.7 IP_s + 0.7 IP_{i-j}$
combination17	$IP_g - 0.7 IP_{i-j}$
combination18	$IP_g - 0.7 IP_s + 0.7 IP_{i-j}$
combination19	$IP_g + 0.7 IP_{i-j}$
Combination20	$IP_g - 0.7 IP_s - 0.7 IP_{i-i}$
Combination21	$IP_g - 0.7 IP_{i-i}$
Combination22	$IP_g - 0.7 IP_s + 0.7 IP_{i-i}$
Combination23	$IP_g + 0.7 IP_{i-i}$

Table 3-2 Combination of the initial imperfection

3.2.3 Analysis type and evaluation strategy

Two types of analysis are performed on the structures:

Linear elastic analysis (LEA) to determine whether the loading and boundary conditions do not impose deformation in the structure. The LEA analysis has been evaluated by controlling the stress in the panel. In this analysis, no stress deviation in the panel should be caused. Geometrical and material nonlinear analysis (GMNIA) to determine the resistance of the panels and stress in the panels during loading.

The structural resistance can be determined by the evaluation of the calculated load-deformation path by taking the lowest resistance from the following two criteria[28]:

C1) The maximum load level of the computed load-deflection path (maximum load limit).

C2) The largest tolerable deformation or strain, in cases where this happens during the loading path before reaching the limit load. The recommended limiting value of the principal membrane strain is 0.05. this criterion is also relevant for panels in compression. [23]

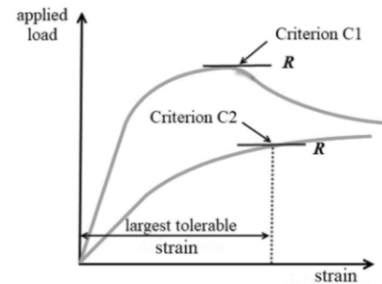


Figure 3:16 Evaluation strategy for ultimate resistance [28]

3.3 Solving method

The ultimate resistance is considered as the maximum load factor on the load-deformation curve, obtained by the arc-length Riks method, which is particularly suitable for numerical problems where non-linear static equilibrium solutions are sought with descending load level and/or displacement along the loading path.

3.4 Boundary condition

In the analysis of the built-up section including the longitudinal stiffeners, support and boundary conditions should be defined with extra care. To prevent additional eccentricity to the structure which will influence the failure mode and the structural behavior.

As shown in Figure3-17, the model has vertical support on four edges of the plate sheet. One support in the transverse direction is applied in the middle of the loaded edge to prevent the rigid body motion in the transverse direction. Two supports in the longitudinal direction are applied to prevent in-plane rotation and rigid body motion in the longitudinal direction. By defining an equation constrain between as equation 3-6 the edge nodes of the plate sheet and a reference point in the middle of it, the relative displacements between the points of the edge are prevented. In the other words, the nodes in the loaded edges of the plate sheet are constrained to move uniformly in the longitudinal direction.

The ability of the loaded edge to deform freely in the longitudinal direction has an influence on the ultimate resistance. In practice, the plate is always part of a structure; therefore, a constraint that maintains uniform stress introduction aligns better with reality. This constrain can be implemented in the model either by applying a load as a displacement, defining an equation constraint, or by specifying a rigid body constraint between the loaded edge and a reference point in the center of the mass. In terms of the resistance and the behavior of a single plate prone to column-like buckling failure, the introduction of edge equation constrain shows better compatibility with analytical results in terms of resistance and the longitudinal stress in the plate.

$$DOF_{u3,global,nodes} - DOF_{u3,global,reference\ point} = 0 \quad (3-6)$$

The load is applied as a shell edge load in a way to ensure a constant stress introduction in all elements of the stiffened plate. If the stiffened plate elements have different thicknesses, it is important to have a shell edge load that causes equal stress introduction in all parts of the panel, following equation 3-7.

$$\frac{F_i}{t_i} = \frac{F_j}{t_j} = \sigma \tag{3-7}$$

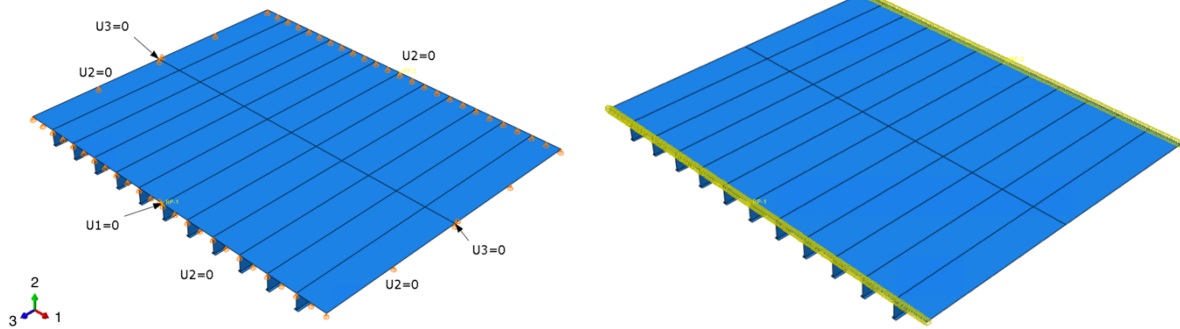


Figure 3:17 Boundary condition for plate with support in all direction

3.5 Validation of the model

Validation is comparing the obtained result with the experimental data or known accurate numerical model. In this study, two validations have been performed both for single unstiffened plate and the stiffened plate with the boundary conditions outlined in part 3-4.

The model is validated for the unstiffened plate regarding the resistance and buckling stress. The reference for the validation is the book ‘Design of Steel Plated Structures with Finite Elements’ [31]. The configuration of the plate is as follows:

$b=1200 \text{ mm}, a=1000\text{mm}, t_p=12 \text{ mm}, f_y=355 \text{ N/mm}^2, \sigma_{Ed}=100 \text{ N/mm}^2.$

The first global mode from eigenmodes was selected as the initial imperfection, with an amplitude of $\min(a/400; b/400)$, to be applied on the model. Comparison between the obtained result with the reference is presented in Table 3-3.

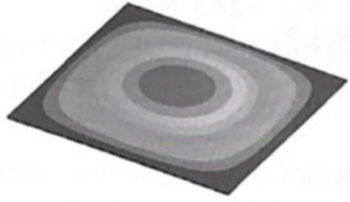
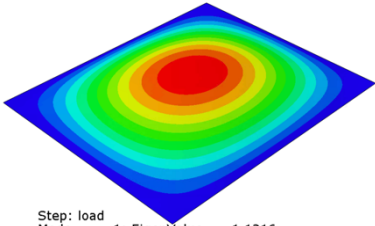
	<i>Design of Steel Plated Structures with Finite Elements’ [31]</i>	<i>Own FEM analysis</i>	<i>differences</i>
<i>First buckling mode</i>	 Mode 1 – $\alpha_{cr,1} = 1.12$ (EBPlate $\alpha_{cr,1} = 1.13$)	 Step: load Mode 1: EigenValue = 1.1216	0%
<i>Resistance</i>	177.25 MPa	178.60	+0.76%

Table 3-3 Validation of the model for unstiffened plate

Validation of the stiffened plated has been performed by using configuration of the model used by Tran [32]. The direction of the applied initial imperfection is towards the plate side and has the shape of first global buckling mode. The stiffened panels included 8 equally spaced flat stiffeners. The load is applied as shell edge load causing a uniform stress distribution equal to 100 MPa in the whole plate. Comparison between the obtained result with the reference is presented in Table 3-5.

with $t_s=16 \text{ mm}, h_s=150 \text{ mm}, t_p=12 \text{ mm}, b=4800\text{mm}, \sigma_{Ed}=100 \text{ N/mm}^2.$



Figure 3:18 Configuration of the stiffened plate for validation of the model

Aspect ratio	Resistance Tran [32]	Resistance Own FEM analysis	Difference
0.5	16.9	17.13	1.36
1	8.2	8.33	1.58
1.5	7.7	7.61	-1.16

Table 3-4 Validation of the model for stiffened plate

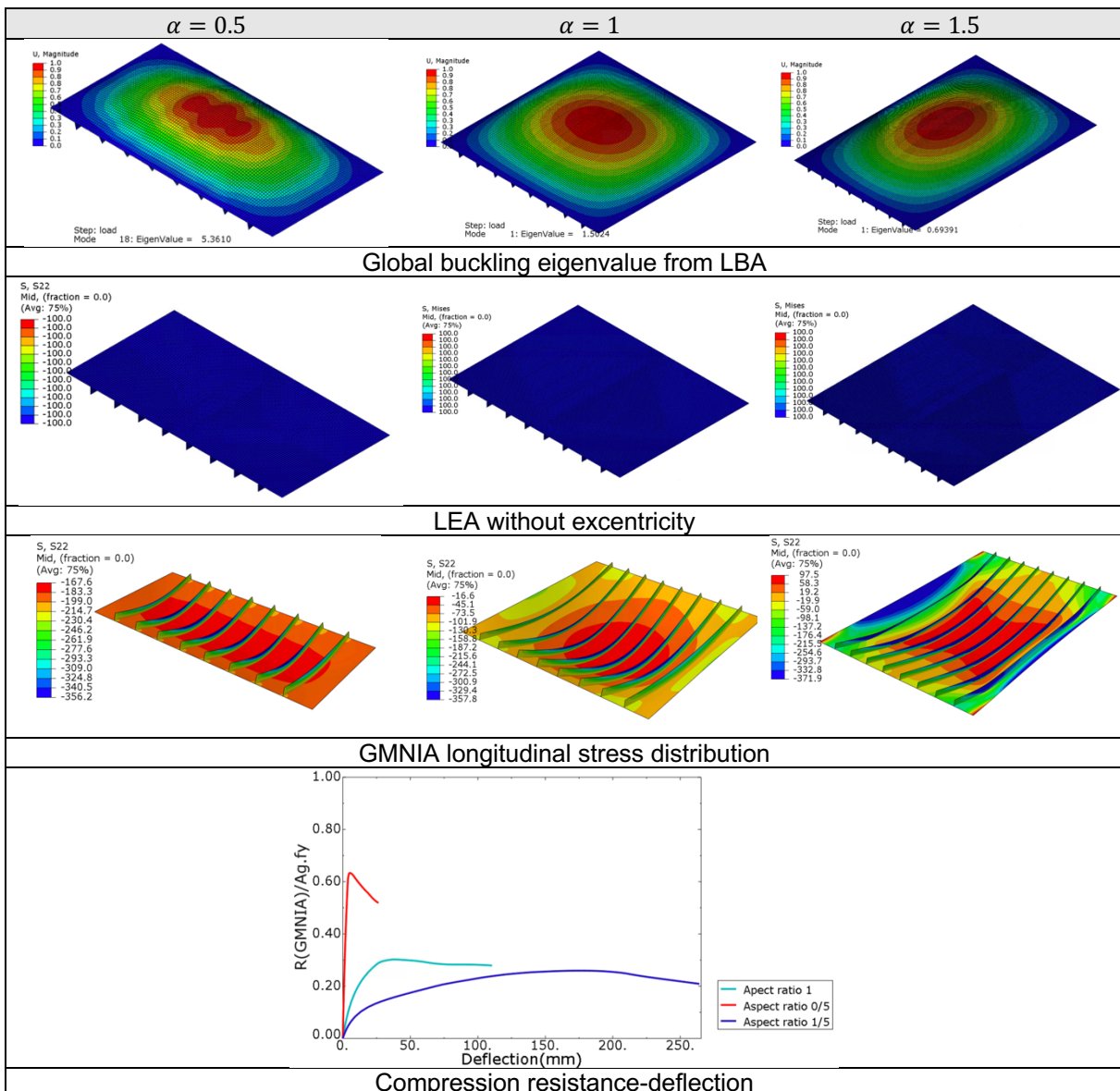


Table 3-5 Results of LBA, LEA and GMNIA analysis.

Model is validated for the stiffened plate with three different aspect ratio. Aspect ratio 0.5 present the pure column like buckling, aspect ratio 1 present the interaction of column-like and plate-like buckling and aspect ratio 1.5 present the pure plate-like buckling.

The model does not include any eccentricity from loading condition as it is clear from the stress pattern in the linear elastic analysis. It can accurately determine the resistance comparing to the resistance determined by the reference and is able to capture differences between stress distribution in plate-like buckling and column-like buckling and the interaction buckling.

3.6 Mesh

For model discretization, four-node shell elements with reduced integration (S4R) are utilized, featuring a mesh size of approximately 25 x 25 mm. The Simpson method is employed for integration along the thickness, and all shell elements are defined having 7 integration points along the thickness. The mesh elements are quadratic linear elements, and the reduced integration technique is employed in shell definition. This method of integration reduces computational effort for the assembly of system matrices and enhance the accuracy of finite element results.

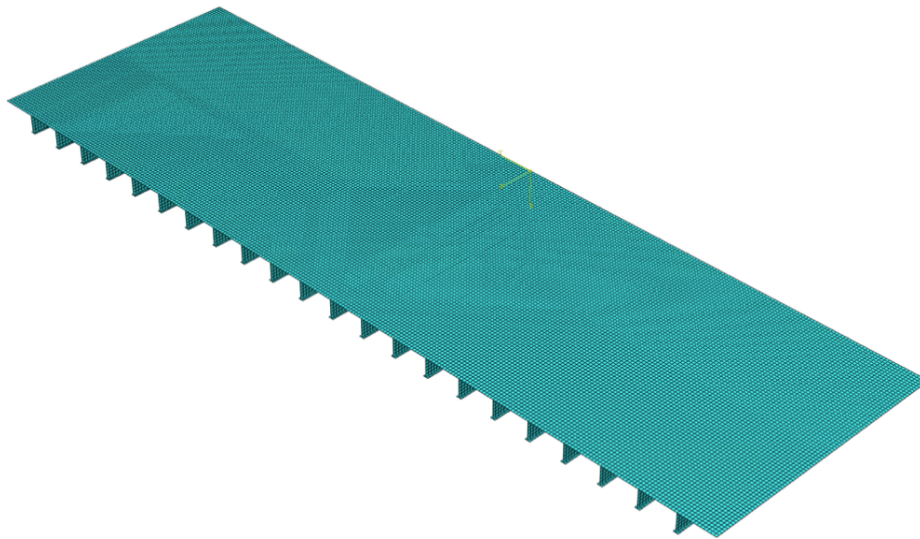


Figure 3:19 FEM mesh in model number 3

3.7 Verification of the model

Verification checks and the sensitivity analysis of the model to the discretization prove the correct application of the numerical model and analysis. In this study verification control has been performed by using finer mesh elements.

Verification control has been performed by controlling.

- a) Discretization error checks
- b) Sensitivity checks of the input parameters and mesh size.

A mesh density corresponding with less than a 5% difference within the obtained result compared to the larger mesh, generally provides a good approximation of the results [23]. The mesh size equal to 25 mm was found to be an equal mesh size based on the sensitivity analysis results, as shown in table 3-6.

Mesh size	50	25	10
Ultimate resistance	100%	99.64%	99.4%
deflection	100%	99.04%	98.1%

Table 3-6 Mesh sensitivity analysis

4

Elastoplastic behavior of stiffened panels with pure column-like buckling failure

To obtain an indication of the stress pattern in wide stiffened panels with an aspect ratio lower than 1, prone to buckling failure in the form of pure column-like buckling, GMNIA analysis of five panels has been performed. Column-like buckling failure is the common buckling mode in bridge applications, as the most economical design for a bridge application is achieved when the aspect ratio of the compression panel falls within the range of 0.2 to 0.3 [10]. In this study, pure column-like buckling is of interest. Plate with aspect ratio equal to 0.19 is representative of the deck of the Haringvliet bridge buckling failure mode.

The plate configurations are considered in a way to study failure of the wide stiffened plate with relative weak stiffeners. In the end the analytical method for addressing absolute maximum compression stress in plate is introduced.

4.1 Parametric study of the elastic-plastic behavior of wide stiffened panels.

The configuration of the panel is chosen to induce pure column-like buckling failure in different stiffened plate with aspect ratios lower than 1. The original stiffeners in the Haringsvliet bridge are double-side bulb stiffeners with a height of 160 mm and a web thickness of 8 mm, as shown in Table 4-1. To use shell elements in the FEM model, these stiffeners are modeled as T-shaped stiffeners with the equivalent area and second moment of inertia.

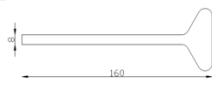

Properties	Bulb stiffener	T shape stiffener
Area(mm ²)	1710	1705.6
eccentricities(mm)	93.30	93.30
Second moment of Inertia(mm ⁴)	4440000	4455381
Dimensions(mm)		

Table 4-1 The equivalent stiffener dimension

The panels are chosen to have different aspect ratios lower than 1 while maintaining a substantial reduction factor (p_c) as the result of global buckling in form of pure column-like buckling. In the parametric study, it becomes clear that shorter panels barely experience any reduction. Subnational reduction is needed to be able to accurately address the ability of effective section properties in determining the stresses. Having aspect ratio lower than 0.5 was also of major interest. Reducing the length and keeping

the width constant for gaining lower aspect ratio will lead to have stocky plate that is fully active is resisting the compression stress. For this reason, in panels with a lower aspect ratio, the width has been increased instead of the length. The final configuration of the analyzed stiffened plates is shown in Table4-2. The plate configuration is chosen in a way that the global reduction factor from plate and column-like buckling is less than 0.85. Analytical calculation based on the EN1993-15 criteria, performed by the Python code presented in annex II, shows the chosen configurations have pure column-like buckling failure ($\xi < 0$) and reduction factor below 0.85, as presented in Table4-3

stiffened compression plate dimension

number	unloaded length (a)	width (b)	Subpanel (b _i)	plate thickness	number of stiffeners	stiffeners thickness	stiffeners height
	mm	mm	mm	mm		mm	mm
1	2760	3450	287.5	10	11	8	160
2	2070	3450	287.5	10	11	8	160
3	2760	6900	300.0	10	22	8	160
4	2070	6900	300.0	10	22	8	160
5	2192	11500	302.6	10	37	8	160

Table 4-2 Dimension of stiffened plate

Compression plate critical buckling stress

number	Relative bending stiffness $\gamma_{sl,i}$	χ_c	ρ_c	ρ	$\sigma_{cr,c}$	$\sigma_{cr,p}$	ξ	a/b	Plate resistance EN1993-1-5
					MPa	MPa			MN
1	46	0.734	0.734	1.0	880.51	854.4	-0.029	0.8	14.14
2	46	0.833	0.833	1.0	1565.30	1517	-0.031	0.6	15.92
3	22.9	0.720	0.720	0.901	845.21	545.7	-0.354	0.4	27.7
4	22.9	0.830	0.830	0.901	1502.6	545.7	-0.639	0.3	31.4
5	13.74	0.795	0.795	0.623	1247.2	197.1	-0.859	0.19	50.50

Table 4-3 Critical buckling stress based on EN1993-1-5

For the defined configurations of the panels local buckling in the subpanels and the web of stiffeners will not happen and subpanels get class 3.

Classification has been performed based on the criteria of table 5-2 EN1993-1-1. All subpanels belong to the category of inner part and the limit defined for the inner elements are used for the classification of the subpanels.

For flange sub-panels in pure compression, the criteria 4-1 should be met to have subpanels of class 3.

$$\frac{c}{t} \leq 42 \epsilon$$

(4-1)

Internal compression parts						
Class	Part subject to bending	Part subject to compression	Part subject to bending and compression			
Stress distribution in parts (compression positive)						
1	$c/t \leq 72\epsilon$	$c/t \leq 33\epsilon$	when $\alpha > 0.5$: $c/t \leq \frac{396\epsilon}{13\alpha - 1}$ when $\alpha \leq 0.5$: $c/t \leq \frac{36\epsilon}{\alpha}$			
2	$c/t \leq 83\epsilon$	$c/t \leq 38\epsilon$	when $\alpha > 0.5$: $c/t \leq \frac{456\epsilon}{13\alpha - 1}$ when $\alpha \leq 0.5$: $c/t \leq \frac{41.5\epsilon}{\alpha}$			
Stress distribution in parts (compression positive)						
3	$c/t \leq 124\epsilon$	$c/t \leq 42\epsilon$	when $\psi > -1$: $c/t \leq \frac{42\epsilon}{0.67 + 0.33\psi}$ when $\psi \leq -1$: $c/t \leq 62\alpha(1 - \psi)(-w)$			
$\epsilon = \sqrt{235/f_y}$	f_y	235	275	355	420	460
	α	1.00	0.92	0.81	0.75	0.71

Table 4-4 Internal compression part classification [33]

* $\psi \leq -1$ applies where either the compression stress $\sigma \leq f_y$ or the tensile strain $\epsilon_t > \epsilon_y/E$

4.2 Result of the GMNIA analysis

In the analysis of the plates, several imperfections and their combinations are considered. The imperfections defined for GMNIA analysis of these plates can be found in Table 3-2. The ultimate resistance result of each imperfection combination is presented in Annex I. Graphical results for three cases of the combinations of initial imperfection are presented in this chapter. They represent the results that led to the lowest resistance for cases of combination of initial imperfection, where the global imperfection direction is towards the plate side, towards the stiffeners side and in the third case, only having the global imperfection towards the plate is considered.

Positive initial imperfection is defined as having the initial global imperfection towards the plate in the combination with other local initial imperfection that leads to the lowest resistance, while negative global imperfection is defined as having the global initial imperfection in the direction of the stiffeners. The imperfection direction not only influences the ultimate resistance but also the stress pattern in the section due to the bowing effect in the middle of the section. The development of the longitudinal stress is observed in the middle of the plate, with stress being measured at the point with zero fraction ratio (middle of the plate thickness). For introducing the analytical method maximum magnitude of the compression stress in the plate sheet with minimum resistance is studied.

4.2.1 Failure behavior

Column-like buckling is determined by considering the most compressed fiber yielding, based on EN1993-1-1. Investigation of the stress reveals that at point A in Figure 4-1, the compression stress will reach the yield stress in the stiffeners. After this load step, plastic strain rapidly develops in the stiffeners of the stiffened plate. Despite the appearance of the first plastic strain, the plate is still capable of resisting the applied load. Due to material hardening and boundary conditions, the stiffened plate can reach a higher resistance, up to limit B. This extra resistance aligns with the yielding of stiffeners and development of plastic strain in them. The analysis of the stiffened panel with weak stiffeners where failure of stiffeners occurs prior to buckling of plating normally overall buckling occurs in the elastic region.

While the stiffened panel with orthotropic behavior, can sustain further loading even after overall buckling in the elastic region occurs. Their ultimate strength is eventually will reach by formation of a large yield region inside the panel and/or along the panel edges. The observation of the failure was based on the expectation. The plate failed in elastic region without any yielding in the plate sheet as it is shown in Figure 4-2 and 4-3.

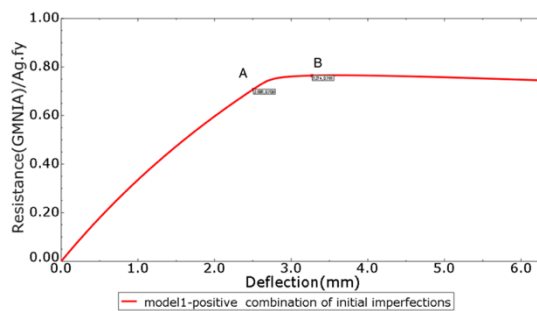


Figure 4.1 Load deflection diagram model 1 at failure

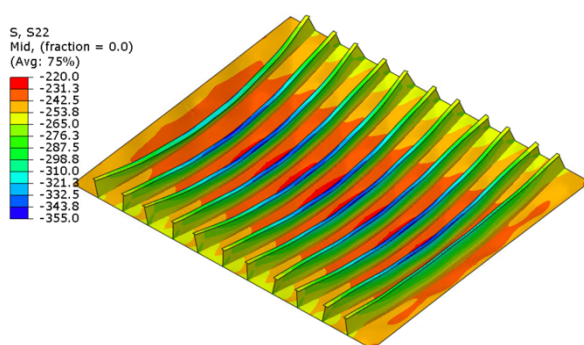


Figure 4.2 Longitudinal stress at point A

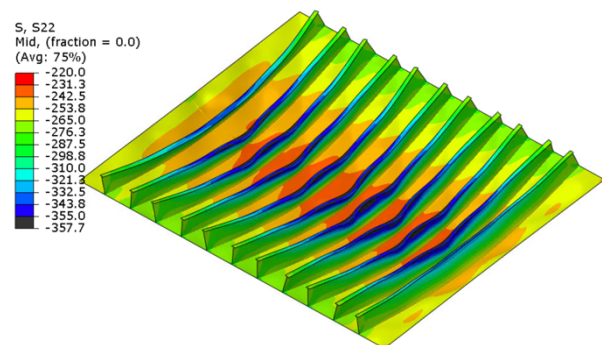


Figure 4.3 Longitudinal stress at point B

4.2.2 Resistance

The results prove that all chosen panel configurations will present failure in the form of pure column-like buckling and the configuration chosen for the panel can be used for further investigation of the panel with pure column-like buckling as the compression flange of the box girder. As it is clear from the stress and the determined ultimate resistance there does not exist any post-buckling resistance, which is one feature of the panel with pure column-like buckling failure.

There is a significant difference between the resistance depending on the direction of the initial imperfection. In general, the panel with imperfection towards the plate side which is positively named in this report leads to the lowest resistance. This conclusion regarding the direction of the initial imperfection is compatible with the result of Manco [26]. They find that in 97% of the cases in the flat stiffened panel imperfection towards the plate will lead to the lowest resistance.

Considering the edge stress equal to the yield stress in the analytical method is not compatible with the actual stress magnitude at the edges (shown in figures 4-11) when the failure is pure column like buckling. This will cause an overestimation of the resistance in the pure compressed plate with such a failure.

Considering local initial imperfection in combination with global initial imperfection in the plate with pure column like buckling, have influence on the loads level in which the first yielding will occurs.

The first kink in the load-deflection diagram takes place at the load level equal to $\chi_{c,first\ plastic} \cdot f_y \cdot A_g$. In the plate with shorter length this limit was lower than the analytical limit from EN1993-1-1. The explanation for that is the resistance and the reduction factor in analytical method is based on having initial imperfection in the form of only half sine wave in the longitudinal direction. In this study the local imperfections were also included combined with global imperfection, and the observation was that local imperfection will show effect on the plates with shorter length. Their influence was lowering the loading step in which the first plastic strain was appeared. The ultimate resistance was in all cases higher than the appearance of the first plastic strain. As the result of material hardening, the plates were able to resist higher resistance trough yielding of the stiffeners. The extra resistance that the plate gained through yielding of the stiffeners was higher in the shorter plates.

If only the ultimate resistance is of concern, it was observed that the reduction factor from GMNIA analysis is almost comparable with the column buckling factor (χ_c) from the EN1993-1-1; however, considering the edge stress equal to yield stress will cause overestimation of the resistance following EN1993-1-5 criteria. It is observable in the plate with pure column like buckling deflection of the plates is relatively low.

	Resistance EN1993-1-5	Resistance GMNIA	difference	χ_c EN1993-1-1	χ_c First plastic strain	difference	χ_c, num Ultimate resistance	difference
	MN	MN	%			%		%
model1 $\alpha = 0.8$	14.14	14.46	2.26	0.734	0.726	-1.09	0.765	4.223
model2 $\alpha = 0.6$	15.92	15.73	-1.19	0.833	0.744	-10.68	0.832	-0.120
model3 $\alpha = 0.4$	27.67	28.28	2.20	0.72	0.718	-0.28	0.748	3.889
model4 $\alpha = 0.3$	31.43	30.48	-3.02	0.83	0.752	-9.40	0.825	-0.60
model5 $\alpha = 0.19$	50.50	51.27	1.52	0.795	0.797	0.25	0.811	2.013

Table 4-5 GMNIA analysis and ultimate resistance

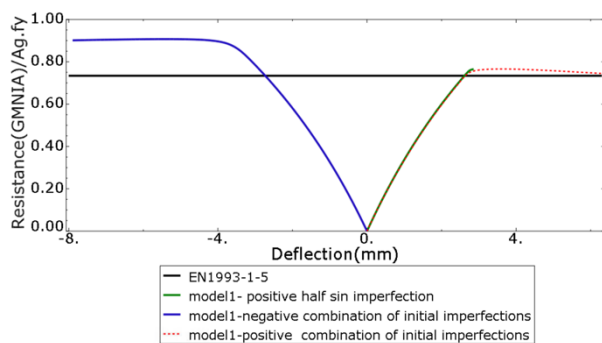


Figure 4.4 Aspect ratio 0.8 a=2760

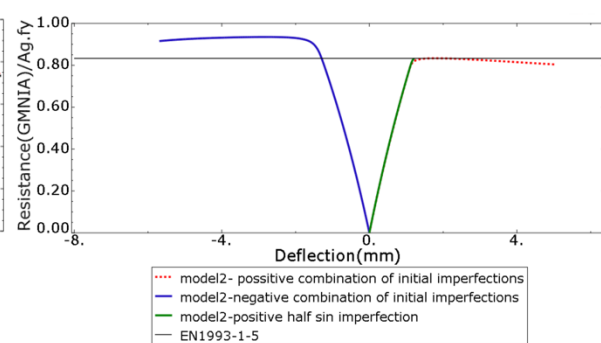


Figure 4.5 Aspect ratio 0.6 a=2070

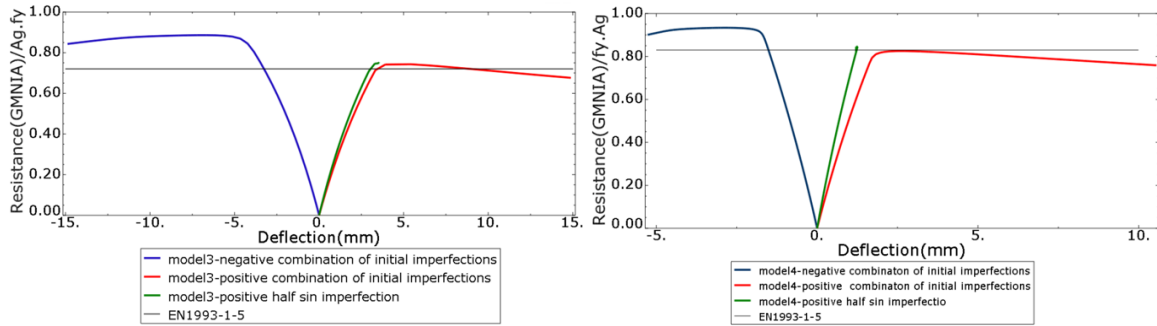


Figure 4:6 Aspect ratio 0.4 a=2760

Figure 4:7 Aspect ratio 0.3 a=2070

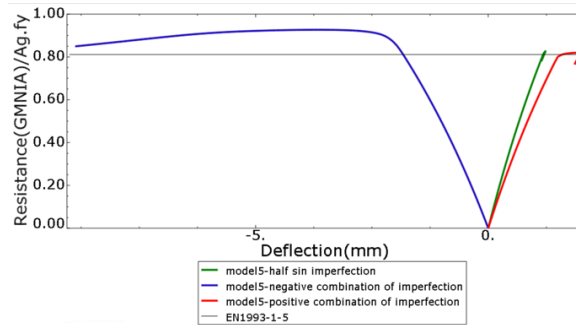


Figure 4:8 Aspect ratio 0.2 a=2192

4.2.3 Initial imperfection

In this study, several imperfections with different directions are considered for the GMNIA analysis. Comparing local, global, and bow imperfections in the stiffeners, it was observed that the global imperfection and its direction has the most significant effect on the resistance and the behavior of the stiffened plate with column-like buckling failure having relative weak stiffeners. In all cases, the combination of the initial imperfection having the contribution of the global imperfection with its direction towards the plate side, has led to the lowest resistance. Having the global initial imperfection towards the stiffeners will cause gaining resistance up to 20% higher than the analytical resistance from EN1993-1-5.

As the result of having a combination of imperfections the appearance of first plastic strain in the most compressed fiber was lower than the buckling stress limit determined from EN1993-1-1 criteria in shorter plates. However, considering the ultimate reduction factor obtained from the GMNIA analysis, resistance and reduction was comparable to the reduction factor determined from EN1993-1-1 [33] criteria. In determining the ultimate resistance considering only global imperfection in the GMNIA analysis will provide accurate enough exact resistance. As it is clear in figure 4-8, the resistance of the models with only half sin initial imperfection is very close to the ultimate resistance from the same model including global and local initial imperfections. The major influence of the local initial imperfections was observed in the model with shorter length meaning models with aspect ratio equal to 0.3 and 0.6 and the length of 2070mm.

4.2.4 Stress

Generally, the longitudinal stress in the middle of the plate sheet is lower than at the edges when the panel is bowing towards the plate side. The longitudinal stress in the middle of the plate sheet will have a higher value when the deflection of the stiffened plate is towards the stiffeners. The local deflection shows an influence on the stress pattern in most outer integration points through the thickness. Stress is studied further in the integration point in the middle of the thickness.

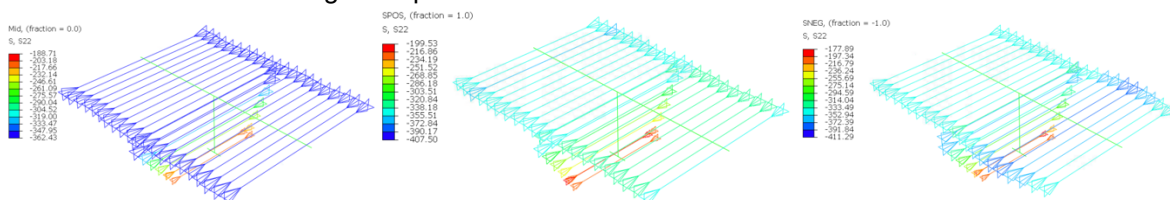


Figure 4:9 Stress in the middle strut having initial imperfection towards stiffeners

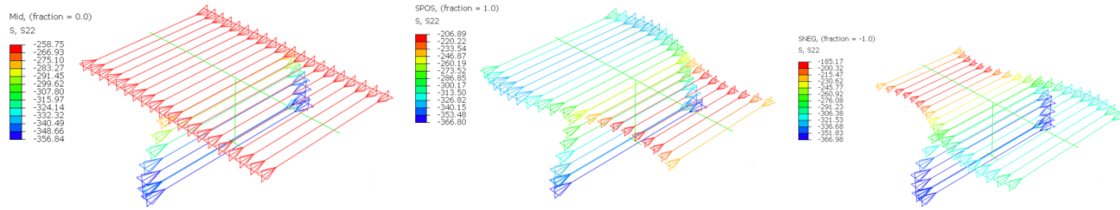


Figure 4:10 Stress in the middle strut having initial imperfection (towards plate)

In general, when the behavior is elastic the stress in the middle can be determined from equation (4.2), in which the stress resulting from an additional moment in the middle of the plate will be accounted for.

$$\sigma_{compression} = \frac{F_c}{A} + \frac{F_c \times deflection}{W} \tag{4-2}$$

The stress in the edges does not have any influence from the bowing effect, therefore it can be calculated from equation 4-3.

$$\sigma_{compression} = \frac{F_c}{A} \tag{4-3}$$

Figure 4-11 shows the development of the stress in the compressed stiffened plate sheet. Since the plate will reach minimum resistance by bowing towards the plate side, the stress in the middle will be lower. Stress in the plate sheet is more uniform in the plates with shorter length than in the plates with longer length when comparing Figure4-11, A and B to Figure B and D. All plates failed by having stress at the edges lower than the yield stress.

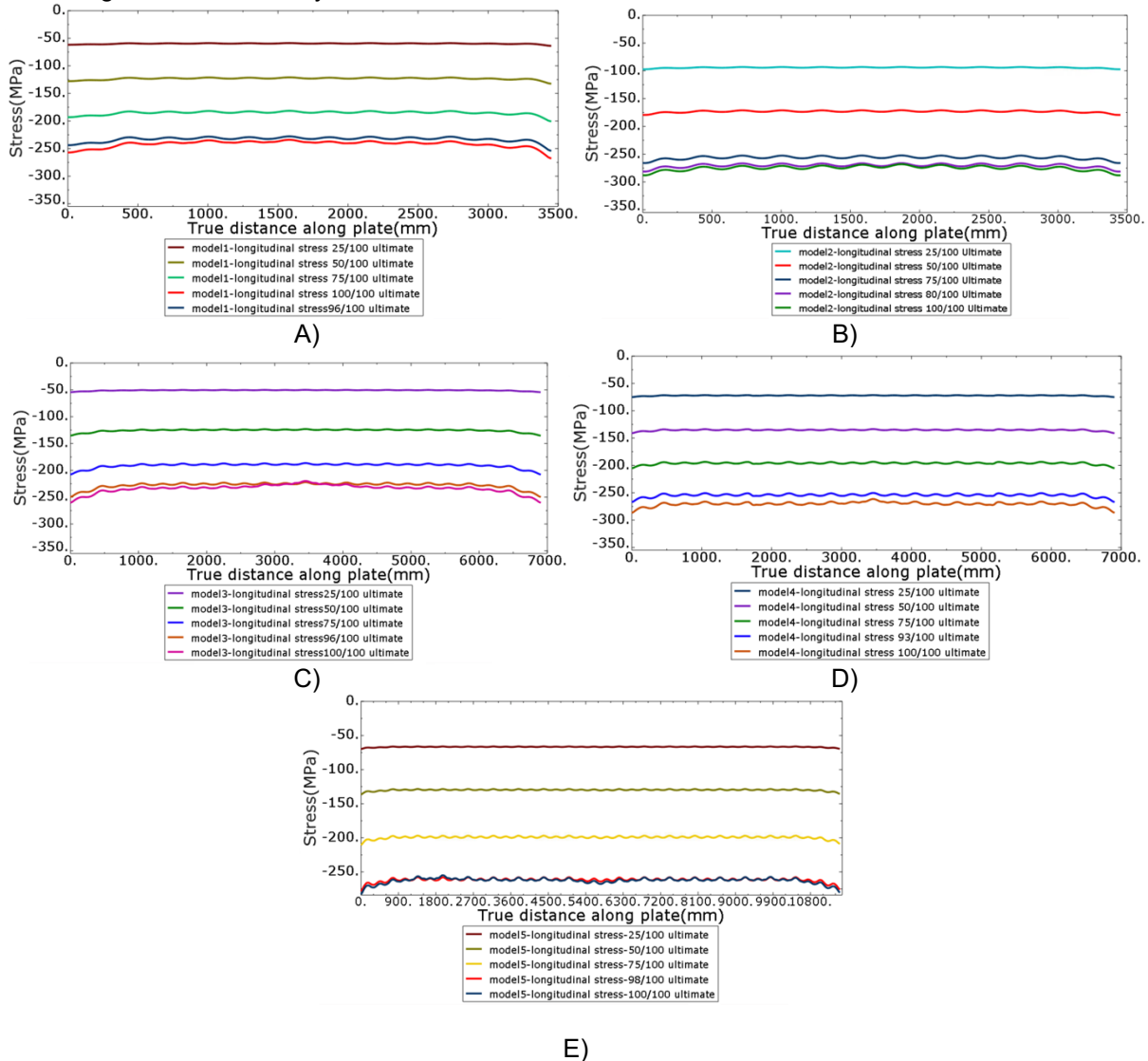


Figure 4:11 Development of the longitudinal stress from GMNIA analysis on the plate A) aspect ratio 0.8, B) aspect ratio 0.6, C) aspect ratio 0.4, D) aspect ratio 0.3 E) aspect ratio 0.2

The question to be answered was which section area is representative of the stress in equation 4-3, the gross section area or the effective section area. To answer this question, the compression stress from GMNIA analysis is derived from the FEM model. In Figure 4-12, the GMNIA compression stress is shown with the blue line. The red line represents the stress determined by dividing the applied force by the gross section area. The value of the compression stress from GMNIA analysis is comparable to the stress from the analytical method in which the gross section area is used for stress determination.

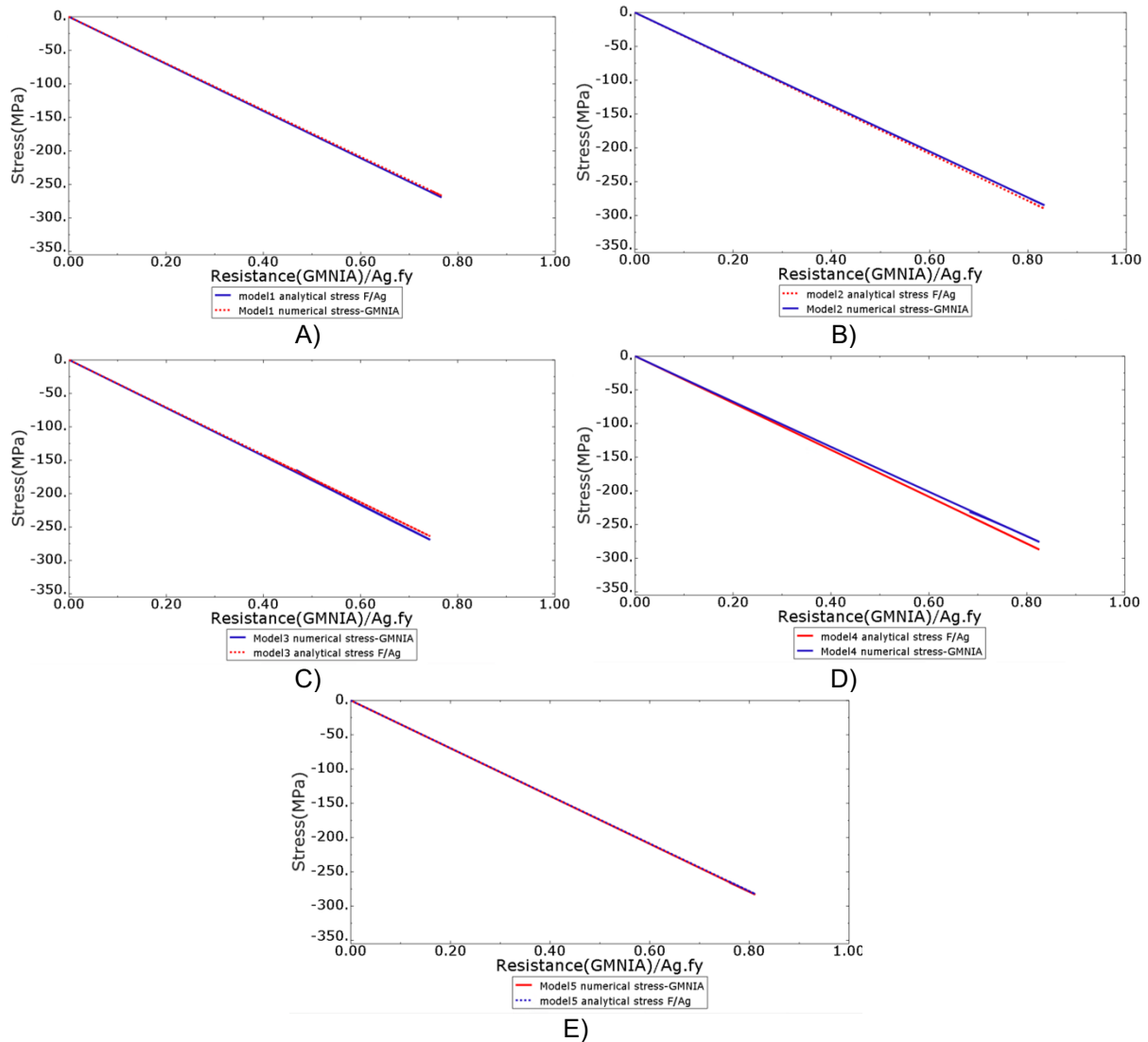


Figure 4:12 Stress from GMNIA analysis compared to stress from gross section properties A) aspect ratio 0.8, B) aspect ratio 0.6, C) aspect ratio 0.4, D) aspect ratio 0.3 E) aspect ratio 0.2

Diagram 4-12 shows that the gross section properties are representative of the maximum stress in the plate sheet. Moreover, the deflections are relatively low. It reveals that, up to column-like buckling resistance limit, the behavior of the panel is linear elastic since the increase of the stress flows a linear line and the deflections do not cause enormous second order effects.

The maximum stress magnitude at the edges is comparable to the value of $p_c \cdot f_y$ in all five plates. In Diagram 4-13, the maximum compression stress occurring at both edges of the plate at failure is plotted against the buckling reduction factor. The stress is limited to the maximum stress magnitude equal to $p_c \cdot f_y$. Since the behavior is purely column-like buckling, the edge stress did not reach the yield stress limit.

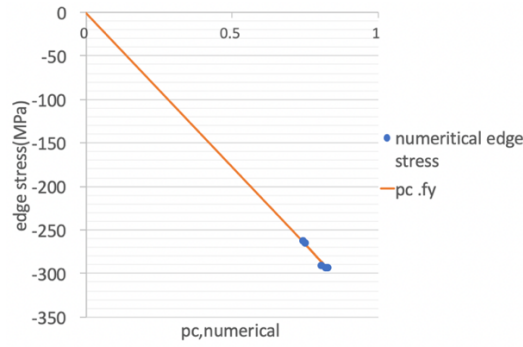


Figure 4:13 Stress at the edges

4.3 Comparing resistance with criteria of a new draft of EN1993-1-5:

4.3.1 Alternative interaction formula:

The draft of the new EN 1993-1-5 (2022) introduces an alternative method for determining the interaction behavior of the stiffened panels. For orthotropic plates with at least three identical stiffeners, the weighting factor ξ may be obtained by equation 4-4 and 4-5.

$$\xi = k_{\sigma,p} \left(\frac{a}{b}\right)^2 \frac{b_{sl,1}}{b_c} \left(\frac{1+\delta}{\gamma}\right) - 1 \quad \text{for } \psi \neq 1 \quad (4-4)$$

$$\xi = \frac{(1+(\frac{a}{b})^2)^2 - 1}{\gamma} \quad \text{for } \psi \neq 1 \text{ and } 0.5 < \frac{a}{b} < \sqrt[4]{\gamma} \quad (4-5)$$

The validity criteria for using this alternative method is not met for three of the under-studied plate configurations. However, it was still used to limit the $\frac{a}{b}$ to the minimum value of 0.5. What is markable in this method is that for panels in pure compression, the ξ factor will always be higher than zero. Therefore, the categorizing of the stiffened panels behavior in the form of pure column-like buckling is missed. ρ_c determined from the alternative method is comparable to the existing method since the ξ factor is almost zero.

	ξ	$\rho_{c,alternative}$
model1	0.0032	0.75
model2	0.0016	0.84
model3	0.0024	0.74
model4	0.0024	0.84
model5	0.0011	0.81

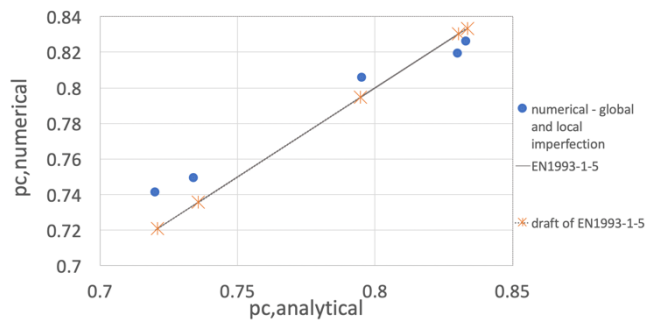


Figure 4:14 $p_{c, numerical}$ and $p_{c, analytical}$

4.3.2 Resistance

Based on the new research, the stiffness in the stiffened plates should have relative flexural rigidity higher than a specified value to be able to form a nodal buckling shape. Plates having weak longitudinal stiffeners should be considered unstiffened plates regarding their resistance to direct stresses.

In the draft of the new EN1993-1-5(2022), There is a minimum stiffness criterion defined for the longitudinal stiffener. In the draft of EN1993-1-5, it is mentioned to use the criteria of the unstiffened plate for determining the resistance of the panel with weak longitudinal stiffeners. The minimum stiffness

criteria is relative to the panel width defined, therefore having the same stiffeners, in the wider panel minimum stiffness criteria of 25 will not wile for narrower plates the criteria will be met.

$$\gamma_{sl,i}^* = \frac{E \cdot I_{sl,i}^*}{bD} > 25. \quad (4-6)$$

In which

$I_{sl,i}^*$: is the second moment of area of the stiffener for out-of-plane bending, its cross-section including a participating width of the plate of $10t_p$ on each side of each stiffener-to-plate junction.

If the relative bending stiffness of each stiffener γ^* is less than 25, the resistance of the stiffened panel may be determined from the criteria of an unstiffened panel.

For the unstiffened panel with aspect ratios lower than 1, a column type of buckling can occur, and the check should be performed on the interaction criteria between column-like and plate-like buckling to determine the final reduction factor ρ_c .

Column-like buckling stress of the unstiffened plate can be determined from equation 4-7.

$$\sigma_{cr,c} = \frac{\pi^2 E t^2}{12(1-\nu^2) a^2}, \quad \bar{\lambda}_c = \sqrt{\frac{f_y}{\sigma_{cr,c}}} \quad (4-7)$$

Plate-like buckling stress for unstiffened panels can be determined from equation 4-8. For panels in pure compression the buckling factor k_σ is equal to 4.

$$\sigma_{cr,p} = k_\sigma \frac{\pi^2 E t^2}{12(1-\nu^2) \bar{b}^2} \quad (4-8)$$

Following the criteria of the unstiffened plate for the panel with weak stiffeners, with relative stiffness lower than 25 will lead to the lower resistance determination for the panels 3,4 and 5.

number	ρ_c	ρ	χ_c	$\sigma_{cr,p}$	$\sigma_{cr,c}$	ξ	a/b	Plate resistance EN 1993-1-5
				MPa	MPa			MN
1	0.734	1.0	0.734	916.42	943.87	-0.029	0.8	14.43
2	0.833	1.0	0.833	1626	1678	-0.031	0.6	15.80
3	0.066	0.066	0.068	1.60	25.63	-0.94	0.40	2.50
4	0.066	0.066	0.011	1.60	4.14	-0.61	0.30	2.50
5	0.040	0.040	0.010	0.57	3.69	-0.84	0.19	2.52

Table 4-6 Stiffened plate resistance based on the criteria of minimum rigidity of the stiffener.

The resistance determined based on the criteria of the draft of new EN1993-1-5 is unrealistic less than the resistance based on the criteria of the current EN1993-1-5. Comparing the resistance to the resistance of the plates from GMNIA analysis in table 4-5 the same was concluded.

4.4 Summary of the result

The plates were vertically supported in four edges in this analysis, which has deviation with the assumption of the Eurocode for determining the column buckling resistance of the plate. The longitudinal support at the unloaded edges did not have a significant effect on the failure behavior of the compressed plate when the behavior was pure column-like buckling.

EN1993-1-5 assumes that the stress in the edges is equal to the yield stress, however, it was observed that the edge of the panel will get stress equal to $\rho_c f_y$. The assumption of reaching yield stress is not valid in all cases of the plate's failure. Reaching yield stress limit at the edges of plate is one of the features of the plates with orthotropic behavior.

The column approach is often used for buckling assessment in design codes. These formulations have the advantage of being relatively simple and provide quick strength estimate. Looking at the deflection mode of the actual stiffened panel, it becomes clear that the columns approach provides the

representation of the real structural response most accurately in the cases that the length of the panel is relatively high.

The longitudinal edges are usually supported in panels; therefore, pure column-like buckling does not exist. Still, it can be observed that if the $\sigma_{cr,p}/\sigma_{cr}$ ratio is small, it can be concluded that pure column-like buckling can exist in a single panel, independent of the longitudinal boundary condition. The boundary condition will have an influence on the deflection; however, the behavior is still pure column-like buckling in terms of resistance with a significant feature of no existence of yield region in the plate sheet.

For better understanding of the behavior of the panel, always the stress pattern in which the failure takes place should be controlled in combination with the load deflection diagram.

In plates with stocky behavior having pure column like buckling, the stress pattern is almost constant, up to failure and the stress from local effects is negligible if the stiffeners are relative weak, especially for lower unity checks. A study on the pure column-like behavior of the stiffened panel showed that in 100% of cases, the direction of the global imperfection that led to the lowest resistance was in the plate direction. Comparing to the global initial imperfection, the effect of local imperfection was almost negligible in panels with a higher length. The local imperfection effect will become more visible and dominant in panels with a shorter length.

The stiffened panel with weak stiffeners where failure of stiffeners occurs prior to buckling of plating normally, overall buckling occurs in the elastic region. For determining the stress on the single panel with stocky behavior and pure column-like buckling failure using gross section properties can be representative of the absolute maximum compression stress in the plate.

5

Definition of the FEM model of steel box girders

Despite the wide application of stiffened plates in practice, relatively little is known about their true behavior, and much design work is based on small-scale experiments. To develop reliable design criteria, it is necessary to obtain a complete analytical understanding of the problem. Therefore, it is essential not only to consider factors such as geometric and material properties, imperfections, and loading conditions but also the effect of interaction between adjacent elements.

The maximum load that a plate can carry, while important for design purposes, cannot be indicative of the true behavior of the structures. Many structures may become unsatisfactory in use before the ultimate load is reached due to the violation of serviceability requirements. Therefore, a complete understanding of the behavior up to collapse is essential.

The purpose is to find how the compression stress can be determined most accurately through an analytical method. To answer this question, the location of the neutral line in the cross-section was controlled, and the maximum stress from GMNIA analysis was compared to the possible analytical method.

The analysis of the studied boxes is performed through geometric and material nonlinear properties using Abaqus. The details of the modeling, including the definition of the material, solving method, and imperfections, were discussed in part 3.

The boundary conditions and definition of meshes for the boxes are illustrated in this part of the report.

5.1 Box girders configurations

Box numbers 1 and 2, which have smaller cross-sections, are considered with unstiffened panels in the web. Box numbers 3 and 4, which have larger cross-sections, are considered to have four equally spaced stiffeners in the web of the section. Motivation for considering two types of cross section was to have also have a geometry containing longitudinal stiffeners in the web. This will be closer to the real configuration of the box girder in the bridge application.

The tension flange thickness and the web thickness of the girders are defined in three categories: A, B, and C. In each category, a specific behavior is of concern. In categories A and B, the assumption of the code that the most compressed fiber reaches the yield stress is valid; therefore, the effective width criteria are applicable for determining the resistance. In type C of the box girder, the tension flange is defined as thin enough to reach the yield stress at the tension flange in the elastic analysis. The compression flange will not reach the yield stress limit, and the stress stays below the critical buckling stress based on linear elastic analysis.

The thickness of the tension flange and the web of the girder per set of the analysis is defined in a related part.

The box girders are composed of the compression flange defined and analyzed in part 4-1. The same scaling dimension used for defining the width of the compression flange is used in defining the height of the web with reference to the Haringvliet bridge. The dimension of the girder is presented in Table 5-1.

Keeping the global deflection effect constant, all the girders are modeled with almost equal length to ensure comparable behavior on a global scale. Therefore, the girders composed of the stiffened panel with a length of 2070 mm are modeled with six transverse stiffeners (7 panels in total), and the stiffened panel with a length of 2760 mm is modeled with 4 transverse stiffeners (5 panels in total).

Model	height (b)	width (b)	transverse stiffeners distance	length of the girder
	mm	mm	mm	mm
1	1605	3450	2760	13800
2	1605	3450	2070	14490
3	3210	6900	2760	13800
4	3210	6900	2070	14490

Table 5-1 Dimension of the girders

5.2 Imperfection

The two imperfection combinations that lead to the lowest resistance, with the global initial imperfection towards the plate side and stiffeners sided in the single panel analysis, are chosen to be applied as the initial imperfection file on the compression flange of the box girders.

Figure 5-1 shows the applied initial global imperfection direction on the whole girders. The imperfection on the cross-section is defined as an external file. The imperfection in the compression flange is combined with the local imperfection that leads to the lowest resistance in the analysis of the single stiffened plate in part 4.2.

For the web, only global imperfection is considered, and the tension flange is without any imperfection defined. The imperfection that has the contribution of the global initial imperfection in the middle field of the girder towards the plate is positively named and shown in Figure 5-1. The negative imperfection is defined with a contribution of the global initial imperfection in the middle field of the compression flange towards the stiffeners side.

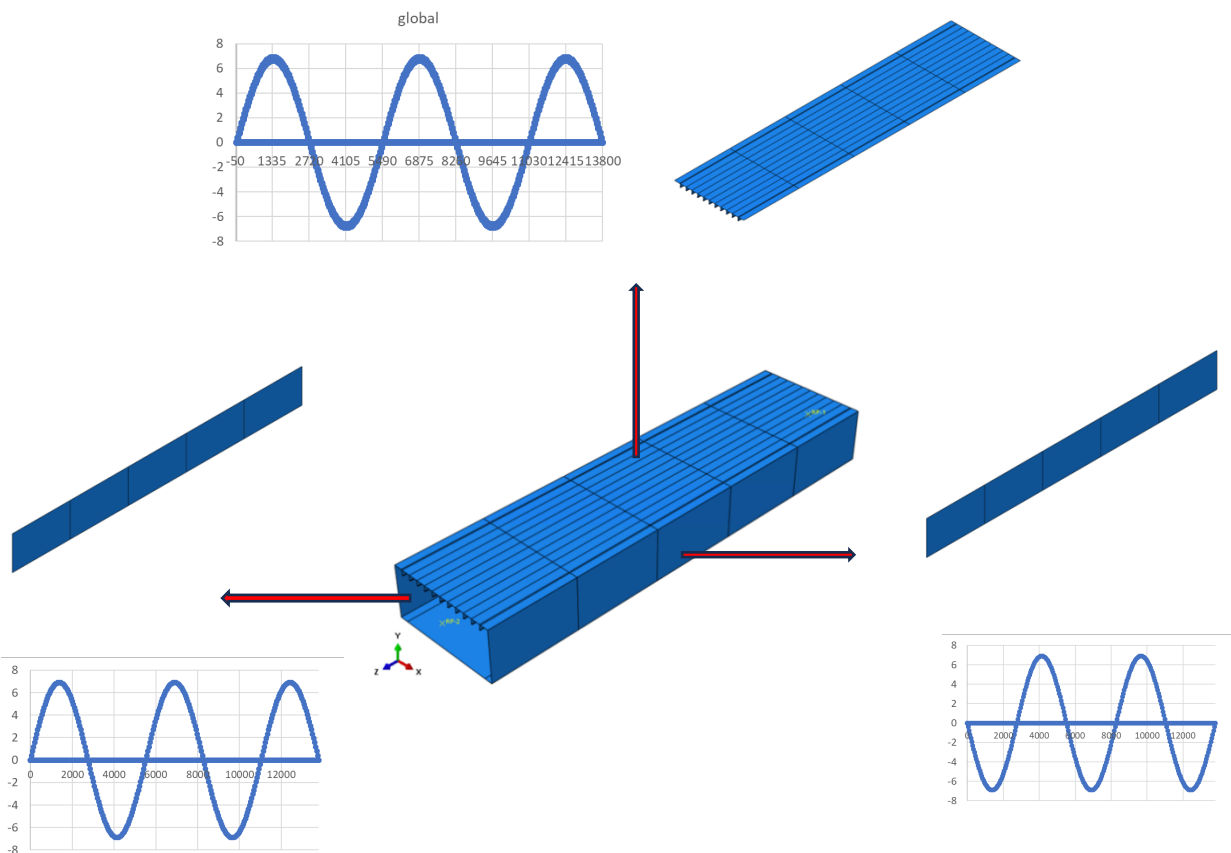


Figure 5:1 Definition of combination of positive initial imperfection

5.3 Definition of boundary conditions

The recommended solution for modeling support in the built-up section is to apply the support and load using a reference point defined at the center of mass on two sides of the girder. In this case, an extra node should be defined at the center of gravity of the cross-section, and all other nodes at the edges of the cross-section should be coupled to the defined node. Coupling can be achieved through rigid elements or constrained equations. This ensures that the end cross-section is maintained as a plane. This method of modeling the boundary supports has several advantages, including the ability to achieve a pure pinned or fixed connection. The rigid end cross-section functions as a diaphragm, meaning that possible local failures at the load introduction zone can be avoided.

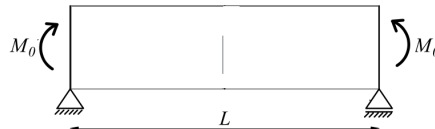


Figure 5:2 Scheme of the model

The reference points are defined in the center of gravity in two edges. Load and boundary conditions are defined on the reference points. All the edge nodes are connected by the rigid body, that relates all 6 degrees of freedom (tie) to the reference point on each side. On one side, all translational degrees of freedom are fixed, and only the rotational degree of freedom is constrained. On the other side, the same degrees of freedom are fixed, except that the translational degree of freedom in the longitudinal direction is kept free. Figure 5-3 shows the modeling of box girder number 1. The transverse stiffeners are thick enough to be sure the half-wave can be developed in the compression flange between them.

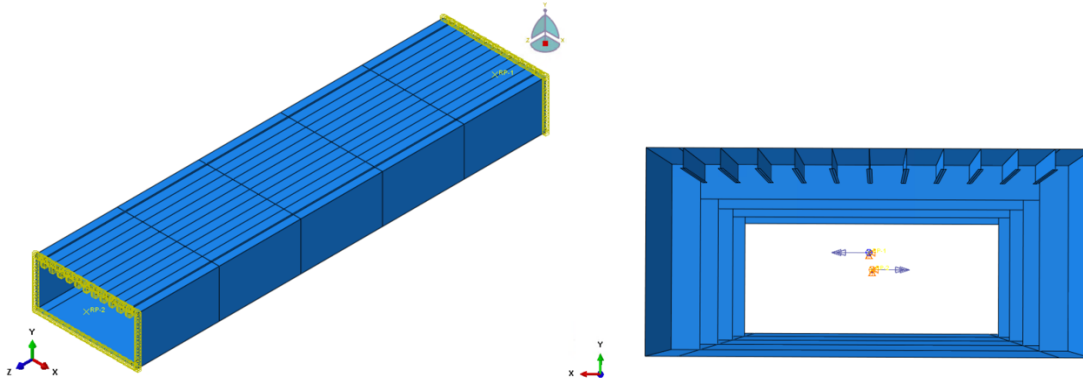


Figure 5:3 Defining the reference point and the boundary conditions on the reference point.

5.4 Transverse stiffeners

Transverse stiffeners have the same dimension in all analyses. The height of the transverse stiffeners in the compression flange is equal to 300 mm and the height of transverse stiffeners in the web is equal to 250 mm. Transverse stiffeners have the same thickness equal to 15 mm in all analyses. The tension flange is defined without transverse stiffeners.

In general, to deal with plate buckling the panels are considered as simply supported at all edges. These boundary conditions reproduce good boundary conditions of the panels in real scenarios. Besides that, these boundary conditions provide results on the safe side where a certain degree of rotational restraint exists (partially or totally clamped). It is worth mentioning that the rotational stiffness of the transverse stiffeners may influence the behavior of the compressed panel when the plate failure is pure column-like buckling. To prevent providing additional stiffness to the panel the transverse stiffeners are defined relatively with a low second moment of inertial.

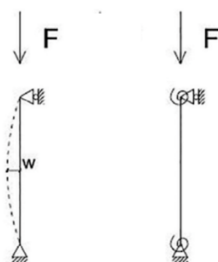


Figure 5:4 Rotation rigidity from the connection to the transverse elements in the longitudinal stiffeners

5.1 Solving method

The ultimate resistance is considered as the maximum load factor on the load-deformation curve, obtained by the arc-length Riks method, which is particularly suitable for numerical problems where non-linear static equilibrium solutions are sought with descending load level and/or displacement along the loading path.

5.2 Mesh

Quadratic four-node mesh elements with reduced integration (S4R) are employed, with a mesh size of approximately 50 x 50 mm. The integration method along the thickness is the Simpson method, and all shell elements are defined with 7 integration points along the thickness. The mesh elements are quadratic linear elements, and the reduced integration technique is used in shell definition to reduce computational effort for the assembly of system matrices and improve the accuracy of the finite element results. Verification of the model with the chosen mesh configuration is performed in part 5.2.2.

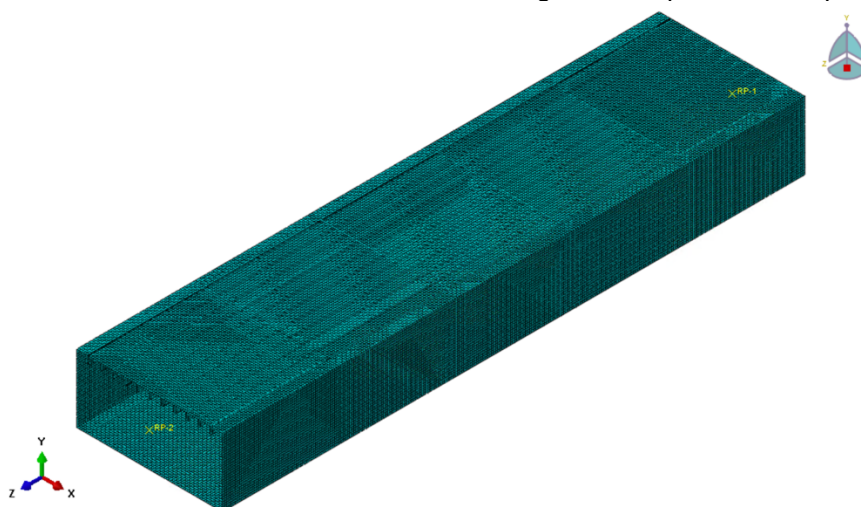


Figure 5:5 Mesh definition on the box girder

5.2.1 Validation

The used methodology for defining the boundary condition and modeling of the box girder was based on the work of Kövesdi and Ljubinković.

Kövesdi [28] suggest modeling edges of the sub models with the rigid body link between edge nodes to the master reference point, he considers the sub models of the box girder with the transverse stiffeners in the middle of the girder.

Ljubinković [34] made the simplified model of the tested box girder using the same boundary condition, he also consider the transverse stiffener as the rigid body link to the reference point.

The boundary conditions defined on the edges reference points by Ljubinković is the same as the boundary conditions defined by Kövesdi.

5.2.2 Verification

Verification checks and the sensitivity analysis of the model to the discretization prove the correct application of the numerical model and analysis. In this study verification control has been performed by using finer mesh elements.

Verification control has been performed by controlling.

- a) Discretization error checks
- b) Sensitivity checks of the input parameters and mesh size.

A mesh density corresponding with less than a 5% difference within the obtained result compared to the larger mesh, generally provides a good approximation of the results.

The mesh size of 50 mm shows less than 5% deviation.

Results of the analysis for the girder with the mesh size of 100, 50 and 25 are presented in the table 5-2. The results are normalized to the resistance and deflection of the girder with the mesh size of 100mm. considering the accuracy of the results and computation time mesh size of 50 mm provides enough accurate results.

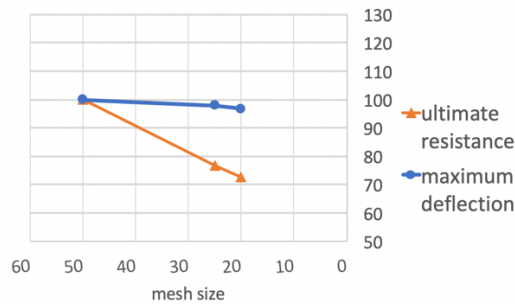


Figure 5:6 Mesh sensitivity analysis of the box girder

	100	50	25
Ultimate resistance	100	97.86	96.82
maximum deflection	100	76.88	72.69

Table 5-2 Mesh sensitivity analysis

5.3 Shear-lag effect

A rigid body is applied along the load introduction place of the model to ensure a realistic uniform stress distribution against actual loading. This definition of the load and boundary condition ensures an equivalent internal force distribution on the defined sub-model as part of the larger structure. When determining the effective cross-section properties, reductions as the result of shear lag in tension and compression regions should be considered.

By performing the linear elastic analysis, and monitoring stress in the middle of the girder, it was confirmed that the model does not exhibit nonlinear stress distribution as a result of shear lag, as shown in Figure 5-7. Since the linear elastic analysis demonstrates uniform compression and tension stress distribution in the flanges of the girder, it was justified that further reduction due to the shear lag effect in the control of the results through analytical method EN1993-1-5, is not needed.

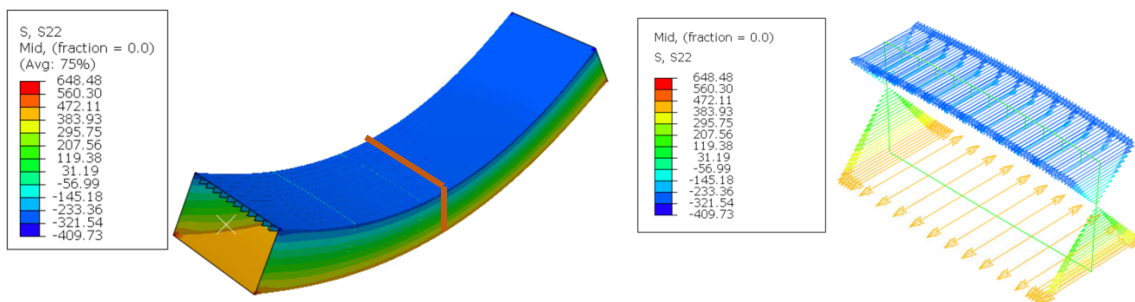


Figure 5:7 Stress distribution from LEA of the model

5.4 Point for monitoring the longitudinal stress

By focusing on the stress in the girder, it is observed that stress in the middle of the plate is depended on the deflection and second order effects as shown Figure 5-8. Since effective section properties are based on the failure modes and the maximum compression stress in the plate field where the failure happens will be at the edge of the plate, stress at the marked edges of the plated will be studied in the section6.

Choosing the point at edges will help studying stress purely as the results of plate buckling and not the second order effects in the middle of the girder.

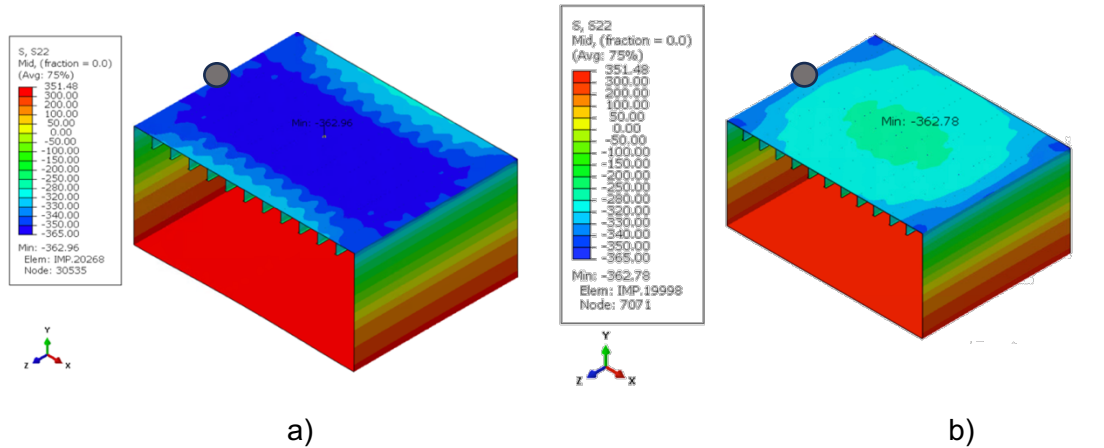


Figure 5:8 Longitudinal stress a) negative global imperfection b) positive global imperfection

6

Behavior of box girders

The methodology to deal with the buckling of the plated cross sections is to consider them as separate plates and determine the reduced area of each single plate. To be able to study interaction between connected plate parts in the flanges and in the webs, in this section the box girder as a whole is analyzed. Box girders are analyzed in three categories. All categories have the same compression flange, height and width; however, the thickness of the web and thickness of tension flange differs in set analysis A, B and C to get favorable type of failure.

The development of the stress and the position of neutral line are monitored in each analysis to find the proper analytical method addressing the maximum compression stress in the girder.

6.1 Model A

In this set of analyses, all other stability failures, such as local and overall buckling of the web in the box girder, are prevented. The reduction of the cross-section area only occurs in the compression flange, determined by the column-like buckling reduction factor using the EN1993-1-5 effective width method. The compressed part of the web is defined to have class 3 in the section with the unstiffened web. In the section with the stiffened web, by having subpanels of class 3 and ρ_c reduction factor as the combination of plate-like and column-like buckling equal to 1, as shown in Table 6-1 and 6-2, it has been ensured that there is not any instability in the web of the box girder.

The tension flange thickness is defined as thick enough to get failure in the compression flange. In other words, to be capable of reaching the yield stress limit in the compression flange while stress in the tension flange stays below the yield stress limit in the linear elastic analysis.

<i>number</i>	<i>Width</i>	<i>thickness of web</i>	<i>thickness of tension flange</i>	$\rho_c \cdot f_{y \text{ flange}}$	$\rho_{\text{local,web}}$
	mm	mm	mm	MPa	
1-a	3450	20	15	260.67	1
2-a	3450	20	20	295.71	1

Table 6-1 Box girder with the unstiffened web model 1 and 2 category A

<i>number</i>	<i>width</i>	<i>Number of web stiffeners</i>	<i>thickness of web</i>	<i>thickness of tension flange</i>	$\rho_c \cdot f_{y \text{ flange}}$	$\rho_{c\text{-web}}$	$\rho_{\text{local,web}}$
	mm		mm	mm	MPa		
3-a	6900	4	20	15	255.60	1	1
4-a	6900	4	20	20	294.65	1	1

Table 6-2 Box girder with stiffened web model 3 and 4 category A

6.1.1 Detecting failure

Detecting the location of the failure is important to correctly study the behavior of the plate as the compression flange of the girder.

To comprehend the behavior of the girder composed of the several stiffened plated elements it is important to understand the failure behavior of the single stiffened panel. From the analysis of the single isolated plate, it becomes evident that the behavior of the plate is elastic, and the failure will take place soon after reaching the yield stress in the most compressed fiber of the stiffened plate. Furthermore, it becomes clear the imperfection combinations that include the global initial imperfection towards the plate side will cause maximum compression in the longitudinal stiffeners. Therefore, the lowest resistance was obtained when the global initial imperfection was towards the plate side which caused additional moments that provided the longitudinal stiffeners with additional compression stress. The sign of failure was a negligible plastic strain in the longitudinal stiffeners.

The girders' webs have class 3 therefore the stability failure will take place only in the compression flange. The compression flange failure behavior is pure column-like buckling. By the failure of one panel, the whole box girder will fail since there is not any post-buckling reserve and redistribution of the stress. The feature of the column-like buckling is that the element will fail by gaining the yield stress in the most compressed fiber and there is not any post-buckling reserve. Figures 6-1 to 6-4 show the plastic strain in the girders cut in the middle. As it is clear from figure number 6-1 to 6-4 the development of the first plastic strain takes place exactly at the same location of the single panel i.e., in the middle of the panel in the longitudinal stiffeners.

In set one of the combinations of initial imperfection global deflection in the middle panel is defined towards the plate. This set of initial imperfections is positive named in the report and is shown in the Figure 6-1 to 6-4 left. In set two of the analysis the global initial imperfection in the middle panel is toward stiffeners. This set of initial imperfections is negative named in the report and is shown in the Figure 6-1 to 6-4 right.

In models number 1 to 3, the point of failure was in the middle of the girder and was achieved by applying positive initial imperfection. The girder has the highest bending moment as the result of the second-order effect in the middle of the section, so this observation was based on the expectation.

However, in box number 4, Figure 6-4, the point of failure was not in the middle of the panel by having positive initial imperfection but in the panel closer to the side of the girder with lower global deflection of girder. The explanation for this behavior is that the global deflection of the girder is in a favorable direction on the other side of applied initial imperfection. This global deflection has higher magnitude in the girders with wider compression flange. Interaction of the global deflection of the girder towards the stiffeners with the tendency of the plate to fail in the plating direction which is in the other side of the global deflection has caused this deviation of the behavior.

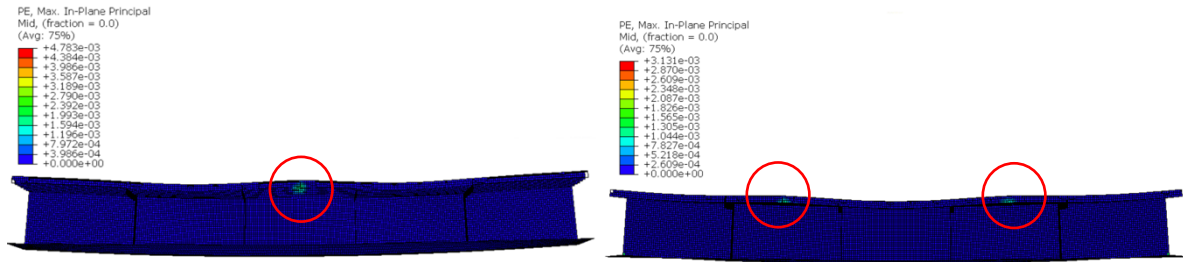


Figure 6:1 Plastic strain at failure of the box number 1 left) global deflection in the middle panel towards plate right) global deflection in the middle panel towards stiffeners

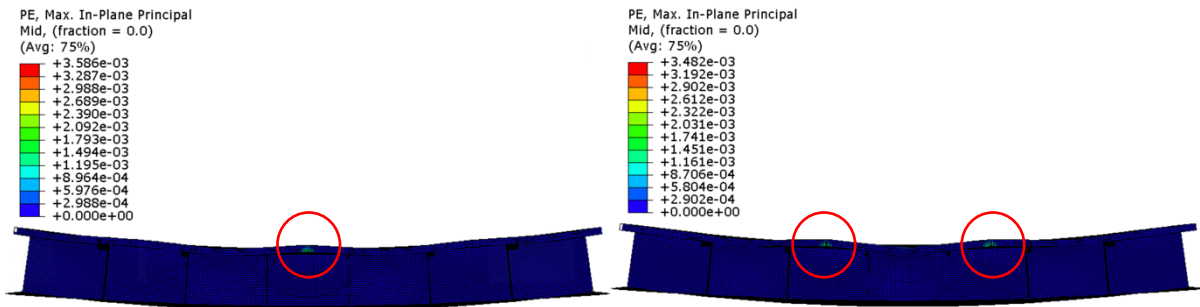


Figure 6:2 Plastic strain at failure of the box number 2 left) global deflection in the middle panel towards plate right) global deflection in the middle panel towards stiffeners

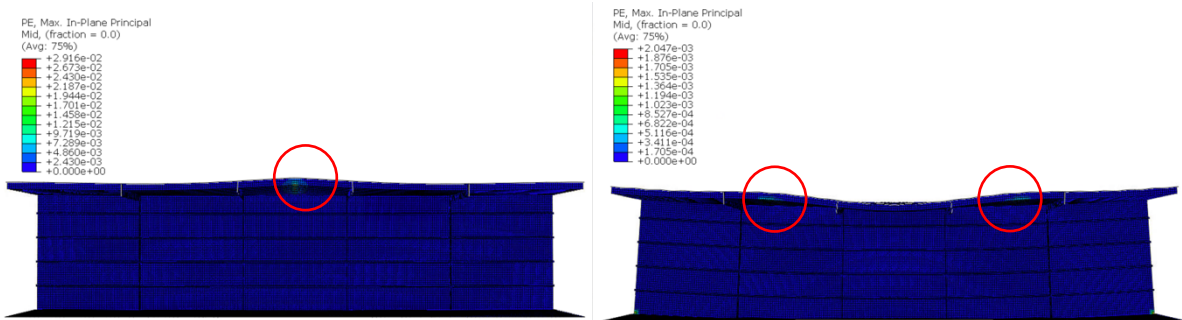


Figure 6:3 Plastic strain at failure of the box number 3 left) global deflection in the middle panel towards plate right) global deflection in the middle panel towards stiffeners

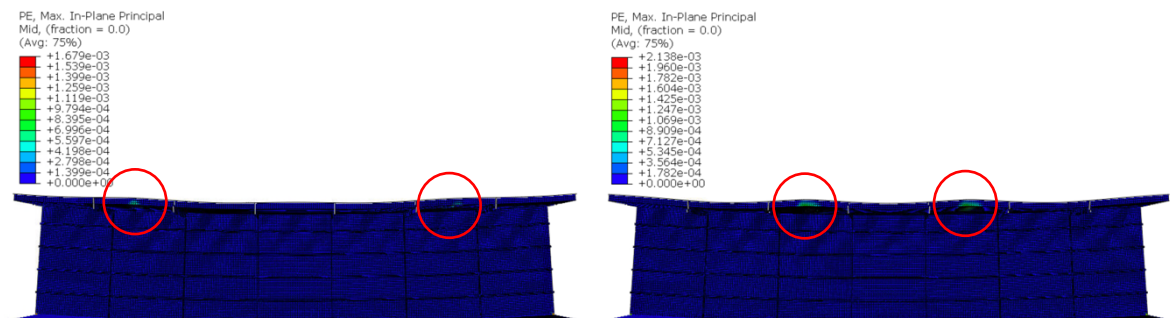


Figure 6:4 Plastic strain at failure of the box number 4 left) global deflection in the middle panel towards plate right) global deflection in the middle panel towards stiffeners

6.1.2 Resistance of the girder

In Figure 6-5, the moment-deflection diagram is plotted for the point in the middle of the girder in model numbers 1a to 3a. In model 4a, for both types of applied initial imperfections, the moment-deflection diagrams have been plotted for the failure point, meaning the middle of the second side panel for positive imperfection, and in the middle of the third side panel in the case of negative imperfection.

Model 1-a (Figure 6-5-A) is the model with a transverse span equal to 2760 mm and an aspect ratio equal to 0.8. The ratio of ξ in the compression flange is -0.029 meaning the pure column-like buckling is the dominant failure following the analytical method and the GMNIA analysis in part 4 of the report. The bending moment determined by EN 1993-1-5 criteria is also plotted for comparison. As it is clear in (Figure 6-5-A), when the compression flange begins to buckle and deflect towards the plate side i.e. the load step in which the slope of the moment deflection begins to change, the resistance from GMNIA analysis of the girders coincides with the resistance that can be determined from EN1993-1-5.

In model 2-a (Figure 6-5-B) the distance between the transverse stiffeners is less and equal to 2070 mm. The compression panel has an aspect ratio equal to 0.6 and the ξ interaction factor in the compression flange is -0.030. For box number 2 the buckling stress level is higher than the resistance from the EN1993-1 this can be the result of having global deflection in a favorable direction. In the single plate analysis, it becomes clear that the plate numbers 2 and 4 with a span length equal to 2070 mm, the resistance is more sensitive to the local initial imperfection. In the analysis of the box girders composed of this panel, it becomes clear that they also show sensitivity to the global deflection of the whole girder and are under-influenced of it. Since the deflection of the girder is in the favorable direction (toward stiffeners) the middle panel was able to resist higher bending moments.

Box number 3 (Figure 6-5-C) is the larger box compared to the girder number 1 and 2. It has four stiffeners in the web. The ξ factor is equal to -0.357 and the aspect ratio is equal to 0.4. In this girder resistance determined from the GMNIA analysis has the best combability with the resistance determined from EN1993-1-5.

Box number 4 (Figure 6-5-D) has the lowest aspect ratio equal to 0.3 with the ξ interaction factor equal to -0.84. Only in this girder, the middle field was not the critical field. The load-deflection diagram is not plotted for the middle of the girder in model 4-a but in the middle of the panels in which plastic stains appear.

As shown in Table 6-3 the ultimate resistance is higher than the resistance from the analytical method in all cases.

	<i>maximum bending resistance/Mel (EN1993-1-5)</i>	<i>bending /Mel first plastic strain (GMNIA)</i>	<i>maximum bending resistance/Mel (GMNIA)</i>	<i>Difference Maximum resistance GMNIA and EN1993-1-5 %</i>
1-a	0.863	0.854	0.937	8.57
2-a	0.881	0.987	0.994	12.03
3-a	0.849	0.851	0.878	3.42
4-a	0.895	0.915	0.957	6.93

Table 6-3 Resistance of the girders set A

Resistance that can be determined from the analytical method from EN1993-1-5 is plotted by black line in Figure 6-5. It exactly coincides with the point when the slope of the moment-deflection diagram begins to change in Figures 6-5 A and C. The behavior after this limit differs in plates depending on their aspect ratios. For the compression plate with an aspect ratio higher than 0.5, the plates showed the ability to resist more bending moment. For plates with an aspect ratio lower than 0.5, this ability was almost negligible.

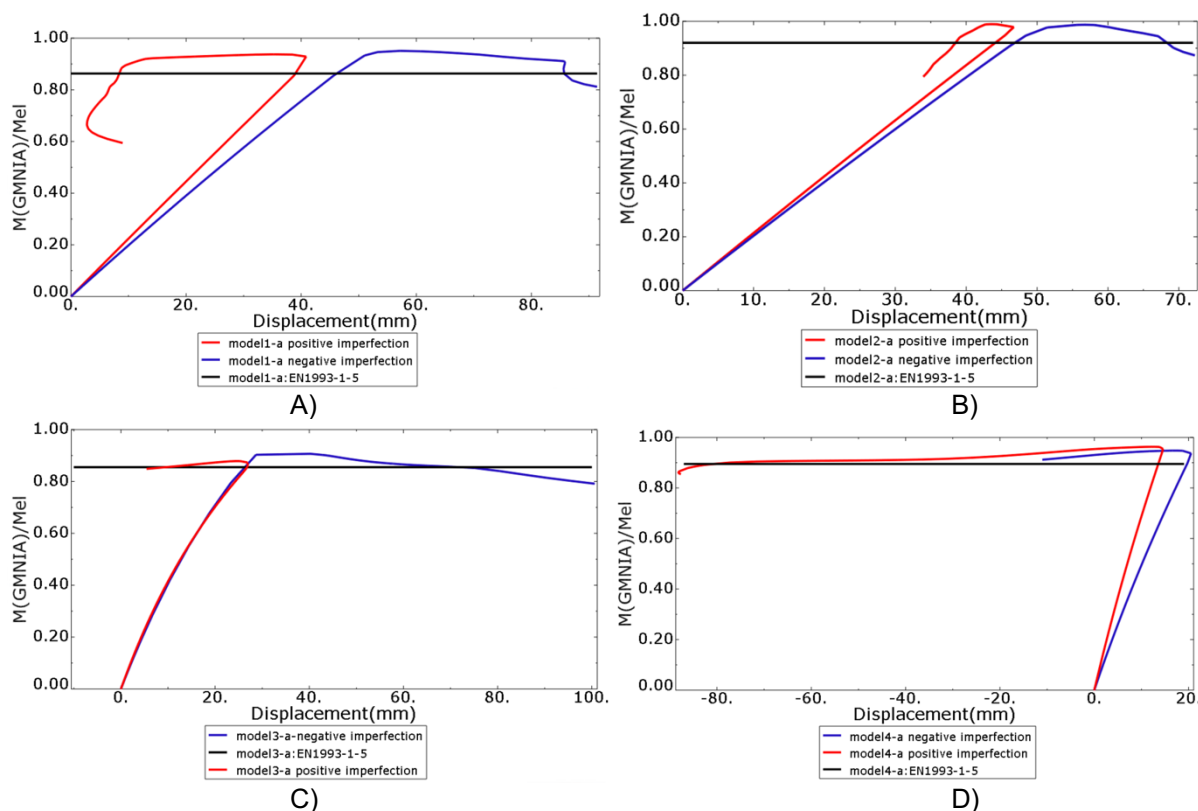


Figure 6:5 Moment deflection diagram from GMNIA analysis A) Model 1a, B) model2a, C)model3 a, D)model4a

6.1.3 Development of the stress in the flange of the girder

The behavior of girders' is studied considering in couple of points on the moment-deflection diagram to monitor the stresses in the web and the flange at the loading level in these points. In Figures 6-6A and B, from point A to C, the behavior of girder is in the elastic stage, and the compression in the flange is lower than the buckling resistance limit ($p_c.f_y$). Point D marks the end of elastic behavior and coincides with reaching the column buckling resistance in the compression flange. From point D, the behavior begins to change. Against the expectation, the stress level at which the compression flange begins to buckle was not the same as stress level at which the buckling resistance of the single compressed plate was reached. The behavior after this point was the same in models 1 and 2; however, both showed differences compared to models 3 and 4. In models 1 and 2 (Figures 6-6 A and B), the aspect ratios were 0.8 and 0.6, respectively, and the ξ was very close to zero. Up to load step D, the stress in the panel was almost uniform. From step D to E, the stress in the compression flange increased, by resisting more bending moment. From point E to F, stress suddenly is transferred to the two sides of the edges connected to the web, and ultimately, the resistance was reached when the stress in the edges reached the value close to f_y . In this region, the edge stress increased without resisting substantial bending moment. Point D coincides with the resistance determined from EN1993-1-5.

The limit between points D and F is representative of the extra bending resistance of the girder and deviation from pure column-like buckling. This additional resistance was achieved for several reasons, including the geometry of the plates i.e an ξ interaction ratio between plate and column-like buckling close to zero, rotational fixity in the connection zone of the longitudinal stiffeners to the transverse stiffeners, and, most importantly, introducing the compression stress gradient on the compression flange as the side effect of applied bending moment.

The behavior in the box number 3 and 4 (Figures 6-6-C and D) was different after reaching column buckling resistance at point D, with the previous models. They have lower aspect ratio equal to 0.4 and 0.3 and the ξ interaction ratio is closer to -1. The stress after point D stays almost unchanged meaning the cross section is not able to resist any more stress. The compression flange ultimately failed without reaching the yield stress limit. In these analyses it was again observed that the stress in the compression flange reach higher stress compared to the single compressed plate.

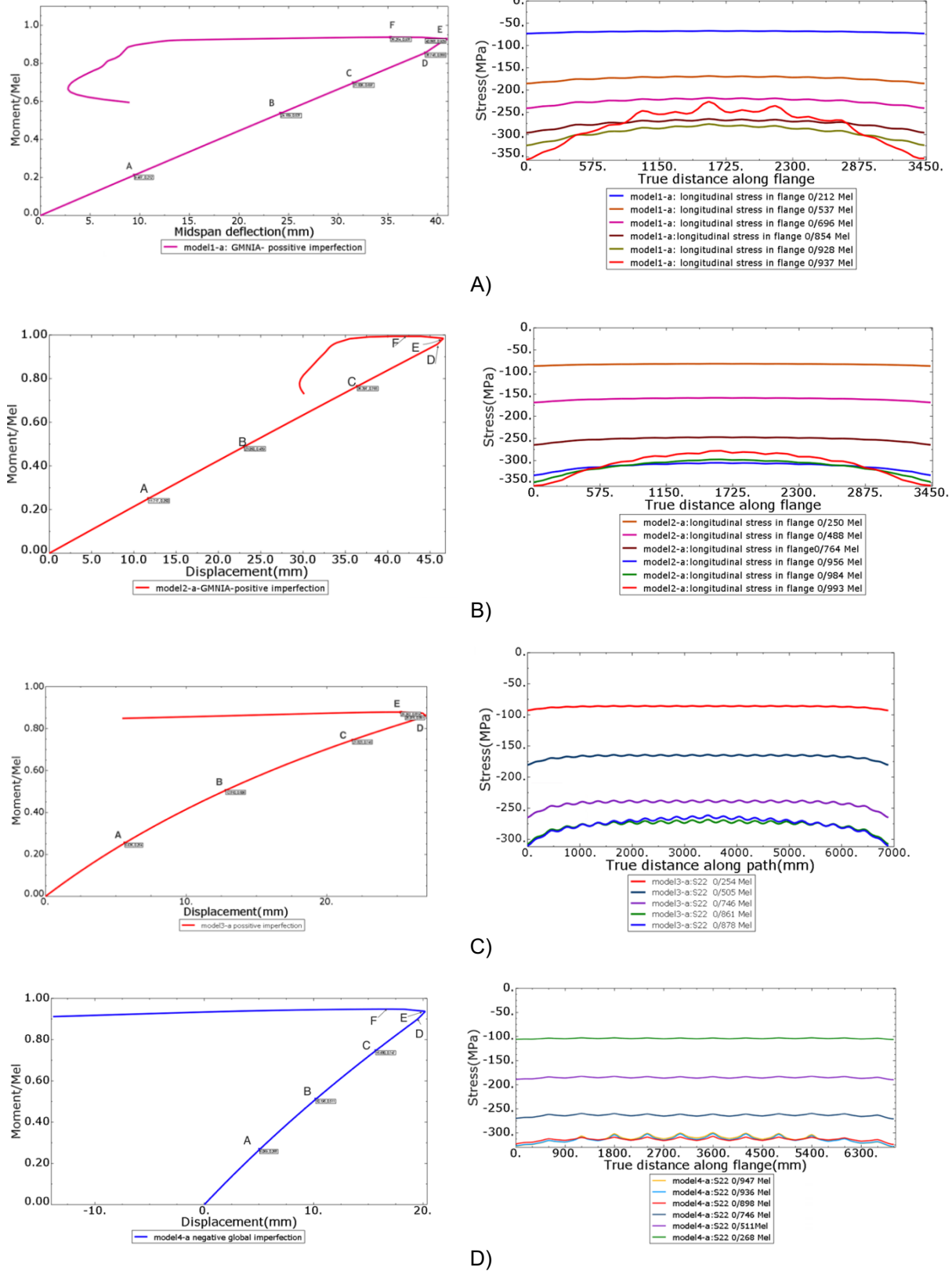


Figure 6:6 Development of the stress in the compression flange GMNIA analysis A) Model 1a, B) model2a, C) model3 a, D)model4a

Figure 6-7 A and B shows the longitudinal stress in the girder in the field where failure take place. As it is clear the model 1a and 2a, with higher aspect ratio, show an increase of the stress at the edges and decreases of the stress in the middle of the compression flange at failure. While in the model 3a and 4a the stress was more uniform whiteout sudden increase.

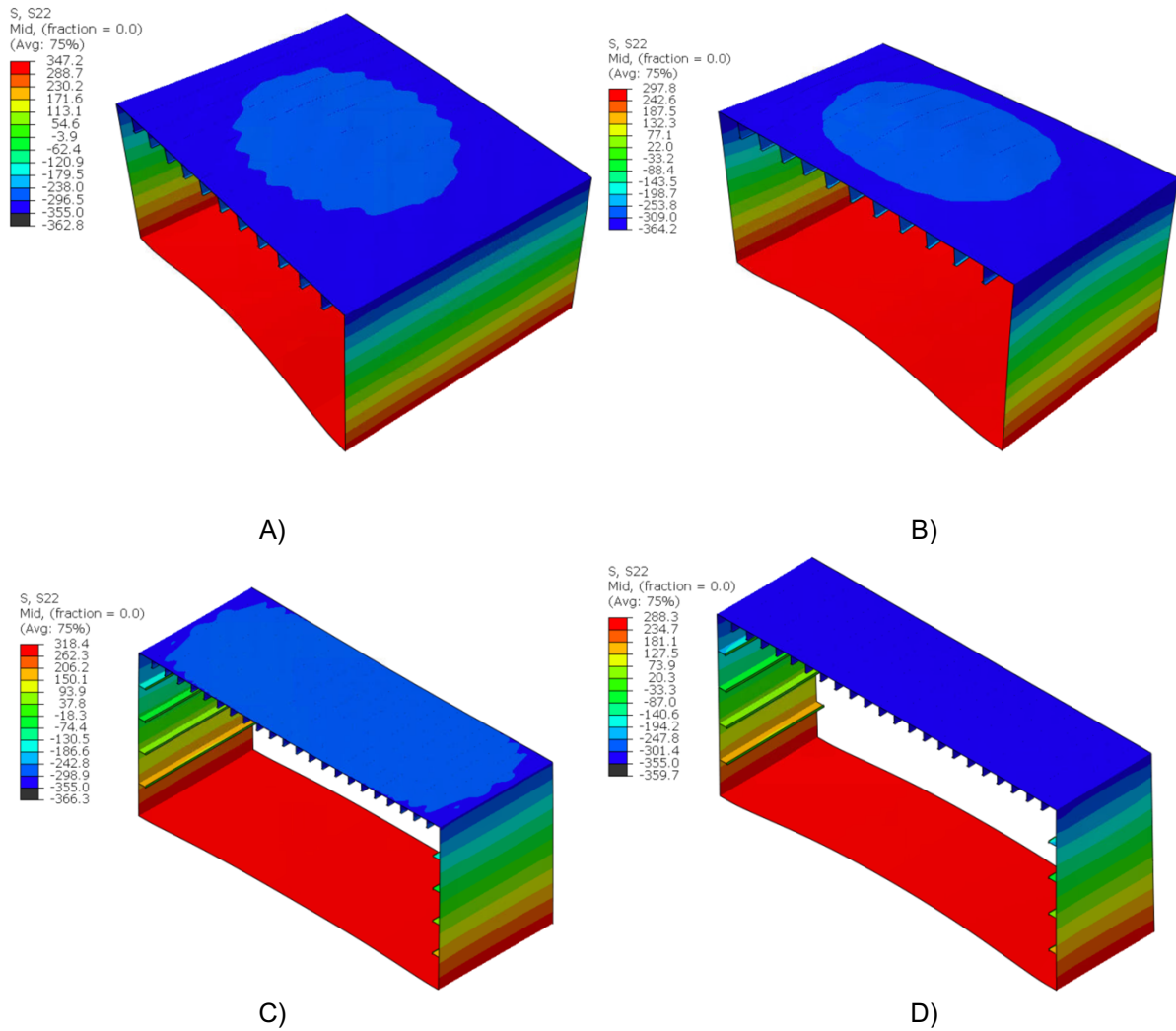


Figure 6.7: Development of the stress in the girder A) Model 1a, B) model2a, C) model3 a, D) model4a

6.1.4 Development of stress in the web of the girder

The development of stress in the web of the box girder is plotted for the same load step as described in part 6-1-3. Since there are no local instabilities in the subpanel of the webs of girders, the stresses in the web remain linear.

Before the buckling of the compression flange which takes place in the load level D in box numbers 1 and 2, as shown in Figure 6-8 A and B, the neutral line position coincides with the position of gross section neutral line. After buckling of the compression flange in figure 6-8A and B, the neutral line position begins to shift towards the tension side. This occurs because of a sudden increase of the longitudinal stress at the edges of the compression flanges in these girders. Ultimately, the compression flange of the box girder fails with a neutral line very close to the neutral line of the effective cross-section. Prior to point D, when there was no sign of buckling in the girder, the position of the neutral line remains unchanged. Results show that the shift in the position of the neutral line may take place when the structure has sudden increase of the stress at the edges and resistance limit beyond the pure column-like buckling resistance.

In the analysis of box numbers 3 and 4 figures 6-8 C and D, some nonlinearities at the location of the longitudinal stiffeners in the web were observed; however, the behavior was based on the expectation linear elastic. The neutral line with zero longitudinal stress coincides with the neutral line of the gross cross-section. Before the column-like buckling limit, which is ultimate resistance limit based on the analytical method of EN1993-1-5, there was no sign of a change in the height of compression zone and shifting of the neutral line. By doing this, the answer to objective number 2 was found. Before the column-like buckling resistance limit, the neutral line does not shift towards the tension side, and the location of the neutral line coincides with the location of the gross section neutral line.

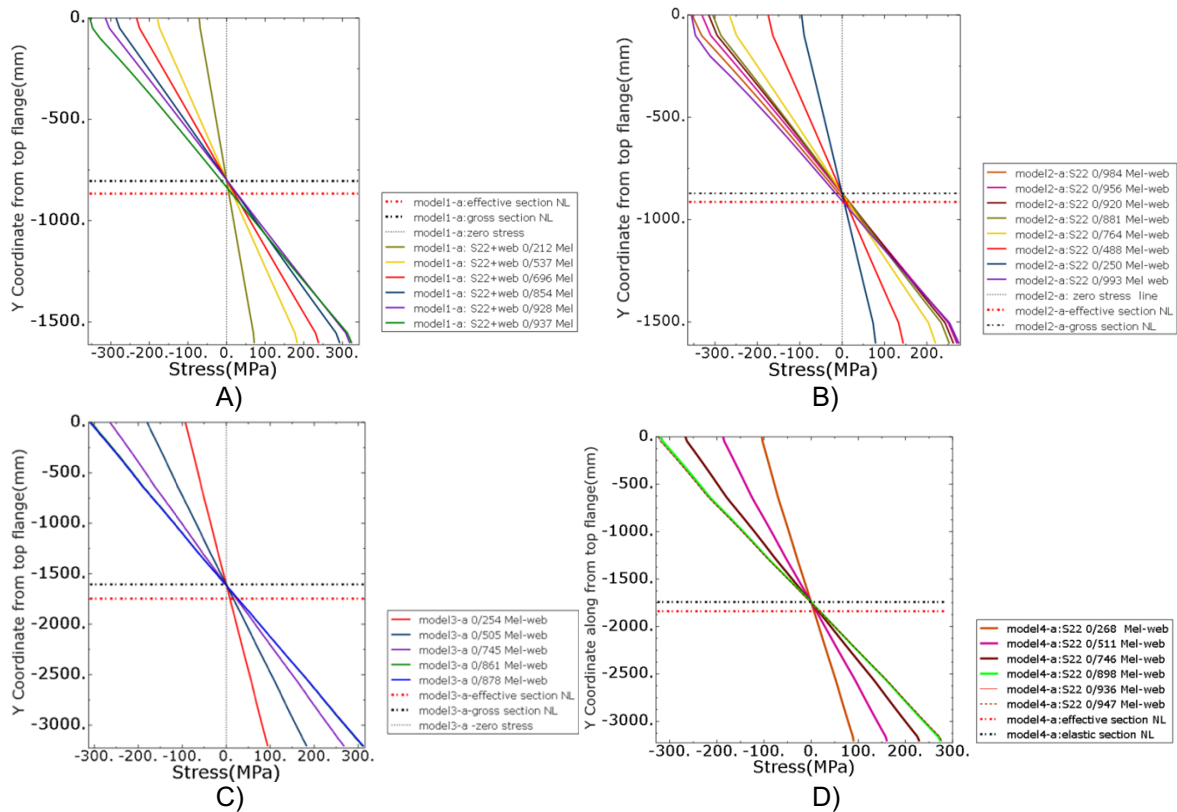


Figure 6:8 Development of the stress in the web of girder GMNIA analysis A) Model 1a, B) Model2a, C) Model3a, D) Model4-a

6.1.5 Section properties representative of the stress

The maximum value of the compression stress in the compression flange is derived from GMNIA analysis. This stress is compared to the stress that can be determined from gross section properties and from effective section properties.

As shown in Figure 6-8, up to a certain limit in all girders, which was found to be the limit of buckling in the compression flange, the stress in the flange derived from GMNIA analysis is completely compatible with the stresses derived from gross section properties.

Only close to the ultimate state, longitudinal stress from the GMNIA analysis has a significant increase in box numbers 1 and 2 as shown in Figures 6-9 A and B. These girders present higher resistance than the EN1993-1-5 effective width methods. The part containing a sudden increase in stress is not considered in the resistance limit based on EN1993-1-5 method. The sudden increase that takes place in the longitudinal stress from GMNIA analysis coincides with the increase of stress from point D to F in the moment deflection diagram in Figure 6-6 A and B. The conclusion is that at this extra resistance region the behavior is not pure column like buckling anymore and the behavior is more representative of the interaction behavior between column like buckling and plate like buckling.

In boxes numbers 3 and 4, Figures 6-9 C and D, without substantial extra resistance after column-like buckling limit, longitudinal compression stress determined from gross section properties was comparable with GMNIA longitudinal stress up to failure. The failure behavior was a sudden collapse after reaching buckling resistance limit.

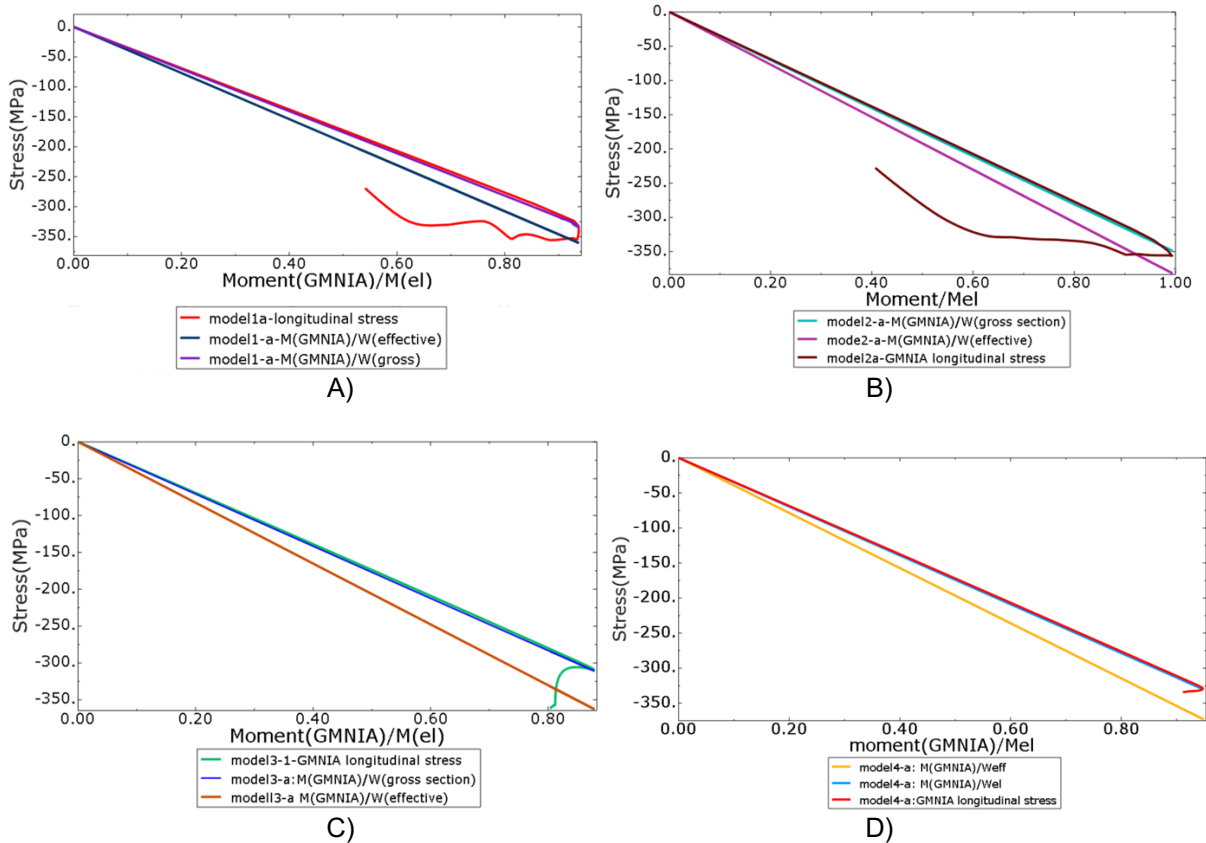


Figure 6:9 Section properties representative of the longitudinal stresses versus GMNIA stress A) Model 1a, B) model2a, C) model3 a, D)model4-a

By doing this, objective number 3 was obtained. The result shows that until column-like buckling resistance of the compression flange in the girder, which coincides with the resistance that can be determined from EN1993-1-5, the gross section area of the compression flange is applicable for determining the section properties with which stress can be determined.

However, It was observed that the stress in the panel, as the compression flange of the girder, has higher magnitudes at the ultimate bending resistance comparing to the single isolated compressed plate analyzed in part4-2-4. This has been justified in section 6-1-6.

6.1.6 Single plate versus plate as the compression flange of the girder in bending

To compare the load-deflection diagram of the single panel in compression to the moment-deflection diagram of the compression flange of the girder, the point in the middle of the failed panel is monitored. By removing the global deflection from this point in the girder, which can be determined from the deflection at the edges of the panel as shown in equation 6-1, pure deflection of the compression flange in the middle of failed field was determined.

$$\Delta = \Delta_{\text{middle of the panel}} - \Delta_{\text{side of the panel}} \quad (6-1)$$

Final moment deflection of the compression flange of the girder and load deflection of the plate is shown in figure 6-10. It is worth mentioning, the coefficient of $M_{GMNIA}/W_g \cdot f_y$ is in this case also representative of the compression resistance of the flange. Since the failure take place as the column buckling of the flange and no other type of failures are involved.

The deflection of the panel in the middle of the girder has also the contribution of the global effects; for this reason, the deflection is not completely compatible with the deflection of the single plate, especially

in girders with a wider flange, Figures 6-1C and D. In terms of deflection, they are not comparable to each other; however valuable information in terms of resistance and stress up to failure can be achieved. Although reaching the compression load level of $p_c \cdot f_y$ in the single plate coincides with the buckling and reaching the ultimate resistance, the panel as part of the girder shows the ability to reach the resistance having a stress magnitude higher than $p_c \cdot f_y$. This is also considered in the effective width method and one of the features of this method is the capability to determine resistance after buckling resistance limit.

$$M_{Rd,analytical} = f_y \times W_{effective\ section} \quad (6-2)$$

$$\frac{M_{Rd,analytical}}{W_g} > \rho_c \cdot f_y \quad (6-3)$$

The additional resistance and extra longitudinal stress in the compression flange mainly result from the introduction of gradient stress into the flange of the box girder with pure bending. This has been justified by analyzing single plates defined in section 4-1 with gradient stress resulting from the bending moment on the compression flange of the girders defined in part 6-1. The results are presented in section 6-1-7.

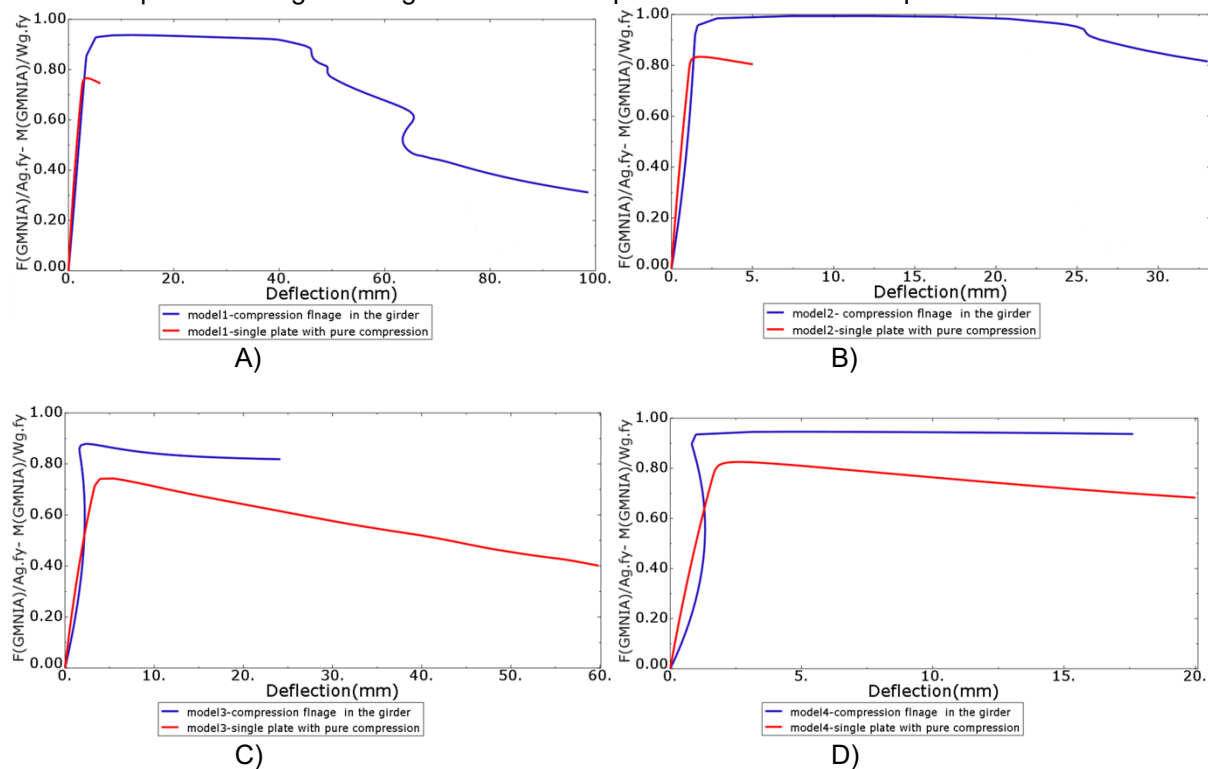


Figure 6:10 Resistance behavior differences in a single plate comparing to plate as the compression flange of the box girder analysis A) Model 1a, B) Model2a, C) Model3 a, D)Model4a

6.1.7 Effect of gradient stress introduction

As discussed in part 4-3, the boundary conditions significantly affect the behavior of the panel. In the box girder, the compression flange is connected to the webs providing rotational and transverse stiffness to the compression panel. Additionally, due to bending moments, stresses are introduced with a gradient distribution on the compression flange and the longitudinal stiffeners. These two factors contribute to an increase in the buckling stress resistance of the panel as the compression flange of the girder, compared to a single panel with simple boundary conditions and uniform loading.

The major reason for the differences in the buckling behavior between a single stiffened plate and the stiffened plate as the compression flange of the girder is the introduction of gradient stress in the compression flange of the girder as the result of loading girder by pure bending moment.

From the analysis performed on the stiffened single plate with uniform compression, it was clear that at failure, stress at the edges was equal to $p_c \cdot f_y$.

Performing GMNIA analysis on the isolated single-plate model of the compression flange with gradient stress, as shown in Figure 6-12B, and comparing it with the gradient stress on the compression flange of the girder, proves that this is the major reason for higher buckling resistance, as evident in Figure 6-

11. The isolated plates with gradient stress exhibit higher resistance, a higher buckling stress limit, and higher stress at both edges of the plate.

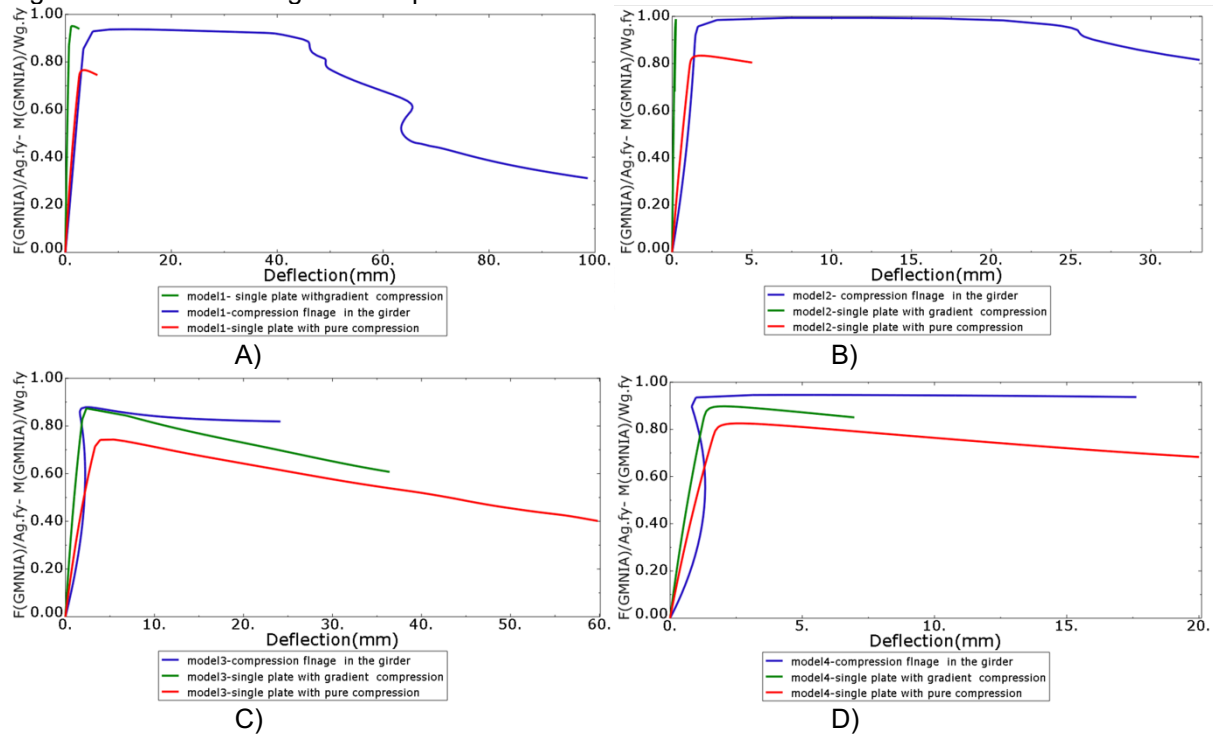


Figure 6:11 Effect of gradient loading on the resistance A) Model 1a, B) Model2a, C) Model3 a, D) Model4a

Figure 6-12 illustrates stresses at the edge strut during the failure stage. In both cases, the plate will reach the higher stress limit at the stiffeners. However, the introduction of gradient stress will delay reaching the yield stress limit in the longitudinal stiffeners and enhance the plate ability to resist compression stress.

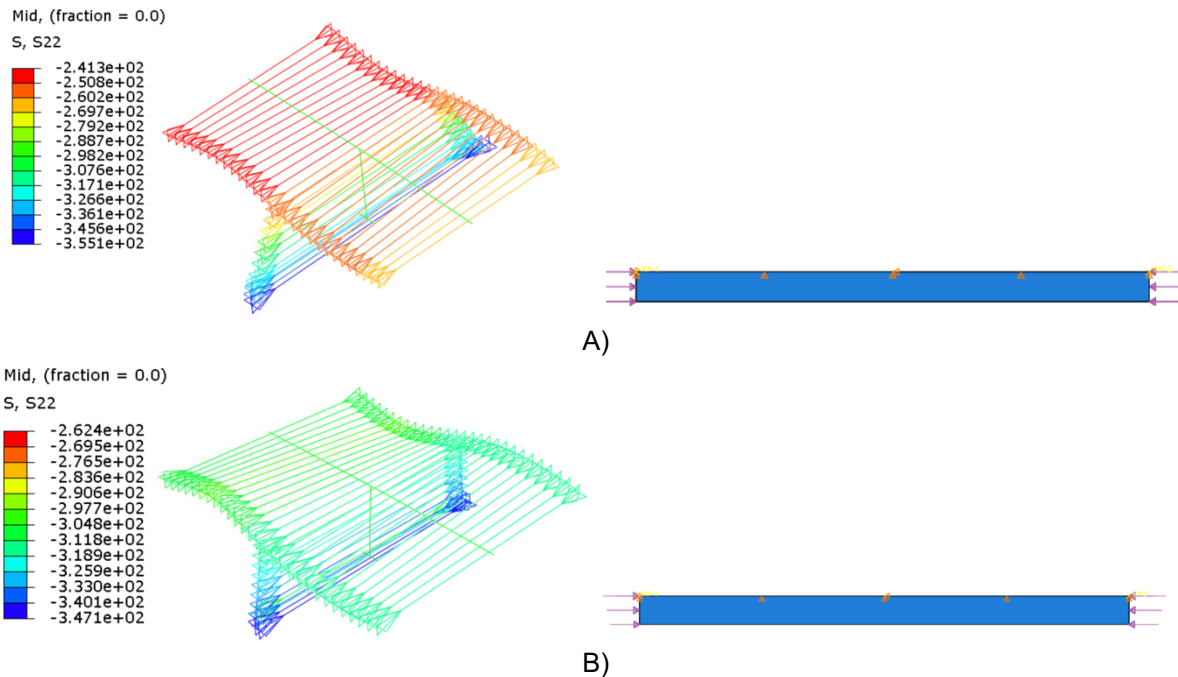


Figure 6:12 A) Stress in the strut of the plate with uniform compression stress b) stress in the strut of the plate with gradient compression stress

The increase in the stress at the compression flange has not been caused by nonlinearity in the structure; this occurs because the girder can resist more compression if the stress is applied gradient,

because of the bending moment. This has been confirmed by modeling plates with gradient stress and comparing the stress at the failure stage to the stress in the compression flange of the girder.

6.2 Model B

In Type B of the analysis, both the compression flange and the tension flange maintain the same configuration as in analysis A. However, by reducing the thickness of the webs as defined in Table 6-4 and 6-5, the sections are categorized as class 4. Before reaching the buckling resistance limit in the compression flange, the web has reached its buckling resistance limit.

number	width	thickness of web	thickness of flange	$\rho_c \cdot f_{y,flange}$	$\rho_{local,web}$
	mm	mm	mm	MPa	
1-b	3450	10	15	260.57	0.543
2-b	3450	10	20	295.71	0.516

Table 6-4 Box girder with the unstiffened web model 1 and 2 category B

number	width	Number of stiffeners	thickness of web	thickness of tension flange	$\rho_c \cdot f_{y,flange}$	$\sigma_{c,max,elastic}$	$\rho_{local,web}$	ρ_{c-web}
	mm		mm	mm	MPa	MPa		
3-b	6900	4	8	15	255.6	355	0.552	0.86
4-b	6900	4	7	20	294.6	355	0.489	0.92

Table 6-5 Box girder with the stiffened web model 3 and 4 category B

6.2.1 Resistance of the girder

As shown in figure 6-13, The resistance determined from EN1993-1-5 is lower than the resistance from analytical method. This indicates that the method of reducing the web is relatively conservative by neglecting the positive effect of the tension region in the web or iterative reduction in combination with compression flange with pure column like buckling. Discussing about the reduced area of the web with gradient stress is not an objective of this research.

	maximum bending resistance (EN1993-1-5)/ M_{el}	maximum bending resistance (GMNIA)/ M_{el}	Difference%
1-b	0.825	0.917	11.18
2-b	0.881	0.956	8.62
3-b	0.810	0.882	8.86
4-b	0.848	0.942	11.03

Table 6-6 Box girder resistance type B

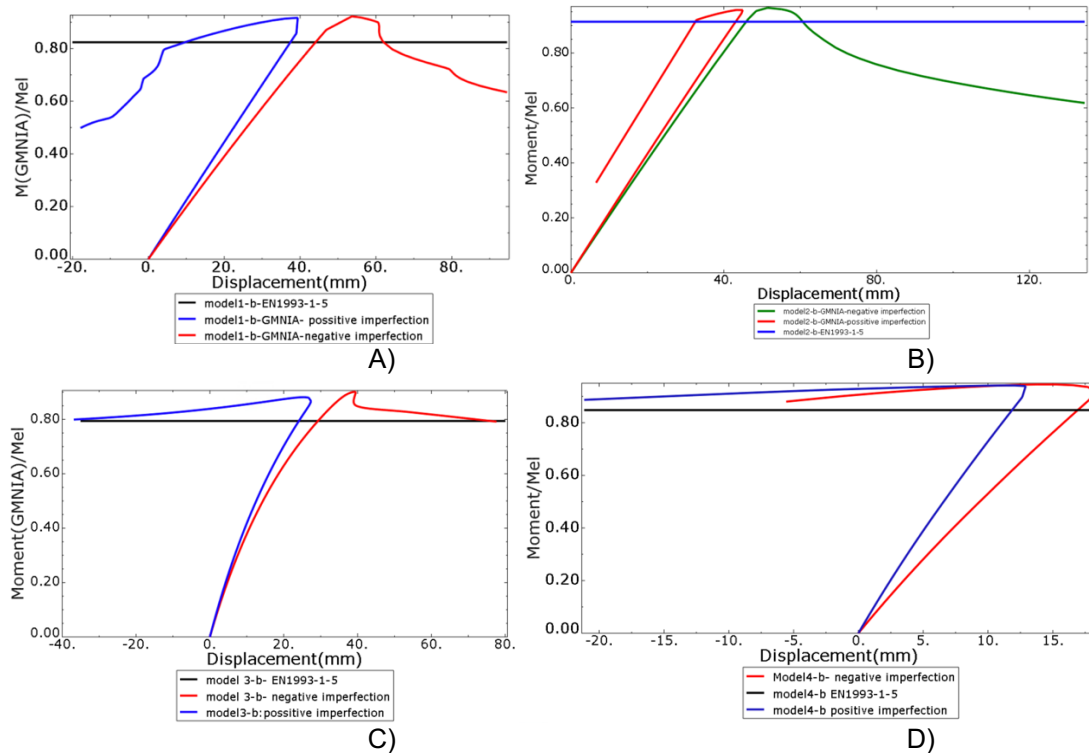


Figure 6:13 Moment deflection diagram from GMNIA analysis A) Model 1b, B) model2b, C) model3 b, D) model4b

6.2.2 Development of stress in the web of the girder

The type A models had a web of class 3, and the only buckling failure will take place in the compression flange. In the type B analysis, the web of the girders has class 4. As a result, a nonlinear stress distribution will develop in the web of the section as shown in figure 6-14. This nonlinear stress distribution will cause the increase of stress at the edge of the compression flange. However, the nonlinear stress did not demonstrate the ability to cause change in the stress distribution in the tension part. Therefore, the height of the tension zone in the cross-section remains unchanged.

In general, it was observed that the tension part will stay in tension and the compression part will stay having compression stress, in this analysis. The position of the line with zero stress stays almost unchanged. Since the influence of the web in the repositioning of the neutral line either in the gross section or effective section is negligible. Moreover, in this study, shifting of neutral line as the result of column-like buckling of the compression flange is of concern.

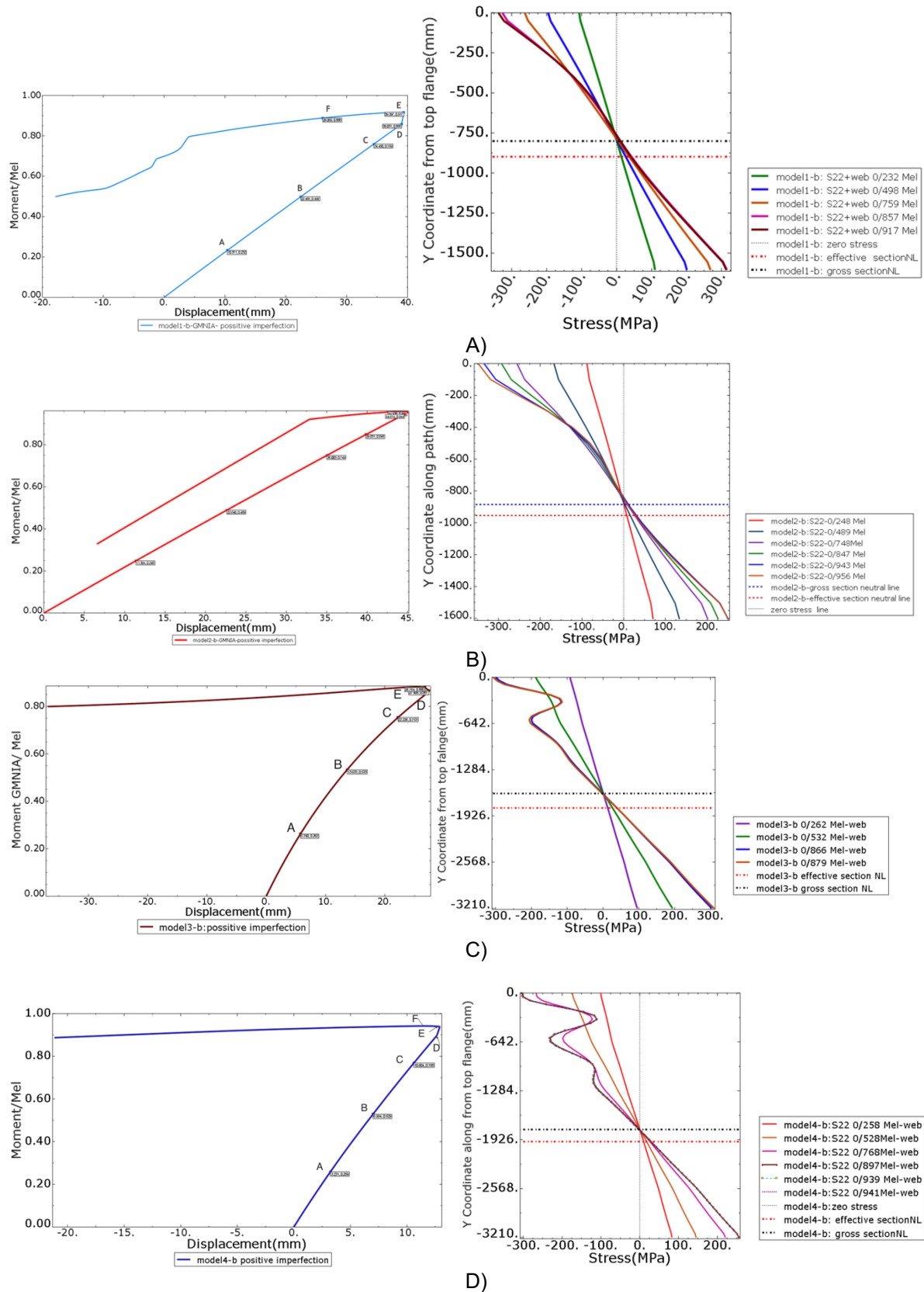


Figure 6:14 Development of the stress in the web of the girder from GMNIA set analysis b. A) Model 1b, B) Model2b, C) Model3 b, D)Model4-b

6.2.3 Section properties representative of the stress

When there are instabilities in the web of the section depending on the slenderness and magnitude of the nonlinearities as the result of the buckling in the slenderest element, web in this case, the gross section properties cannot be used to determine the internal stresses anymore. Transfer of the stress towards the compression flange as the result of buckling of the web will cause having higher stress in the compression flange edges. The stress from GMNIA analysis is compared to the stress that can be determined from gross section, effective section with the reduction in the web and in the flange and effective width determined only from web reduction in Figure 6-15. It becomes clear that section properties determined from reducing the web can be representative of the stresses prior to the buckling of the flange and after buckling of the web in the girders with column-like buckling failure.

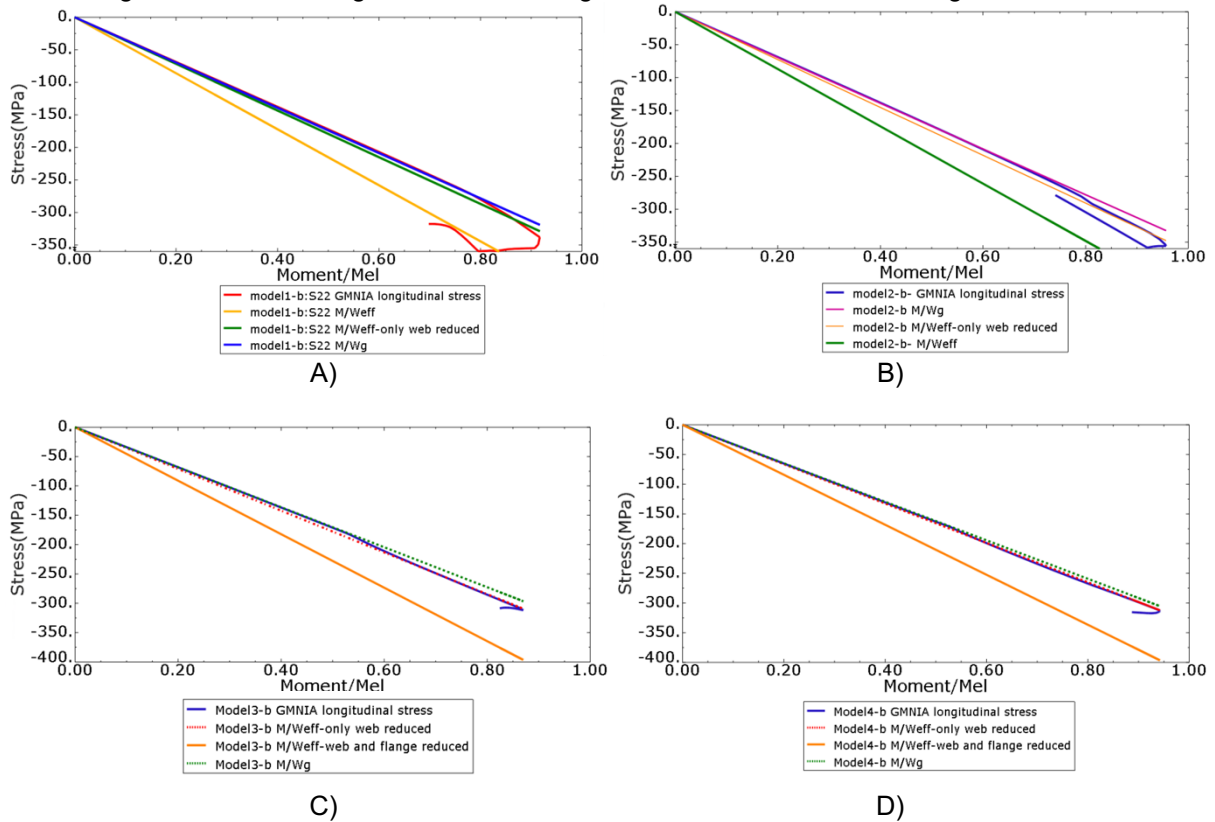


Figure 6:15 Section properties representative of the maximum stress GMNIA set analysis. A) Model 1b, B) Model2b, C) Model3 b, D) Model4-b

6.1 Model C

Most of the plated box girders in bridge applications have unsymmetric sections with a wider stiffened compression deck, similar to the cross-section of the Haringvliet bridge. This causes the gross section neutral line to be closer to the compression deck of the girder. As a result, tension failure can become the determining criteria limiting the bending resistance of the girder. The configuration of the box girder is presented in table 6-7 and 6-8.

In Type C of the box girders, the bottom tension flange is thin enough to meet the yield stress limit. The compression flange will not reach the yield stress limit, and the stress remains below the critical buckling stress. Classification of the section can be performed based on EN1993-1-1 Table 5-2 [33].

It is mentioned in this table when the compression stress in lower than the yield stress criteria of $\psi < -1$, should be applied.

$$\text{limit for class3 : } \psi < -1: \frac{c}{t} < 62 \varepsilon(1 - \psi) \times \sqrt{-(\psi)} \tag{6-4}$$

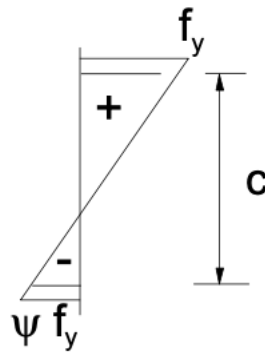


Figure 6:16 Classification of the part with gradient stress

Following this criterial subpanel of the web were determined to have class 4 in all girders and therefore using effective section properties was essential.

The major assumption in the classification of the section is to have the yield stress at the most compressed fiber. According to EN1993-1-5, when the compression stress is below the yielding stress, the slenderness of the plate element can be reduced using Equation 6-5. The final reduction factor for the reduced slenderness can either be determined from annex E of EN1993-1-5 or by replacing $\bar{\lambda}_p$ with $\bar{\lambda}_{p,red}$.

$$\bar{\lambda}_{p,red} = \bar{\lambda}_p \cdot \sqrt{\frac{\sigma_{com,Ed}}{\frac{f_y}{\gamma_{M0}}}} \tag{6-5}$$

number	height	thickness of web	thickness of flange	$\rho_c \cdot f_y \text{ flange}$	$\rho_{local,web, reduced}$ slenderness	$\sigma_{c,max,elastic}$
	mm	mm	mm	MPa		MPa
1-c	1605	8	8	260.57	1	228.1
2-c	1605	8	8	295.71	1	228.1

Table 6-7 Box girder with the unstiffened web model 1 and 2 category C

number	height	Number of stiffeners	thickness of web	thickness of tension flange	$\rho_c \cdot f_y \text{ flange}$	$\sigma_{c,max,elastic}$	ρ_{c-web}	$\rho_{local,web,min,r}$
	mm		mm	mm	MPa	MPa		
3-c	3210	4	8	8	255.60	230	0.95	0.579
4-c	3210	4	8	8	294.65	230	0.89	0.579

Table 6-8 Box girder with the unstiffened web model 3 and 4 category C

Following the criteria of the reduced slenderness method, the girder with an unstiffened web receives a local reduction factor equal to 1, meaning being full active and the absence of a nonlinear stress

distribution. Conversely, the larger girders with the stiffened webs have been determined to get both local and global reduction factors therefore it was expected to observe nonlinear stress distribution in the web of these girders. Coefficients of the plate buckling reduction factor for the reduced slenderness is presented in Table 6-7 and 6-8. For the compression flange, such criteria of the reduced slenderness method is not defined since it has column like buckling failure.

6.1.1 Resistance of the girder

In the analysis of the single plate, it was observed that having an initial imperfection towards the stiffeners leads to higher compression resistance, while having an initial imperfection towards the plate side leads to the lowest compression resistance. The same conclusion was reached in the analysis of box girders composed of these plates, regarding the bending moment, when the box girder fails in tension part, the imperfection of the compression part does not have a significant influence on the resistance, as shown in Figure 6-17. All plated girders exhibited plastic resistance. In the plastic region, the deflection of the girder increases significantly. In sections with slender elements, it is not allowed to consider the plastic resistance of the girders based on EN1993-1-1. For this reason, only behavior prior to elastic resistance is further studied.

Criteria of the reduced slenderness method is not defined for the plates with column like buckling failure. The observation was that if the compression stress from linear elastic analysis is lower than the column like buckling resistance of the compression flange ($\rho_c \cdot f_{y,flange}$), no sign of failures in the compression flange will be observed, before elastic bending resistance of the girder. Following the criteria of the effective width method need extra care in this case. Since through the iteration process and the reduction of the compression part even higher resistance can be determined, if in the reduced section again the tension failure is the governing failure. The conclusion is that, in plated box girders with tension failure, the elastic bending moment resistance can be the actual representative of the bending resistance in this case. Considering elastic resistance will be conservative by neglecting the plastic bending resistance of the girder.

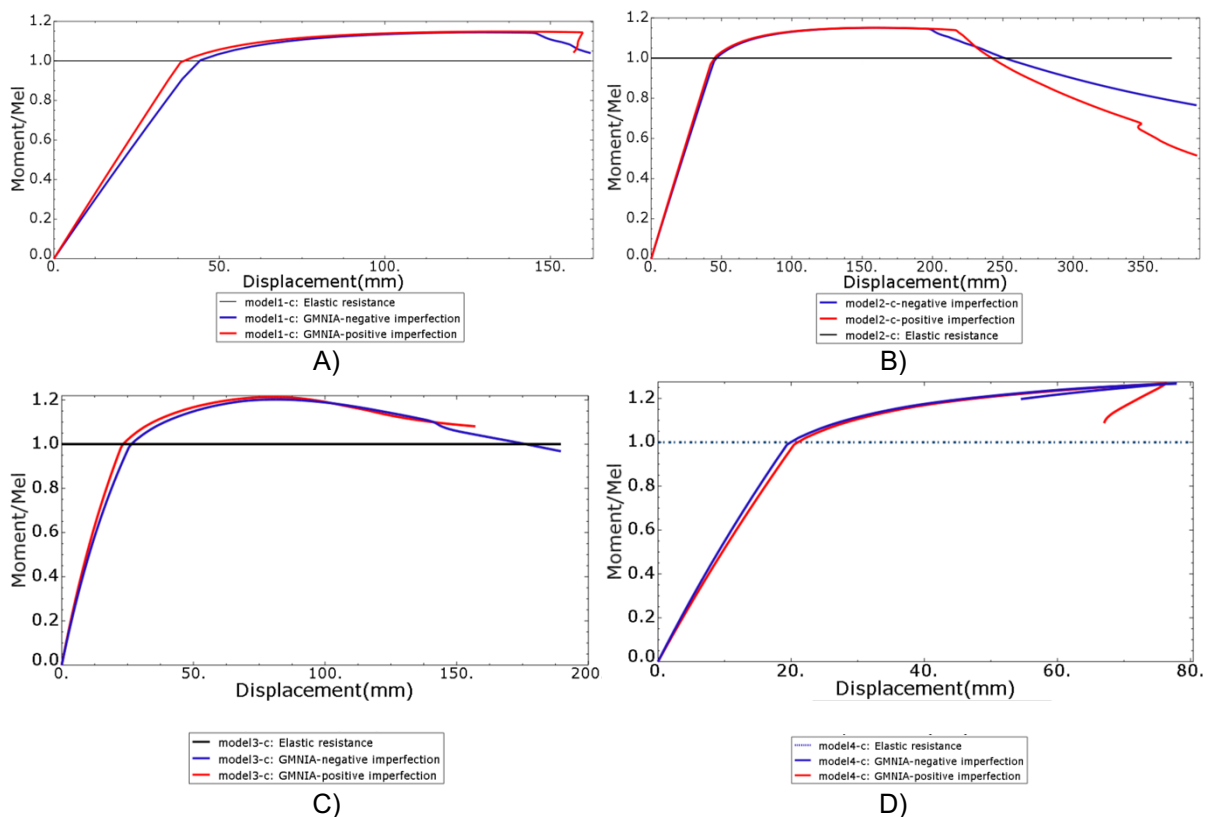


Figure 6:17 Resistance of the girder type C analysis . A) Model 1c, B) Model2c, C) Model3 c, D) Model4c

6.1.2 Development of the stress in the web

Monitoring the stress in the web of the section shows a linear stress distribution in the girder's web, as shown in figure 6-18. Although the web was determined to have reduction as the result of nonlinearities in boxes number 3 and 4 by following the reduced slenderness method no sign of nonlinearity was observed in the web of the section.

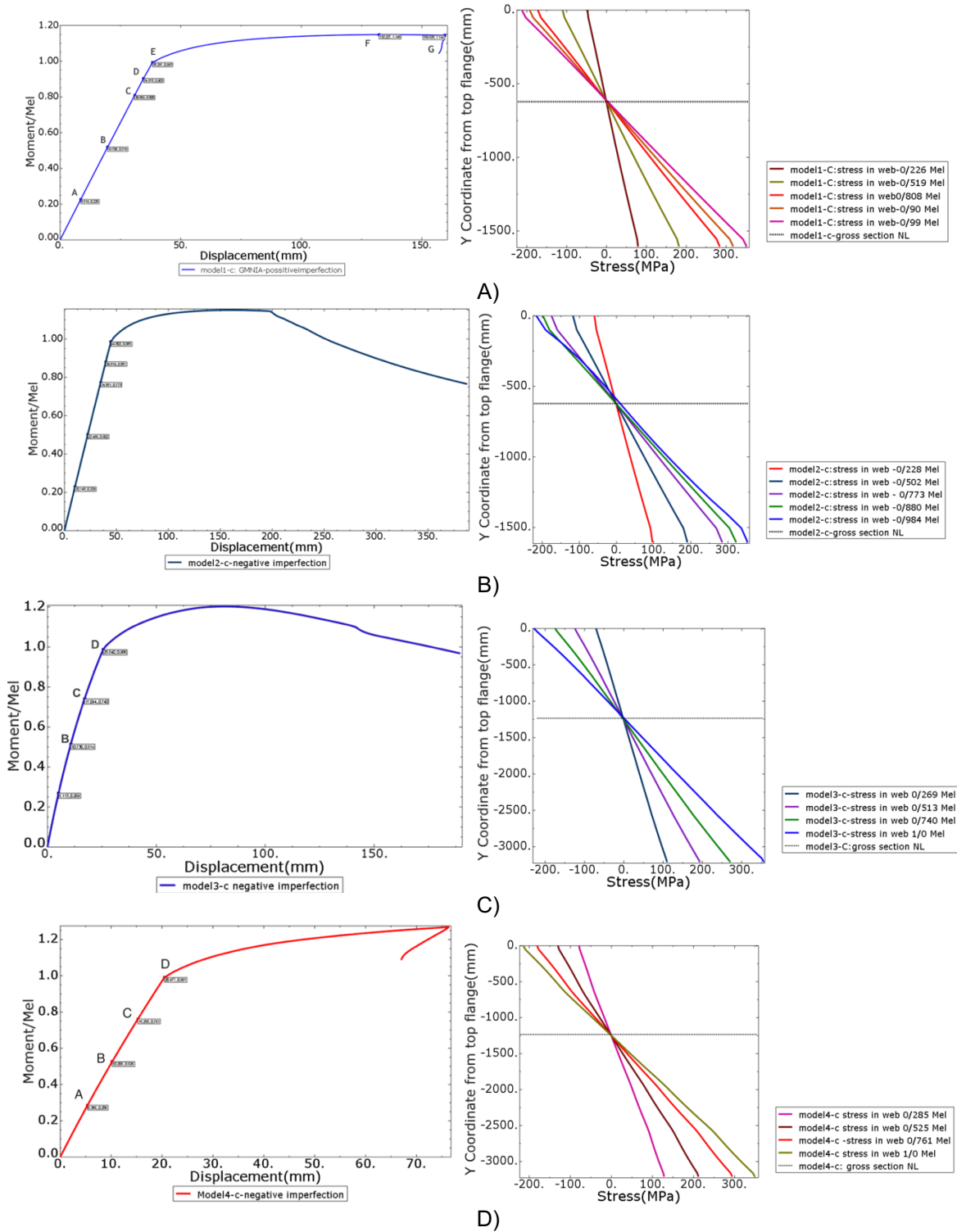


Figure 6:18 Type C analysis stress in the web of the girder A) Model 1c, B) Model 2c, C) Model 3c, D) Model 4c

6.1.3 Section properties presentative of the stresses

Stress at the reference point define in section 5-4 on the edges of the compression flange and another point below it in the tension flange is monitored in the GMNIA Analysis. Comparing the stress to the stress that can be determined from gross section properties, shown in Figure 6-19, reveals that up elastic bending moment resistance behavior is linear and elastic. For this reason, the stress determined from LEA can be representative of the edge stresses.

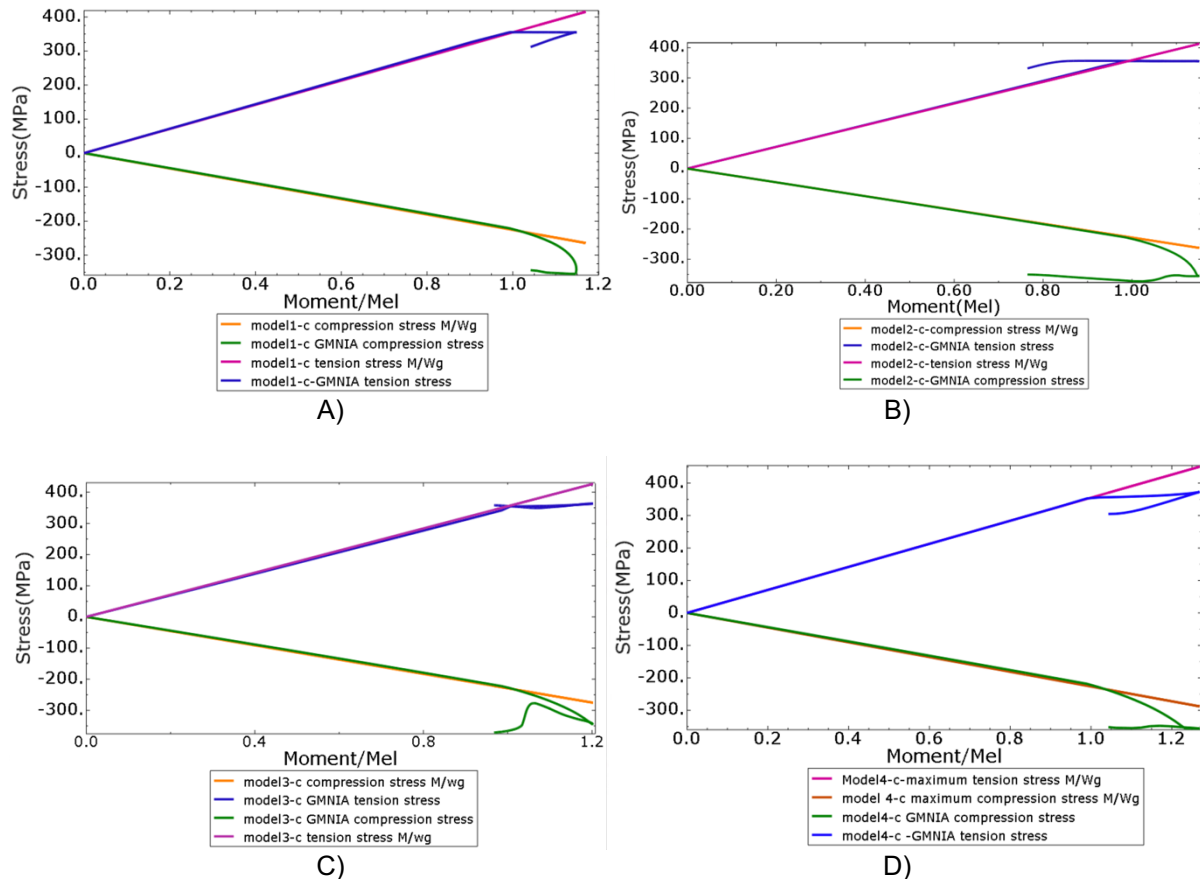


Figure 6-19 type C analysis compression and tension in the flange of the box girder A) Model 1c, B) Model 2c, C) Model 3c, D) Model 4c

6.2 Summary of the results

In the compression flange containing stiffened plate with ξ interaction ratio close to zero and the aspect ratio above 0.5, the compression flange exhibited the ability to resist extra bending moment. In this extra resistance limit, the maximum stress at the edges of the flange sheet experienced a sudden increase, which happened in the resistance limit above column-like buckling resistance limit. Depending on the geometry, the ability of the girder to reach higher bending resistance differs. So that, when the ξ interaction ratio was close to -1 and the aspect ratio below 0.5, compression flange and consequently girder in bending failed with a sudden failure without sustaining substantial extra bending moment. In this case the stress at the edges of the compression flange sheet did not experience any sudden increase close to failure.

Most of the plated girders in bridge application have aspect ratio between 0.2 to 0.3 for economic reasons [10]. The failure of box girders with such configurations happens mainly in a sudden manner in the form of pure column-like buckling. The result of analysis shows performing GMNIA analysis barely shows extra resistance comparing to the analytical method for such configuration. If GMNIA analysis is going to be performed for determining the resistance of girders with such configuration the possible phenomena having favorable effect in resisting more force should be accurately addressed in the FEM model otherwise the resistance will be overestimated.

In general buckling resistance of the plate as the compression flange of girder with bending moment was higher than the buckling resistance of a single isolated compressed panel regarding. Single plate loaded by uniform compression stress failed with the maximum stress at the edge equal to $p_c \cdot f_y$; however, the plate as the compression flange of the girder failed by having higher compression stress magnitude at the edges of flange sheet.

This occurs mainly as a result of gradient stress introduction in the compressed flange, as a side effect of the bending moment on the girder. The effective width method can consider the ability of the compression flange in gaining extra compression stress. Although the magnitude of compression stress at edges was higher than $p_c \cdot f_y$, the behavior of the plate was still linear-elastic.

When the buckling behavior is in the form of pure column-like buckling, there is no instability prior to buckling. When there is no other instability problem involved in the cross section the stress determined from elastic analysis is representative of the actual stress in the plated structure. Since the nature of the behavior before column-like buckling in the plate is linear-elastic, using effective section properties by reducing the compression flange area with pure column-like buckling reduction for determining the internal stresses will cause a significant overestimation of the internal stresses.

This was confirmed by controlling the position of the neutral line and controlling the maximum compression stress in the flange, which occurs on both sides of the flange edge. When the post-buckling reserve is not considered in the resistance and the plate fails with sudden column-like buckling behavior, the position of the neutral line stays on the location of gross section neutral line.

GMNIA longitudinal stresses in the girder shows better compatibility with the stresses determined from section properties containing gross section area of the compression flange with column-like buckling failure. The reason is that before column-like buckling limit, the behavior is elastic in the plate.

The stocky compression flange can be combined with the slender web. When the web of the box girders has a slender element, buckling of this element will cause extra stress in the compression flange of the girder. In this case, this extra stress should be considered in the design. It was observed by using the gross area of the compression flange and the effective area of the compressed part of the web this effect can be considered.

By focusing on the tension failure, it was observed that the resistance can be increased up 20%. In plastic region. In the criteria of the effective width method of Eurocode it is mentioned that the effective width method is applicable when the compression flange reaches the yield stress. Suggestion for the deviation from this assumption is to use reduce slenderness method. This find to be conservative, moreover, it is not general since it does not cover the situation when the compression flange has overall buckling in the form of pure column-like buckling.

It was observed when the elastic resistance can be determined by tension failure and the stress in the compression flange are bellow buckling stress limit, elastic bending resistance will be a safe estimation of the bending resistance.

6.3 Discussion

The study has provided valuable insights into the column-like behavior of the stiffened plates under various conditions and the analytical method addressing the maximum longitudinal stress in the stiffened plate.

Initially, the column-like buckling of single isolated plates under pure compression load was studied. The failure of stocky plates with relatively weak stiffeners experiencing pure column-like buckling failure begins with the yielding of the longitudinal stiffeners. Without any development of yield region in the plate sheet the ultimate resistance will be reached.

In terms of ultimate resistance, the plates with pure column-like buckling are considered to have free longitudinal edges. The study shows that the plate will not benefit from having vertical supports at unloaded edges in resisting more compression force. The exact reduction factor can be determined from the analytical method based on EN1993-1-1.

However, it was observed that the resistance from GMNIA can be lower than the resistance from the analytical method based on EN1993-1-5.

EN1993-1-5 assumes that the stress at the edges is equal to the yield stress; however, it was observed that the edges of the panel will experience stress equal to $p_c \cdot f_y$ in the plates with column-like buckling without any local buckling in the subpanels. In fact, reaching yield stress at side edges is one of the features of the plates with orthotropic behavior. Considering stress at side edges equal to yield stress in all cases of the plate failure, will cause over estimation of the resistance. The observation in the case of plate with pure column-like buckling failure was that considering edges stress equal to $f_y \cdot p_c$ will provide a better presentation of the real stress in the plate edges.

For a better understanding of the panel's behavior, it is crucial to control the stress pattern in the failure step. Doing this will provide valuable information about type of failure in the plate. The stiffeners reached yield stress limit; however, the location of the maximum absolute compression stress in the plate sheet was at side edges with maximum magnitude of $f_y \cdot p_c$.

The stiffened plate as the compression flange of the girder under pure bending will not exhibit exact the same behavior as the single isolated plate, meaning it will not fail by reaching $p_c \cdot f_y$ at failure stage. The reasons for this different behavior can be categorized into two main factors, the influence of the geometry and the influence of the gradient load introduction into the flange of the box girder with pure bending moment.

The gradient load introduction showed the major influence causing deviation of the behavior comparing to single isolated plate. Failure of the plate, in both isolated plate and the plate as the compression flange of the girder begin by reaching yielding stress at the longitudinal stiffeners. In the plates with gradient stress introduction, by having higher stress magnitude at the plate sheet and lower stress magnitude in the longitudinal stiffeners the column-like buckling limit will increase. Therefore, the plate will fail by gaining stress higher than $p_c \cdot f_y$ at failure stage.

Effective width method can consider this extra resistance in the girder. The ultimate bending resistance that can be determined from the effective width method when only column-like buckling reduction of the compression flange is involved in the effective section (meaning all other reduction factors are equal to 1), is exactly equal to the buckling limit of the compression flange with gradient stress.

Extra resistance after this point is observed in some cases depending on the geometrical configuration of the girder.

7

Conclusion

This section presents the conclusions, which address the research objectives aimed at achieving a more accurate assessment of stress in the compression flange of box girders subjected to bending moment when the compression flange is stocky and experiences pure column-like buckling failure.

7.1 Conclusions

Determining longitudinal stress in the plate through an analytical method was the major interest of this research.

In the single stiffened plate, the observation was using gross section properties in equation 7-1 for determining the stress on the compressed plate can be representative of the absolute maximum compression stress in it. The location of the maximum absolute compression stress was at side edges. The deflection up to failure was relatively low. Looking at the stress from the analytical method and relatively low deflection in the plate, can be indicative that LEA can be suffice for finding the maximum stress in the plate sheet.

$$\sigma_{GMNIA, longitudinal} = \frac{F_{Ed}}{A_g} \quad (7-1)$$

The longitudinal stiffeners in this case will experience higher stress magnitude and they will reach yield stress in the ultimate limit state.

The analytical method for addressing the compression stress at failure location in the flange of the girder, has contributions from the distance between the compression flange to the neutral line and the second moment of inertia. If the compression flange fails due to pure column-like buckling and features subpanels of class 3, it is observed that the neutral line of the section aligns with the gross section neutral line up to column-like buckling failure of the compression flange.

Up to level 1 which is buckling of limit of the web the behavior of the whole girder is elastic and stress can be determined from gross section area of the girder. In the resistance limit after level 1 in which the post buckling resistance of the web is considered the stress should be determined from effective section properties determined by reduced web area and the gross section area of the compression flange. Level 2 coincides with the buckling of the compression flange. If the compression flange fails by pure column-like buckling and the subpanels have calss3, the further reduction of the compression by column like buckling reduction factor is not needed for determining the longitudinal stress.

$$\left\{ \begin{array}{l} \text{level1: } \sigma_{GMNIA, longitudinal} = \frac{M_{y \text{ gross section}}}{I_{\text{gross section}}} \\ \text{level2: } \sigma_{GMNIA, longitudinal} = \frac{M_{y \text{ effective-web reduced}}}{I_{\text{effective-web reduced}}} \end{array} \right. \quad (7-2)$$

In general criteria of effective width method is not valid in the box girder that have tension failure. In case of the tension failure modification is needed for classification of section and determining the slenderness.

If the girder fails due to tension failure of the tension flange and the stress at the compression flange is lower than the column-like critical buckling stress limit, it was observed that the compression flange is active with its full area in resisting the stress from bending moment. For the web although reduction was determined in the girders with the stiffened plate, no sign of nonlinearity or sign of deviation from linear elastic theory was observed up to elastic bending resistance. This reveals that the criteria of the reduced slenderness method can be conservative, and even in the EN1993-1-5 it is also mentioned to be conservative.

In the girders with tension failure due to the development of a tension block, the resistance will exceed the elastic bending resistance. In this resistance region, the stiffness of the girder will significantly decrease, and consequently, the deflection will increase. In the girders with slender elements considering plastic bending resistance is not allowed based on the current EN1993-1-1.

7.2 Future research

Based on the results gathered in this report, certain subjects can be further studied to have a complete analytical method addressing the maximum compression stress at the compression flange.

The expectation is that the compression flange with class 4 subpanels and pure column-like buckling failure of the compression flange, the reduction of the compression flange area by column-like buckling reduction factor will also lead to the conservative longitudinal stress estimation. The analytical method for addressing the stress magnitude in such cases needs further investigation.

In the plates with interaction behavior between plate-like and column-like buckling, the magnitude of compression stress at the side edges of the plate needs further study. The expectation is that in such configurations, the compression stress at the edge will have a magnitude between $p_c \cdot f_y$ and f_y .

In this study, the open T-shape stiffeners are relatively weak considered. For closed stiffeners or the stiffeners with higher relative bending stiffness, the applicability of the finding needs further investigations. These investigations should be focused on addressing whether the pure column-like buckling exists in plates with such configurations and whether the gross section of the plate can be used for addressing the maximum compression stress.

It was observed that in the plate with gradient stress introduction, the column-like buckling resistance can be higher. Further research can be performed on this type of loading regarding plate-like buckling and interaction of plate and column buckling. Result of such research can be guided to the less conservative estimation of the resistance based on the reduced slenderness method.

In case of tension failure, future research focused on determining less conservative method than the reduced slenderness method is of interest.

References

- [1] EN1993-1-5.
- [2] L. Euler, "Euler's calculation of buckling loads for columns of non uniform section," *In The Rational Mechanics of Flexible or Elastic Bodies*, 1757.
- [3] W. Ayrton and J. Perry, "On struts," *Engineer*, vol. 62, p. 464–465, 1886.
- [4] J. Caldwell, "Ultimate longitudinal strength," *InTrans.RINA*, vol. 107, p. 411, 1956.
- [5] L. Navier, "Resume des lecons de mecanique," 1819.
- [6] G. Kirchhoff, "Uber das Gleichgewicht und die Bewegung einer elastischen Scheibe," *j Reine Angew*, vol. 40, pp. 51-58, 1850.
- [7] T. von Kármán, "Festigkeitsproblem im Maschinenbau," *Encyk. D. Math. Wiss*, vol. IV, pp. 311-385, 1910.
- [8] L. Gardner and M. Theofanous, "Discrete and continuous treatment of local buckling in stainless steel elements," *Journal of Constructional Steel Research*, 2008.
- [9] B. Johansson, R. Maquoi, G. Sedlacek, C. Müller and D. Beg, "Commentary and Worked Examples to EN 1993-1-5 "Plated Structural Elements"," 2007.
- [10] P. Dubas and E. Gehri, in *Behaviour and design of steel plated structures*, Honggerberg, Applied statics and steel structures.
- [11] G. Winter, "Commentary on the 1968 Edition of the Specification for the Design of Cold-Formed Steel Structural Members," *American Iron and Steel Institute*, 1970.
- [12] D. Faulkner, "Compression tests on welded eccentrically stiffened plate panels," *Steel plated structures*, no. 581 617, 1977.
- [13] G. Gerard, "Minimum weight analysis of orthotropic plates under compressive loading," *Aerospace Sci*, vol. 27, pp. 21-26, 1960.
- [14] K. Kloppel, R. Schmied and J. and Schubert, "Die Traglast mittig und aussermittig gedruckter dunnwandiger Kasten-trager unter Verwendung der nichtlinearen Beultheorie," *Der Stahlba*, p. 321, 1966.
- [15] R. Maquoi and ch. Massonnet, "Theorie non-lineaire de la resistance postcritique des grandes poutres en caisson raidies," *Memoires de l'AIPC*, Vols. 31-II, 1971.
- [16] B. Johansson and M. Veljkovic, "Steel plated structures," no. DOI: 10.1002/, p. 59, 2001.
- [17] S. E. Webb, " Stiffened plating under combined in-plane and lateral loading," Imperial College of Science and Technology, London, 1980.
- [18] S. E. WEBB and P. J. DOWLING, "Large-deflection elasto-plastic behaviour of discretely stiffened plates," *Proc. Instn Ciu. Engrs.*, vol. 2, no. 69, pp. 375-401, 1980.
- [19] J. K. Paik, A. K. Thayamballi and B. J. Kim, "Large deflection orthotropic plate approach to develop ultimate strength formulations for stiffened panels under combined biaxial compression/tension and lateral pressure," *Thin-Walled Structures*, vol. 39, no. 215-246, pp. DOI: 10.1016/S0263-8231(00)00059-8, 2001.
- [20] P. Jetteur, R. Maquoi and C. Massonnet, "Simulation of the Behaviour of Stiffened Box Girders With and Without Shear Lag," *Thin-Walled Structure*, vol. 1, pp. 211-237, 1983.
- [21] K. Moxham, "theoretical prediction of the strength of welded steel plates in compression," *University of Cambridge*, 1971.
- [22] K. O. F. N. A Hasegawa, "buckling strength of multiple stiffened plates," *Methods of structural analysis*, vol. 2, no. ASCE, pp. 937-956, 1976.

- [23] D. Beg, U. Kuhlmann, L. Davaine and B. Braun, "Design of Plated Structures : Eurocode 3: Design of Steel Structures, Part 1-5: Design of Plated Structures," 2010.
- [24] R. Tenchev, "Shear lag in orthotropic beams/plates and plates with stiffeners," *IN t.J. Solid structures*, no. Vol.33, 1996.
- [25] E. Byklum, "Ultimate strength analysis of stiffened steel and aluminium panels using semi-analytical method," 2002.
- [26] T. J. d. C. Manco, "Behaviour of unstiffened and stiffened curved steel panels under in-plane and out-of-plane actions," August 2018.
- [27] A. V. 6. Documentation. [Online].
- [28] B. Kovesdi, "Finite Element model-based design of stiffened welded plated structures subjected to the combine loading," *Periodica polutechnica civil engineering*, no. 677, pp. 677-689, 2021.
- [29] "PrEN 1993-1-14".
- [30] B. Kovesdi, M. Z. Haffar and S. Adany, "Buckling resistance of longitudinally stiffened plates: Eurocode-based design for column-like and interactive behavior of plates with closed-section stiffeners," *Thin-Walled Structures*, vol. 159, no. <https://doi.org/10.1016/j.tws.2020.107266>, 2021.
- [31] B. Braun, R. Chacón, H. Degée, Y. D. L. Dunai, B. Kövesdi, U. Kuhlmann, G. Lener, V. Pourostad, F. Sinur and R. Timmers, Design of steel plated structures with finite elements.
- [32] K. Tran, "Étude de la résistance et de la stabilité des tôles courbes cylindriques en acier.," Application aux ouvrages d'art. PhD thesis Université Paris-Est, Paris, 2012.
- [33] EN1993-1-1.
- [34] F. Ljubinković, "Cylindrically Curved Steel Panels in Bridge Design," PhD thesis University of Coimbra, 2020.
- [35] L. Davaine, F. Imbert, J. Raoul, E. Gogny, B. Prevost, J. Resplendido, P. Schmitt and F. Tavakoli, "Guidance book - Eurocodes 3 and 4 Application to steel-concrete composite road bridges," SETRA, 2007, pp. 162-167.

ANNEX I

In this appendix of the report result from GMNIA analysis of the stiffened plates with 26 combinations of initial imperfection are presented in the tables.

Plate number 1

Imperfection name	Imperfection type	Imperfection magnitude	resistance (MN)		difference%
			GMNIA	EN1993-1-5	
combination1	Global mode	-6.90	16.978	14.143	20.05
combination2	Global mode	6.90	14.500	14.143	2.52
combination3	local 9 sin waves	1.44	18.368	14.143	29.87
combination4	local 9 sin waves	-1.44	18.368	14.143	29.87
combination5	local 10 sin waves	1.38	18.245	14.143	29.00
combination6	local 10 sin waves	-1.38	18.245	14.143	29.00
combination7	stiffeners	h/50	18.703	14.143	32.24
combination8	- IP _g +0.7 IP _s +0.7 IP _{l-j}		16.818	14.143	18.91
combination9	- IP _g +0.7 IP _{l-j}		16.797	14.143	18.77
combination10	- IP _g +0.7 IP _s -0.7 IP _{l-j}		16.818	14.143	18.91
combination11	- IP _g -0.7 IP _{l-j}		16.839	14.143	19.06
combination12	- IP _g +0.7 IP _s +0.7 IP _{l-i}		16.781	14.143	18.65
combination13	-IMP3+0.7 IP _{l-i}	h/50	16.797	14.143	18.77
combination14	- IP _g +0.7 IP _s -0.7 IP _{l-i}		16.781	14.143	18.65
combination15	- IP _g -0.7 IP _{l-i}		16.797	14.143	18.77
combination16	IP _g -0.7 IP _s -0.7 IP _{l-j}		14.461	14.143	2.25
combination17	IP _g -0.7 IP _{l-j}		14.492	14.143	2.47
combination18	IP _g -0.7 IP _s +0.7 IP _{l-j}		14.460	14.143	2.24
combination19	IP _g +0.7 IP _{l-j}		14.492	14.143	2.47
Combination20	IP _g -0.7 IP _s -0.7 IP _{l-i}		14.510	14.143	2.59
Combination21	IP _g -0.7 IP _{l-i}		14.505	14.143	2.56
Combination22	IP _g -0.7 IP _s +0.7 IP _{l-i}		14.490	14.143	2.45
Combination23	IP _g +0.7 IP _{l-i}		14.505	14.143	2.56

Plate number 2

<i>Imperfection name</i>	<i>Imperfection type</i>	<i>Imperfection magnitude</i>	<i>resistance (MN)</i>		<i>difference%</i>
			GMNIA	EN1993-1-5	
<i>combination1</i>	global mode (IP_g)	-5.175	17.691	15.923	11.103
<i>combination2</i>	global mode. (IP_g)	5.175	16.108	15.923	1.162
<i>combination3</i>	local 7 sin waves (IP_{l-j})	1.479	18.410	15.923	15.619
<i>combination4</i>	local 7 sin waves (IP_{l-j})	-1.479	18.410	15.923	15.619
<i>combination5</i>	local 8 sin waves(IP_{l-i})	1.438	18.256	15.923	14.652
<i>combination6</i>	local 8 sin waves(IP_{l-i})	-1.438	18.261	15.923	14.683
<i>combination7</i>	Stiffeners (IP_s)	$h/50$	18.746	15.923	17.729
<i>combination8</i>	- IP_g +0.7 IP_s +0.7 IP_{l-j}		17.558	15.923	10.268
<i>combination9</i>	- IP_g +0.7 IP_{l-j}		17.585	15.923	10.438
<i>combination10</i>	- IP_g +0.7 IP_s -0.7 IP_{l-j}		17.558	15.923	10.268
<i>combination11</i>	- IP_g -0.7 IP_{l-j}		17.585	15.923	10.438
<i>combination12</i>	- IP_g +0.7 IP_s +0.7 IP_{l-i}		17.468	15.923	9.703
<i>combination13</i>	- IP_g +0.7 IP_{l-i}		17.489	15.923	9.835
<i>combination14</i>	- IP_g +0.7 IP_s -0.7 IP_{l-i}		17.468	15.923	9.703
<i>combination15</i>	- IP_g -0.7 IP_{l-i}		17.489	15.923	9.835
<i>combination16</i>	IP_g -0.7 IP_s -0.7 IP_{l-j}		15.815	15.923	-0.678
<i>combination17</i>	IP_g -0.7 IP_{l-j}		15.796	15.923	-0.798
<i>combination18</i>	IP_g -0.7 IP_s +0.7 IP_{l-j}		15.731	15.923	-1.206
<i>combination19</i>	IP_g +0.7 IP_{l-j}		15.796	15.923	-0.798
<i>Combination20</i>	IP_g -0.7 IP_s -0.7 IP_{l-i}		15.799	15.923	-0.779
<i>Combination21</i>	IP_g -0.7 IP_{l-i}		15.824	15.923	-0.622
<i>Combination22</i>	IP_g -0.7 IP_s +0.7 IP_{l-i}		15.837	15.923	-0.540
<i>Combination23</i>	IP_g +0.7 IP_{l-i}		15.824	15.923	-0.622

Plate number 3

<i>Imperfection code</i>	<i>Imperfection type</i>	<i>Imperfection magnitude</i>	<i>resistance (MN)</i>		<i>difference%</i>
			GMNIA	EN1993-1-5	
<i>combination1</i>	global mode	6.9	28.389	27.673	2.587
<i>combination2</i>	global mode	-6.9	33.954	27.673	22.697
<i>combination3</i>	local 9 sin waves	1.5	36.463	27.673	31.764
<i>combination4</i>	local 9 sin waves	-1.5	36.474	27.673	31.804
<i>combination5</i>	local 10 sin waves	1.38	36.175	27.673	30.723
<i>combination6</i>	local 10 sin waves	-1.38	36.175	27.673	30.723
<i>combination7</i>	stiffeners	h/50	37.549	27.673	35.688
<i>combination8</i>	- IP _g +0.7 IP _s +0.7 IP _{i-j}		33.459	27.673	20.908
<i>combination9</i>	- IP _g +0.7 IP _{i-j}		33.491	27.673	21.024
<i>combination10</i>	- IP _g +0.7 IP _s -0.7 IP _{i-j}		33.459	27.673	20.908
<i>combination11</i>	- IP _g -0.7 IP _{i-j}		33.491	27.673	21.024
<i>combination12</i>	- IP _g +0.7 IP _s +0.7 IP _{i-i}		33.331	27.673	20.446
<i>combination13</i>	-IMP3+0.7 IP _{i-i}		33.371	27.673	20.590
<i>combination14</i>	- IP _g +0.7 IP _s -0.7 IP _{i-i}		33.331	27.673	20.446
<i>combination15</i>	- IP _g -0.7 IP _{i-i}		33.371	27.673	20.590
<i>combination16</i>	IP _g -0.7 IP _s -0.7 IP _{i-j}		28.282	27.673	2.201
<i>combination17</i>	IP _g -0.7 IP _{i-j}		28.453	27.673	2.819
<i>combination18</i>	IP _g -0.7 IP _s +0.7 IP _{i-j}		28.326	27.673	2.360
<i>combination19</i>	IP _g +0.7 IP _{i-j}		28.453	27.673	2.819
<i>Combination20</i>	IP _g -0.7 IP _s -0.7 IP _{i-i}		28.413	27.673	2.674
<i>Combination21</i>	IP _g -0.7 IP _{i-i}		28.499	27.673	2.985
<i>Combination22</i>	IP _g -0.7 IP _s +0.7 IP _{i-i}		28.499	27.673	2.985
<i>Combination23</i>	IP _g +0.7 IP _{i-i}		28.413	27.673	2.674

Plate number 4

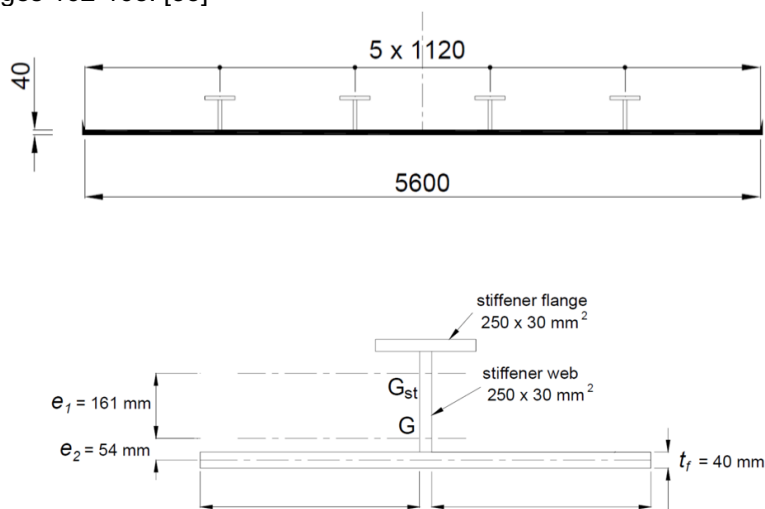
<i>Imperfection name</i>	<i>Imperfection type</i>	<i>Imperfection magnitude</i>	<i>resistance (MN)</i>		<i>difference%</i>
			GMNIA	EN1993-1-5	
<i>combination1</i>	global mode	5.175	31.897	31.430	1.486
<i>combination2</i>	global mode	-5.175	35.632	31.430	13.369
<i>combination3</i>	local 7 sin waves	-1.478571429	36.665	31.430	16.656
<i>combination4</i>	local 7 sin waves	1.478571429	36.708	31.430	16.793
<i>combination5</i>	local 6 sin waves	1.5	36.495	31.430	16.115
<i>combination6</i>	local 6 sin waves	-1.5	36.495	31.430	16.115
<i>combination7</i>	stiffeners	h/50	36.495	31.430	16.115
<i>combination8</i>	- IP _g +0.7 IP _s +0.7 IP _{l-j}		37.507	31.430	19.335
<i>combination9</i>	- IP _g +0.7 IP _{l-j}		35.355	31.430	12.488
<i>combination10</i>	- IP _g +0.7 IP _s -0.7 IP _{l-j}		34.801	31.430	10.725
<i>combination11</i>	- IP _g -0.7 IP _{l-j}		34.806	31.430	10.741
<i>combination12</i>	- IP _g +0.7 IP _s +0.7 IP _{l-i}		34.626	31.430	10.169
<i>combination13</i>	-IMP3+0.7 IP _{l-i}		35.174	31.430	11.912
<i>combination14</i>	- IP _g +0.7 IP _s -0.7 IP _{l-i}		34.620	31.430	10.150
<i>combination15</i>	- IP _g -0.7 IP _{l-i}		35.174	31.430	11.912
<i>combination16</i>	IP _g -0.7 IP _s -0.7 IP _{l-j}		30.491	31.430	-2.987
<i>combination17</i>	IP _g -0.7 IP _{l-j}		30.490	31.430	-2.990
<i>combination18</i>	IP _g -0.7 IP _s +0.7 IP _{l-j}		30.500	31.430	-2.960
<i>combination19</i>	IP _g +0.7 IP _{l-j}		30.590	31.430	-2.672
<i>Combination20</i>	IP _g -0.7 IP _s -0.7 IP _{l-i}		30.589	31.430	-2.676
<i>Combination21</i>	IP _g -0.7 IP _{l-i}		30.586	31.430	-2.685
Combination22	IP _g -0.7 IP _s +0.7 IP _{l-i}		30.485	31.430	-3.007
<i>Combination23</i>	IP _g +0.7 IP _{l-i}		30.491	31.430	-2.988

Plate number 5

<i>Imperfection code</i>	<i>Imperfection type</i>	<i>Imperfection magnitude</i>	<i>resistance (MN)</i>	<i>Resistance (MN)</i>	<i>difference%</i>
			GMNIA	EN1993-1-5	
<i>combination1</i>	global mode	5.48	52.299	50.50	3.562
<i>combination2</i>	global mode	-5.48	59.064	50.50	16.958
<i>combination3</i>	local 7 sin waves	1.57	60.399	50.50	19.602
<i>combination4</i>	local 7 sin waves	-1.57	60.399	50.50	19.602
<i>combination5</i>	local 8 sin waves	1.51	60.549	50.50	19.899
<i>combination6</i>	local 8 sin waves	-1.51	60.549	50.50	19.899
<i>combination7</i>	stiffeners	h/50	62.638	50.50	24.036
<i>combination8</i>	- IP _g +0.7 IP _s +0.7 IP _{l-j}		58.155	50.50	15.158
<i>combination9</i>	- IP _g +0.7 IP _{l-j}		58.179	50.50	15.206
<i>combination10</i>	- IP _g +0.7 IP _s -0.7 IP _{l-j}		57.943	50.50	14.739
<i>combination11</i>	- IP _g -0.7 IP _{l-j}		57.967	50.50	14.786
<i>combination12</i>	- IP _g +0.7 IP _s +0.7 IP _{l-i}		58.394	50.50	15.632
<i>combination13</i>	-IMP3+0.7 IP _{l-i}		58.412	50.50	15.667
<i>combination14</i>	- IP _g +0.7 IP _s -0.7 IP _{l-i}		58.394	50.50	15.632
<i>combination15</i>	- IP _g -0.7 IP _{l-i}		58.412	50.50	15.667
<i>combination16</i>	IP _g -0.7 IP _s -0.7 IP _{l-j}		52.393	50.50	3.749
<i>combination17</i>	IP _g -0.7 IP _{l-j}		52.724	50.50	4.404
<i>combination18</i>	IP _g -0.7 IP _s +0.7 IP _{l-j}		51.291	50.50	1.566
<i>combination19</i>	IP _g +0.7 IP _{l-j}		52.850	50.50	4.653
<i>Combination20</i>	IP _g -0.7 IP _s -0.7 IP _{l-i}		51.283	50.50	1.550
<i>Combination21</i>	IP _g -0.7 IP _{l-i}		52.724	50.50	4.404
Combination22	IP _g -0.7 IP _s +0.7 IP _{l-i}		51.270	50.50	1.525
<i>Combination23</i>	IP _g +0.7 IP _{l-i}		52.724	50.50	4.404

ANNEX II

The python script for determining the ultimate resistance of the stiffened plate. The code is able to determine the critical plate-like buckling stress, critical column-like buckling stress and the ultimate resistance of the single stiffened plate base on the criteria of the EN1993-1-5. The code is verified with an example from the Guidance book Eurocodes 3 and 4 – “Application to steel- concrete composite road bridges”, pages 162-168. [35]



Input		Unit
Width of the plate	5600	mm
Length of the plate	4000	mm
Thickness of the plate	40	mm
Number of the stiffeners	5	
Area of one stiffener	15000	mm ²
Second moment inertia of one stiffeners	113125000	mm ⁴
Eccentricity from the plate inner edge	195	mm

Out put	reference [35]	Python script
Plate-like buckling factor	127.83	127.7
σ_E	9.68	9.68
Critical plate-like buckling stress	1237.4	1236.9
Critical column-like buckling stress	1383	1383.2
ξ	0	0
p	1	1
χ_c	0.808	0.804
p_c	0.808	0.804

The python script for determining the ultimate bending resistance of the box girder is presented in this annex. The code is able to determine the bending resistance base on the criteria of the EN1993-1-5.

```

%matplotlib inline
import numpy as np
import matplotlib.pyplot as plt
import pandas as pd

#The outerest coordinate of the plate
x1=0;x2=5600
#Thickness of the plate
ttf=40
#yield stress of the stell
fy=355
#length of the plate
a=4000
E=2.1* 10**5
epsilon=(235/fy)**0.5
v=0.3
#number of the stiffeners
nf=4;
#dimention of the web of the stiffeners
t_stf=30 ;h_stf=250;
#section properties of a single stiffner
l_flange_stiffeners=113125000
A_flange_stiffeners=15000
e_flange_stiffeners=195
Ag = (x2 - x1) * ttf + nf * A_flange_stiffeners
di=(x2 - x1) * ttf**2 / 2 + nf*A_flange_stiffeners*(e_flange_stiffeners+ttf)
nlg=di/Ag
lg=(x2-x1)*ttf**3/12+(x2-x1)*ttf*(nlg-ttf/2)**2 + nf*l_flange_stiffeners+ (nf*A_flange_stiffeners) * (e_flange_stiffeners+ttf-nlg)**2
A_sl_star=A_flange_stiffeners+ (10*ttf**2 +t_stf) * ttf
di_star = (A_flange_stiffeners * (e_flange_stiffeners+ ttf) +( 10*ttf**2 +t_stf) * ttf * ttf / 2)/ A_sl_star
l_sl_star = l_flange_stiffeners+ ( 10*ttf**2 +t_stf) * ttf**3 / 12 + ( 10*ttf**2 +t_stf) * ttf * (di_star - ttf / 2) ** 2+ A_flange_stiffeners *
(e_flange_stiffeners+ttf-di_star)**2
#Minimum stiffness of the stiffeners based on the criteria of the draft of new EN1993-1-5
Relative_bending_stiffness=E* l_sl_star/(x2 - x1)/(E*ttf**3/12/(1-v**2))
if Relative_bending_stiffness>25:
    print('Relative bending stiffness=',Relative_bending_stiffness, 'requirement satisfied')
else:
    print('Relative bending stiffness=',Relative_bending_stiffness, 'requirement not satisfied')
#Classification of the plate
# ψ used in Table 4.2 for web should be obtained using a stress distribution based on the effective area of the compression
flange and the gross area of the web.
# ψ used in Table 4.2-EN1993-1-5 for flange should be obtained using a stress distribution based on the gross area of the
section.
ULS=1
if (x2-x1 - nf *t_stf)/ttf/(nf+1)> 42:
    labda_bar_p=(x2-x1- nf *t_stf)*ULS/ttf/(nf+1)/28.4/epsilon/4**0.5
    if labda_bar_p >0.673:
        p_local=(labda_bar_p-0.055*(1+3))/(labda_bar_p)**2
        if p_local>1:
            p_local=1
    if labda_bar_p <=0.673:
        p_local=1
    print ('distance between stiffeners has class 4 reduce the element by',p_local )
    local_buckling_plate=p_local
else:
    print('flange subpanels have class 3')
    local_buckling_plate=1
# classification of the stiffeners in plate
if ((h_stf)/t_stf)> 42* epsilon:
    si=1
    k_sigma=0.578/(0.34+si)
    labda_bar_p=(h_stf)/t_stf/28.4/epsilon/k_sigma**0.5

    if labda_bar_p >0.5+(0.085-0.055*si)**0.5:
        p_local=(labda_bar_p-0.188)/(labda_bar_p)**2
        if p_local>1:
            p_local=1
    if labda_bar_p <=0.5+(0.085-0.055*si)**0.5:
        p_local=1

```

```

print ('stiffeners has class 4 reduce the element by',p_local )
local_buckling_stiffeners=p_local
else:
print('stiffeners have class 3')
local_buckling_stiffeners=1.0
#Plate-like buckling in plate with pure compression
if nf==0:
sigma_cr_p=4*(np.pi**2*E*tf**2)/(12*(1-v**2)*(x2 - x1 )**2)
beta_a_c=1
print(sigma_cr_p)
if 0<nf<=2:
b1=(x2-x1)/(nf+1)
b2=b1
di=(A_flange_stiffeners*(e_flange_stiffeners+ttf)+(b1+b2)/2*tf**2/2)/(A_flange_stiffeners+(b1+b2)/2*tf)
Asl=A_flange_stiffeners+(b1+b2)/2*tf
l_sl_i=l_flange_stiffeners+((b1+b2)/2)*12*tf**3+(b1+b2)/2*tf*(di-ttf/2)**2+A_flange_stiffeners*(e_flange_stiffeners+ttf-di)**2
print(l_sl_i)
a_c=4.33*(l_sl_i*b1**2*b2**2/tf**3/(x2-x1-2))**0.25
if a>= a_c:
sigma_cr_sl=1.05*E/Asl*(l_sl_i*tf**3*(x2-x1))**0.5/b1/b2
elif a< a_c:
sigma_cr_sl=np.pi**2*E* l_sl_i/Asl/a**2+(E*tf**3*(x2-x1)*a**2)/(4*(np.pi)**2*(1-v**2)*Asl*b1**2*b2**2)
Asl_lumped= 2*Asl
l_sl_lumped =2*l_sl_i
b1=b2=(x2-x1)/2
a_c=4.33*(l_sl_lumped*b1**2*b2**2/tf**3/(x2-x1))**0.25
if a>= a_c:
sigma_cr_sl_lumped=1.05*E/Asl_lumped*( l_sl_lumped*tf**3*(x2-x1))**0.5/b1/b2
elif a< a_c:
sigma_cr_sl_lumped=np.pi**2*E* l_sl_lumped /Asl_lumped/a**2+(E*tf**3*(x2-x1)*a**2)/(4*(np.pi)**2*(1-
v**2)*Asl_lumped*b1**2*b2**2)
sigma_cr_p=min( sigma_cr_sl_lumped, sigma_cr_sl)
elif nf>2:
Asl_p = A_flange_stiffeners * nf + (x2 - x1 ) * ttf
di =(A_flange_stiffeners* nf * (e_flange_stiffeners + ttf) +(x2 - x1 ) * ttf** 2/ 2)/ Asl_p
l_sl = l_flange_stiffeners * nf + (x2-x1) / 12 * ttf**3 + (x2 - x1 ) * ttf * (di - ttf / 2) ** 2+ A_flange_stiffeners *
(e_flange_stiffeners+ttf-di)**2 * nf
lp=(x2-x1)*tf**3/10.92
Asl=A_flange_stiffeners
gamma= l_sl/lp; delta=(Asl)*nf/((x2-x1)*ttf)
alpha= max(a/(x2-x1), 0.5)
if alpha <= (gamma)**0.25:
k_p =2* ((1+alpha**2)**2 +gamma -1)/(alpha**2*(1+delta))
elif alpha > (gamma)**0.25:
k_p= (4* (1+gamma**0.5))/(2*(1+delta))
sigma_cr_p =k_p * np.pi**2 * E * (ttf/(x2-x1))**2 /12 / (1-v**2)
beta_a_c=1
labda_bar_p=(beta_a_c*fy/sigma_cr_p)**0.5
if labda_bar_p >0.673:
p_plate=(labda_bar_p-0.055*(1+3))/(labda_bar_p)**2
elif labda_bar_p <=0.673:
p_plate=1
p_plate= min(1,p_plate )
print ('critical plate-like buckling stress=',sigma_cr_p,'plate-like buckling reduction factor=',p_plate )
p_cr=sigma_cr_p*(x2-x1)*ttf/1000*local_buckling_plate
print(f'Sigma_E = {np.pi**2 * E * (ttf/(x2-x1))**2 /12 / (1-v**2):0.5}')

#Column-like buckling in plate with pure compression
Asl_1 = A_flange_stiffeners + (x2 - x1 ) / (nf + 1) * ttf
Asl_1_eff=A_flange_stiffeners+ (x2 - x1 ) / (nf + 1) * ttf*local_buckling_plate
beta_a_c=Asl_1_eff/Asl_1
di=(A_flange_stiffeners*(e_flange_stiffeners+ttf)+(x2-x1)/(nf+1)*tf**2/2*p_plate)/ Asl_1
l_sl_1=l_flange_stiffeners+(x2-x1)*p_plate/(nf+1)/12*tf**3+((x2-x1)*p_plate/(nf+1))*tf*(di-
ttf/2)**2+A_flange_stiffeners*(e_flange_stiffeners+ttf-di)**2
i=(l_sl_1/Asl_1)**0.5
e=max(np.abs(di-ttf/2),np.abs(e_flange_stiffeners+ttf-di))
beta_a_c=1
sigma_cr_c=(np.pi**2*E*l_sl_1)/(Asl_1*a**2)
labda_bar_c=(beta_a_c*fy/sigma_cr_c)**0.5
alpha_e=0.49+0.09/(i/e)
phi=0.5*(1+alpha_e*(labda_bar_c-0.2))+labda_bar_c**2)
chi_c=1/(phi+(phi**2-labda_bar_c**2)**0.5)
epsi=sigma_cr_p/sigma_cr_c-1
print(f'critical stress coloumn like buckling = {sigma_cr_c:0.05} coloumn like buckling reduction factor= {chi_c:0.2}')
#plate-like and column-like reduction factor
print(epsi)

```

```
if epsi < 0:
    epsi=0
    print('ξ<0 behavioe pure coloumn like buckling')
elif epsi>1:
    epsi=1
    print('ξ>1 behavioe pure plate-like buckling')
else:
    print('global buckling is combination of coloumn like and plate-like')
pc_flange=(p_plate -chi_c)*(epsi)*epsi*(2-epsi)+chi_c
pc_flange=min(pc_flange,1)
print(f'plate and coloumn like buckling reduction factor in top flange{pc_flange:0.03}')
# effective area of the compression flange and ultimate resistanc ebased on EN1993-1-5
A_c_eff=(x2 - x1) * ttf/(nf+1)*ULS*local_buckling_plate+pc_flange*(A_flange_stiffeners *local_buckling_stiffeners*nf+ (x2 - x1)
* ttf* (nf)/(nf+1)*ULS*local_buckling_plate)
F_ULTIMATE=A_c_eff*fy/10**6
print(f'ultimate compression resistance= {F_ULTIMATE:0.5} MN')
print(A_c_eff)
print('ratio=',F_ULTIMATE* 10**6/fy/Ag)
```


Annex III

Python script for determining the bending resistance of the plated girder.

```

#Plate-like buckling in flange with pure compression
sigma_E=MeI/g*(nlg)
for iteration in range (5):
print('beginning of iteration ',iteration+1,'in the whole section ')
if (x2-x1-2*tw - nf *t_stf)/tff*(nf+1)> 42:
labda_bar_p=(x2-x1-2*tw - nf *t_stf)*ULS/tff*(nf+1)/28.4/epsilon/4**0.5
labda_bar_p=(sigma_E/ty)**0.5 *labda_bar_p
if labda_bar_p >0.673:
p_local=(labda_bar_p-0.055*(1+3))/(labda_bar_p)**2
if p_local>1:
p_local=1
if labda_bar_p <=0.673:
p_local=1
print('distance between stiffeners has class 4 reduce the element by {p_local:0.4} ')
local_buckling_plate=p_local
else:
print('flange subpanels have class 3')
local_buckling_plate=1

#Stiffeners classification in flange
if ((h_stf)/t_stf)> 42* epsilon:
si=1
k_sigma=0.578/(0.34+si)
labda_bar_p=(h_stf)/t_stf/28.4/epsilon/k_sigma**0.5
if labda_bar_p >0.5+(0.085-0.055*si)**0.5:
p_local=(labda_bar_p-0.188)/(labda_bar_p)**2
if p_local>1:
p_local=1
if labda_bar_p <=0.5+(0.085-0.055*si)**0.5:
p_local=1
print('stiffeners has class 4 reduce the element by {p_local:0.4} ')
local_buckling_stiffeners=p_local
else:
print('stiffeners have class 3')
local_buckling_stiffeners=1.0

if nf==0:
sigma_cr_p=4*(np.pi**2*E*tw**2)/(12*(1-v**2)*(x2 - x1 - 2 * tw)**2)

if 0<nf<2:
beta_a_c=1
b1=(x2-x1-2*tw)/(nf+1)
b2=b1
di=(A_flange_stiffeners*(e_flange_stiffeners+tff)+(b1+b2)/2**tff**2/2)/(A_flange_stiffeners*(b1+b2)/2**tff)
Asl=A_flange_stiffeners*(b1+b2)/2**tff
l_sl_i=flange_stiffeners*((b1+b2)/2)/12**tff**3+(b1+b2)/2**tff*(di-tff/2)**2+A_flange_stiffeners*(e_flange_stiffeners+tff-di)**2
a_c=4.33*(l_sl_i*b1**2*b2**2/tff**3*(x2-x1-2*tw)**0.25
if a>= a_c:
sigma_cr_sl=1.05*E/Asl*(l_sl_i**tff**3*(x2-x1-2*tw)**0.5/b1/b2
elif a< a_c:
sigma_cr_sl=np.pi**2*E* l_sl_i/Asl/a**2+(E*tff**3*(x2-x1-2*tw)*a**2)/(4*(np.pi)**2*(1-v**2)*Asl*b1**2*b2**2)
Asl_lumped=2*Asl
l_sl_lumped=2*l_sl_i
b1=b2=(x2-x1-2*tw)/2
a_c=4.33*(l_sl_lumped*b1**2*b2**2/tff**3*(x2-x1-2*tw)**0.25
if a>= a_c:
sigma_cr_sl_lumped=1.05*E/Asl_lumped*( l_sl_lumped**tff**3*(x2-x1-2*tw)**0.5/b1/b2
elif a< a_c:
sigma_cr_sl_lumped=np.pi**2*E* l_sl_lumped /Asl_lumped/a**2+(E*tff**3*(x2-x1-2*tw)*a**2)/(4*(np.pi)**2*(1-v**2)*Asl_lumped*b1**2*b2**2)
sigma_cr_p=min( sigma_cr_sl_lumped, sigma_cr_sl)
elif nf>=2:
Asl_p = A_flange_stiffeners * nf * (x2 - x1 - 2 * tw ) * tff
di =(A_flange_stiffeners * nf * (e_flange_stiffeners + tff) +(x2 - x1 - 2 * tw ) * tff** 2/ 2)/ Asl_p
l_sl = l_flange_stiffeners * nf + (x2-x1-2*tw) / 12 * tff**3 + (x2 - x1 - 2 * tw ) * tff * (di - tff / 2) ** 2+ A_flange_stiffeners * (e_flange_stiffeners+tff-di)**2 * nf
lp=(x2-x1-2*tw)*tff**3/10.92
Asl=A_flange_stiffeners
gamma= l_sl/lp, delta=(Asl)*nf/((x2-x1)*tff)
alpha= max(alpha((x2-x1), 0.5)
if alpha <= (gamma)**0.25:
k_p =2* ((1+alpha**2)**2 +gamma -1)/(alpha**2*2*(1+delta))
elif alpha > (gamma)**0.25:
k_p = (4* (1+gamma**0.5))/(2*(1+delta))
sigma_cr_p =k_p * np.pi**2 * E * (tff*(x2-x1))**2 / 12 / (1-v**2)

beta_a_c=1
labda_bar_p=(beta_a_c*fy/sigma_cr_p)**0.5
original= labda_bar_p
if sigma_E<355:
labda_bar_p=(sigma_E/ty)**0.5 *labda_bar_p
p_plate=min((1-0.055*4/labda_bar_p)/labda_bar_p+0.18*(original-labda_bar_p)/(original-0.6), 1)
elif labda_bar_p >0.673:
p_plate=(labda_bar_p-0.055*(1+3))/(labda_bar_p)**2
elif labda_bar_p <=0.673:
p_plate=1.0000
p_plate= min(1,p_plate )
print('critical plate-like buckling stress= {sigma_cr_p:0.4} plate-like buckling reduction factor= {p_plate}')
p_cr=sigma_cr_p*(x2-x1)*tff/1000*local_buckling_plate

#columnn like buckling for flange with pure compression
A_sl_star=A_flange_stiffeners + (10*tff**2 +t_stf ) * tff
di_star = (A_flange_stiffeners * (e_flange_stiffeners + tff) +(10*tff**2 +t_stf ) * tff * tff / 2)/ A_sl_star
l_sl = l_flange_stiffeners + (10*tff**2 +t_stf ) * tff**3 / 12 + (10*tff**2 +t_stf ) * tff * (di_star - tff / 2) ** 2+ A_flange_stiffeners * (e_flange_stiffeners+tff-di_star)**2

Relative_bending_stiffness=E* l_sl/(x2 - 2 * tw - x1)/(E*tff**3/12/(1-v**2))

Asl_1 = A_flange_stiffeners + (x2 - x1 - 2*tw) / (nf + 1) * tff
Asl_1_eff=A_flange_stiffeners+ (x2 - x1-2*tw) / (nf + 1) * tff*local_buckling_plate
beta_a_c=Asl_1_eff/Asl_1
di=(A_flange_stiffeners*(e_flange_stiffeners+tff)+(x2-x1-2*tw)/(nf+1)*tff**2/2*p_plate)/Asl_1
l_sl_1=flange_stiffeners*(x2-x1-2*tw)*p_plate/(nf+1)/12**tff**3+(x2-x1-2*tw)*p_plate/(nf+1)*tff*(di-tff/2)**2+A_flange_stiffeners*(e_flange_stiffeners+tff-di)**2
i=(l_sl_1/Asl_1)**0.5
e=max(np.abs(di-tff/2),np.abs(e_flange_stiffeners+tff-di))

sigma_cr_c=(np.pi**2 * E * l_sl_1)/(Asl_1 * a**2)
labda_bar_c=(beta_a_c*fy/sigma_cr_c)**0.5
alpha_e=0.49+0.09/(i/e)
phi=0.5*(1+alpha_e*(labda_bar_c-0.2))+labda_bar_c**2)
chi_c=1/(phi+(phi**2-labda_bar_c**2)**0.5)
epsi=sigma_cr_p/sigma_cr_c -1

print('critical stress coloumn like buckling {sigma_cr_c:0.4} coloumn like buckling reduction factor {chi_c:0.4}')

```

```

#combination
print(f'ξ= {epsi:0.4}')

epsi=sigma_cr_p/sigma_cr_c-1
if sigma_cr_p/sigma_cr_c-1 < 0:
    epsi=0
    print('epsi=0 behaviour pure column like buckling')
elif sigma_cr_p/sigma_cr_c-1>1:
    epsi=1
    print('epsi>1 behaviour pure plate-like buckling')
else:
    print('global buckling is combination of column like and plate-like')
pc_flange=(p_plate-chi_c)*(epsi)*epsi*(2-epsi)+chi_c

print(f'plate and column like buckling reduction factor in top flange {pc_flange:0.4}')

#####
#####

# cross section with effective compression flange for wb classifications

Ae = (local_buckling_stiffeners*ntf * A_flange_stiffeners + (((x2 - 2 * tw - x1)-(x2 - 2 * tw - x1)/(nf+1)) * ttf*ULS*local_buckling_plate))*pc_flange+(x2 - 2 * tw - x1)/(nf+1) *
ttf*local_buckling_plate+(x3 - x4 - 2 * tw) * ULS * tbf+(y1 - y4) * tw ** 2 +(nw - 1) * A_WEB_stiffeners ** 2
di=((x2 - 2 * tw - x1)-(x2 - 2 * tw - x1)/(nf+1)) * local_buckling_plate * (ttf**2) / 2 * ULS * pc_flange + (x2 - 2 * tw - x1)/(nf+1) * (ttf**2)/2 * local_buckling_plate + (y1 - y4)**2/2 * tw ** 2 + (x3 - x4 -
2 * tw) * tbf * ULS * (y1 - y4 - tbf/2) + local_buckling_stiffeners * ntf * A_flange_stiffeners * (e_flange_stiffeners + ttf) * pc_flange
sumation=0
for i in range(nw-1):
    sumation = 2 * A_WEB_stiffeners * (y1 - y4) / nw * (i + 1)
    di = di + sumation
nle = di / Ae
le = (x2 - 2 * tw - x1) - (x2 - 2 * tw - x1) / (nf + 1) * local_buckling_plate * ttf**3/12 * ULS * pc_flange + (x2 - 2 * tw - x1) - (x2 - 2 * tw - x1) / (nf + 1) * local_buckling_plate * ULS * pc_flange * ttf**2 +
(y1 - y4) ** 3 * tw ** 2 / 12 + 2 * (y1 - y4) / 2 * tw * ULS * (x3 - x4 - 2 * tw) * tbf**3/12 + (x3 - x4 - 2 * tw) * ULS * tbf * (y1 - y4 - tbf/2 - nlg)**2 + local_buckling_stiffeners * ntf * flange_stiffeners * pc_flange +
ntf * A_flange_stiffeners * (e_flange_stiffeners + ttf - nlg)**2 * local_buckling_stiffeners * (x2 - 2 * tw - x1) / (nf + 1) * (ttf**3/12 * local_buckling_plate + (x2 - 2 * tw - x1) / (nf + 1) * ttf * local_buckling_plate - nlg -
ttf/2)**2
sumation = 0
for i in range(nw-1):
    sumation = 2 * I_WEB_stiffeners + 2 * A_WEB_stiffeners * ((y1 - y4) / nw * (i + 1) - nlg)**2
    le = le + sumation
We = min(le/nle, le/(y1 - nle))
Mel = fy * We / 10**9
print('effective section properties reduced by flange effective width:')
print(f'we={We:0.4} mm3 ; Ae={Ae:0.4} mm2; le={le:0.4} mm4; neutral line from top = {nle:0.4} mm')
print(f'Mel= {fy*We/10**9:0.4} GN.mm - MN.m')
print(f'tension stress= {Mel/le*(y1-nle)*10**9:0.4} compression stress= { Mel/le*(nle)*10**9:0.4}')

if nw>1:
    for j in range(5):
        print('web subpanels class from top to bottom')
        panel_in_compression= int(nle/ ((y1-y4-ttf-tbf)/nw)+1)
        sub_panel=np.zeros(nw, 3)
        for i in range(panel_in_compression):
            si=(nle-ttf-(i+1)*(y1-y4-ttf-tbf)/nw)/((nle-ttf-i)*(y1-y4-ttf-tbf)/nw)
            if si>=0:
                state= 42*epsi/n
                if i==0:
                    sub_panel[(i,1)]=(y1-y4-ttf-tbf)/nw-(3-si)/(5-si)*y1/nw
                    sub_panel[(i,2)]=(3-si)/(5-si)*y1/nw
                else:
                    sub_panel[(i,1)]=(2)/(5-si)*y1/nw
                    sub_panel[(i,2)]=(3-si)/(5-si)*y1/nw
            elif -1<si<0:
                state= 42*epsi/n/(0.67+0.33*si)
                sub_panel[(i,1)]=0.4*(nle-ttf-i)*(y1-y4-ttf-tbf)/nw
                sub_panel[(i,2)]=y1/nw-(nle-ttf-i)*(y1-y4-ttf-tbf)/nw
            elif si<-1:
                state=62*epsi/n*(1-si)*(si)**0.5
                sub_panel[(i,1)]=0.4*(nle-ttf-i)*(y1-y4-ttf-tbf)/nw
                sub_panel[(i,2)]=y1/nw-(nle-ttf-i)*(y1-y4-ttf-tbf)/nw
            if ((y1-y4-ttf-tbf)/nw) / tw > state:
                if 0<=si<=1:
                    k_p=8.2/(1.05+si)
                    if -3<=si<=-1:
                        k_p=5.98/(1-si)**2
                    sigma_cr_web=np.pi**2*E*tw**2/12/((y1 - y4) - ttf-tbf)**2/(1-v**2)*k_p
                    labda_bar_web=(y1-y4-ttf-tbf)/tw/nw/(28.2*epsi/n*k_p**0.5)
                    if labda_bar_web > 0.673:
                        p_local_web=(labda_bar_web-0.055*(si+3))/(labda_bar_web)**2
                    elif labda_bar_web <= 0.673:
                        p_local_web=1
                    local_buckling_web=min(p_local_web,1)
                    print('subpanel',i+1,'has class 4, 'ψ=,si, 'p_local_web=', local_buckling_web)
                    sub_panel[(i,0)]=local_buckling_web
                else:
                    p_local_web=1
                    print('subpanel',i+1,'has class 3, 'ψ=,si, 'p_local_web=', p_local_web)
                    sub_panel[(i,0)]=p_local_web
            if p_local_web==1:
                sub_panel[(i,1)]=y1/nw/2
                sub_panel[(i,2)]=y1/nw/2

        for i in range(panel_in_compression,nw):
            print(f'subpanel {i+1}, is in tension')
            sub_panel[(i,0)]= 1
            sub_panel[(i,1)]=y1/nw/2
            sub_panel[(i,2)]=y1/nw/2
# print('gross section width=')
# print(sub_panel)
sub_panel_local=sub_panel
sub_panel_local[:,1]=sub_panel[:,0]*sub_panel[:,1]
sub_panel_local[:,2]=sub_panel[:,0]*sub_panel[:,2]
print('local section width=')
print(sub_panel_local)

if int(nle/ ((y1-y4-ttf-tbf)/nw)+1)>2:
    Asl_p = A_WEB_stiffeners * (nw-1) * (y1) * tw
    di=(A_WEB_stiffeners * (nw-1) * (e_WEB_stiffeners + tw) + (y1) * tw ** 2 / 2) / Asl_p
    I_sl = I_WEB_stiffeners * (nw-1) * (y1) / 12 * tw**3 + (y1) * tw * (di - tw / 2) ** 2 + A_WEB_stiffeners * (e_WEB_stiffeners+tw-di)**2 * (nw-1)
    Ip=(y1) ** 3 / 10.92
    si_w=max(nle/ (nle-(y1)), 0.5)
    Asl=A_WEB_stiffeners
    gamma= I_sl/Ip; delta=(Asl)*(nw-1)/((y1) * tw)
    alpha= max(a/(y1) , 0.5)

    if alpha <= (gamma)**0.25:

```

```

k_p = 2 * ((1 + alpha ** 2) ** 2 + gamma - 1) / (alpha ** 2 * (si_w + 1) * (1 + delta))
elif alpha > (gamma) ** 0.25:
    k_p = 4 * (1 + gamma ** 0.5) / ((si_w + 1) * (1 + delta))
sigma_cr_p = k_p * np.pi ** 2 * E * (tw / (y1)) ** 2 / 12 / (1 - nu ** 2)

#####

beta_a_c = (A_WEB_stiffeners + (y1 / nw) * sub_panel[(0,0)] * tw) / (A_WEB_stiffeners + (y1 / nw) * tw)
labda_bar_p = (beta_a_c * fy / sigma_cr_p) ** 0.5
labda_bar_p = (sigma_E / fy) ** 0.5 * labda_bar_p

if labda_bar_p > 0.673:
    p_web = (labda_bar_p - 0.055 * (1 + 3)) / (labda_bar_p) ** 2
elif labda_bar_p <= 0.673:
    p_web = 1
p_web = min(1, p_web)
print('critical plate-like buckling stress=', sigma_cr_p, 'plate-like buckling reduction factor=', p_web)
p_cr = sigma_cr_p * (x2 - x1) ** 2 / 1000 * local_buckling_plate

#column-like buckling

Asl_1 = A_WEB_stiffeners + (sub_panel[(0,2)] + sub_panel[(0,1)]) * tw
Asl_1_eff = A_WEB_stiffeners + sub_panel_local[(0,2)] + sub_panel_local[(0,1)] * tw
beta_a_c = Asl_1_eff / Asl_1
di = (A_WEB_stiffeners * (e_WEB_stiffeners + tw) + (sub_panel[(0,2)] + sub_panel[(0,1)]) * tw ** 2) / Asl_1
l_sl_1 = (A_WEB_stiffeners * (sub_panel[(0,2)] + sub_panel[(0,1)]) / 12 * tw ** 3 + (sub_panel[(0,1)]) * tw * (di - tw / 2) ** 2 + A_WEB_stiffeners * (e_WEB_stiffeners + tw - di) ** 2) / (l_sl_1 / Asl_1) ** 0.5
e = max(np.abs(di - tw / 2), np.abs(e_WEB_stiffeners + tw - di))

sigma_cr_sl = (np.pi ** 2 * E * l_sl_1) / (Asl_1 * a ** 2)
sigma_cr_c = sigma_cr_sl * nle / (nle - y1 / nw)
labda_bar_c = (beta_a_c * fy / sigma_cr_c) ** 0.5
alpha_e = 0.49 + 0.09 / (i / e)
phi = 0.5 * (1 + alpha_e * (labda_bar_c - 0.2) + labda_bar_c ** 2)
chi_c = 1 / (phi + (phi ** 2 - labda_bar_c ** 2) ** 0.5)
epsi = sigma_cr_p / sigma_cr_c - 1

print('critical stress coloumn like buckling', sigma_cr_c, 'coloumn like buckling reduction factor', chi_c)
epsi = sigma_cr_p / sigma_cr_c - 1
print('xi=(epsi:0.5)')
if sigma_cr_p / sigma_cr_c - 1 < 0:
    epsi = 0
    print('epsi=0 behavioe pure coloumn like buckling')
elif sigma_cr_p / sigma_cr_c - 1 > 1:
    epsi = 1
    print('epsi>1 behavioe pure plate-like buckling')
else:
    print('global buckling is combination of coloumn like and plate-like')
pc_web = (p_web - chi_c) * (epsi) * epsi ** (2 - epsi) + chi_c
print('plate and coloumn like buckling reduction factor in web', pc_web)

di = ((x2 - 2 * tw - x1) - (x2 - 2 * tw - x1) * (nf + 1)) * local_buckling_plate * (ttf ** 2) / 2 * ULS * pc_flange + (x2 - 2 * tw - x1) * (nf + 1) * (ttf ** 2) / 2 * local_buckling_plate + (x3 - x4 - 2 * tw) * tbf * ULS * (y1 - y4 - tbf / 2) + local_buckling_stiffeners * nf * A_flange_stiffeners * (e_flange_stiffeners + ttf) * pc_flange
Ae = (local_buckling_stiffeners * nf * A_flange_stiffeners + ((x2 - 2 * tw - x1) - (x2 - 2 * tw - x1) * (nf + 1)) * ttf * ULS * local_buckling_plate) * pc_flange + (x2 - 2 * tw - x1) * (nf + 1) * ttf * local_buckling_plate + (x3 - x4 - 2 * tw) * ULS * tbf + (nw - 1) * A_WEB_stiffeners * 2

for i in range(panel_in_compression):
    Ae = Ae + (sub_panel_local[(i,2)] + sub_panel_local[(i,1)]) * tw * 2 * pc_web
    if i == 0:
        Ae = Ae - sub_panel_local[(i,1)] * tw * 2 * pc_web + sub_panel_local[(i,1)] * tw * 2
    di = di + sub_panel_local[(i,1)] * tw * 2 * (y2 / nw) + sub_panel_local[(i,1)] / 2 * pc_web + sub_panel_local[(i,2)] * tw * 2 * (y2 / nw) + (i + 1) - sub_panel_local[(i,2)] / 2 * pc_web
    if i == 0:
        di = di - sub_panel_local[(i,1)] * tw * 2 * (y2 / nw) + sub_panel_local[(i,1)] / 2 * pc_web + sub_panel_local[(i,1)] * tw * 2 * (y2 / nw) + sub_panel_local[(i,1)] / 2 * pc_web
for i in range(panel_in_compression, nw):
    Ae = Ae + (sub_panel_local[(i,2)] + sub_panel_local[(i,1)]) * tw * 2
    di = di + sub_panel_local[(i,1)] * tw * 2 * (y2 / nw) + sub_panel_local[(i,1)] / 2 + sub_panel_local[(i,2)] * tw * 2 * (y2 / nw) + (i + 1) - sub_panel_local[(i,2)] / 2

sumation = 0
for i in range(panel_in_compression - 1):
    sumation = sumation + 2 * A_WEB_stiffeners * (y1 - y4) / nw * (i + 1) * pc_web
for i in range(panel_in_compression - 1, nw - 1):
    sumation = sumation + 2 * A_WEB_stiffeners * (y1 - y4) / nw * (i + 1)
di = di + sumation
nle = di / Ae
le = ((x2 - 2 * tw - x1) - (x2 - 2 * tw - x1) * (nf + 1)) * local_buckling_plate * ttf ** 3 / 12 * ULS * pc_flange + ((x2 - 2 * tw - x1) - (x2 - 2 * tw - x1) * (nf + 1)) * local_buckling_plate * ULS * pc_flange * ttf * (nlg - ttf / 2) ** 2 + ULS * (x3 - x4 - 2 * tw) * tbf ** 3 / 12 + (x3 - x4 - 2 * tw) * ULS * tbf * (y1 - y4 - tbf / 2 - nlg) ** 2 + local_buckling_stiffeners * nf * A_flange_stiffeners * pc_flange + nf * A_flange_stiffeners * (e_flange_stiffeners + ttf - nlg) ** 2 * local_buckling_stiffeners + (x2 - 2 * tw - x1) * (nf + 1) * (ttf ** 3) / 12 * local_buckling_plate + (x2 - 2 * tw - x1) * (nf + 1) * ttf * local_buckling_plate * (nlg - ttf / 2) ** 2

for i in range(panel_in_compression):
    le = le + pc_web * (sub_panel_local[(i,1)] ** 3) * tw * 2 / 12 + pc_web * (sub_panel_local[(i,2)] ** 3) * tw * 2 / 12 + pc_web * sub_panel_local[(i,1)] * tw * 2 * (nle - (y2 / nw) * i + sub_panel_local[(i,1)] / 2) ** 2 + pc_web * sub_panel_local[(i,2)] * tw * 2 * (nle - (y2 / nw) * (i + 1) + sub_panel_local[(i,2)] / 2) ** 2
    if i == 0:
        le = le - pc_web * (sub_panel_local[(i,1)] ** 3) * tw * 2 / 12 + (sub_panel_local[(i,1)] ** 3) * tw * 2 / 12 - pc_web * sub_panel_local[(i,1)] * tw * 2 * (nle - (y2 / nw) * i + sub_panel_local[(i,1)] / 2) ** 2
sumation = 0
for i in range(panel_in_compression):
    sumation = 2 * A_WEB_stiffeners * pc_web + 2 * A_WEB_stiffeners * (y1 - y4) / nw * (i + 1) * nlg ** 2 * pc_web
le = le + sumation
sumation = 0
for m in range(panel_in_compression - 1, nw - 1):
    sumation = 2 * A_WEB_stiffeners + 2 * A_WEB_stiffeners * (y1 - y4) / nw * (m + 1) - nlg ** 2
le = le + sumation
for i in range(panel_in_compression - 1, nw - 1):
    le = le + (sub_panel_local[(i,1)] ** 3) * tw * 2 / 12 + (sub_panel_local[(i,2)] ** 3) * tw * 2 / 12 + sub_panel_local[(i,1)] * tw * 2 * ((nle - (y2 / nw) * i + 1) + sub_panel_local[(i,1)] / 2) ** 2 + sub_panel_local[(i,2)] * tw * 2 * ((nle - (y2 / nw) * (i + 1) + sub_panel_local[(i,2)] / 2) ** 2
We = np.abs(min(le / nle, le / (y1 - nle)))
Meff = fy * We / 10 ** 9
print('f in iteration (i+1) we={We:0.4} mm3; Ae={Ae:0.4} mm2; le={le:0.4} mm4; neutral line from top = {nle:0.4} mm; momet resistance(Meff:0.4)')
sigma_E = np.abs(min(Meff ** 10 ** 9 / le * nle, 355))
print('sigma_E=', sigma_E)
print('-----')

if nw == 1:
    for i in range(5):
        si = (nle + tbf - y1) / (nle - ttf)
        if -1 < si < 0:
            k_p = 7.81 - 6.29 * si + 9.78 * si ** 2
        elif -3 < si < -1:
            k_p = 5.98 * (1 - si) ** 2
        sigma_cr_web = np.pi ** 2 * E * tw ** 2 / 12 / ((y1 - y4) - ttf - tbf) ** 2 / (1 - nu ** 2) * k_p
        labda_bar_web = (y1 - y4) - ttf - tbf / tw / (28.4 * epsilon * (k_p ** 0.5))
        if si > -1:
            state = 42 * epsilon / (0.67 + 0.33 * si)
        elif si < -1:
            state = 62 * epsilon * (1 - si) * (-si) ** 0.5
        if (y1 - y4 - ttf - tbf) / tw > state:

```

```

if labda_bar_web > 0.673:
    p_local = (labda_bar_web - 0.055 * (1 + 3)) / (labda_bar_web) ** 2
elif labda_bar_web <= 0.673:
    p_local = 1
    local_buckling_web = min(p_local, 1)
    print('unstiffed web has section 4 local buckling=', local_buckling_web)
    local_buckling_web = p_local
else:
    print('whole web is active and has class 3')
    local_buckling_web = 1
    b_effective_web_compression = local_buckling_web * (nle - ttf)
    b_e_1_web = 0.4 * b_effective_web_compression
    b_e_2_web = 0.6 * b_effective_web_compression
    b_effective_web_tension = (y1 - y4) * (nle - ttf)

Ae = (local_buckling_stiffeners * nf * A_flange_stiffeners + ((x2 - 2 * tw - x1) * (x2 - 2 * tw - x1) / (nf + 1)) * ttf * ULS * local_buckling_plate) * pc_flange + (x2 - 2 * tw - x1) / (nf + 1) *
ttf * local_buckling_plate + (x3 - x4 - 2 * tw) * ULS * tbf + (nw - 1) * A_WEB_stiffeners * 2 * b_effective_web_tension * tw * 2 + (b_e_1_web + b_e_2_web) * tw * 2
di = ((x2 - 2 * tw - x1) * (x2 - 2 * tw - x1) / (nf + 1)) * local_buckling_plate * (ttf ** 2) / 2 * ULS * pc_flange + (x2 - 2 * tw - x1) / (nf + 1) * (ttf ** 2) / 2 * local_buckling_plate + (x3 - x4 - 2 * tw) * tbf * ULS * (y1 - y4 - tbf / 2) +
local_buckling_stiffeners * nf * A_flange_stiffeners * ((e_flange_stiffeners + ttf) * pc_flange + b_effective_web_tension * (-b_effective_web_tension / 2 + (y1 - y4)) * tw * 2 + b_e_1_web * (b_e_1_web / 2) * tw
* 2 + b_e_2_web * (b_effective_web_compression - b_e_2_web / 2) * tw * 2
sumation = 0
for i in range(nw - 1):
    sumation = 2 * A_WEB_stiffeners * (y1 - y4) / nw * (i + 1)
di = di + sumation
nle = di / Ae
le = ((x2 - 2 * tw - x1) * (x2 - 2 * tw - x1) / (nf + 1)) * local_buckling_plate * ttf ** 3 / 12 * ULS * pc_flange + (x2 - 2 * tw - x1) * (x2 - 2 * tw - x1) / (nf + 1) * local_buckling_plate * ULS * pc_flange * ttf * (nlg - ttf / 2) ** 2
+ ULS * (x3 - x4 - 2 * tw) * tbf ** 3 / 12 + (x3 - x4 - 2 * tw) * ULS * tbf * (y1 - y4 - tbf / 2 - nlg) ** 2 + local_buckling_stiffeners * nf * A_flange_stiffeners * pc_flange + nf * A_flange_stiffeners * (e_flange_stiffeners + ttf - nlg) ** 2
local_buckling_stiffeners * (x2 - 2 * tw - x1) / (nf + 1) * (ttf ** 3) / 12 * local_buckling_plate + (x2 - 2 * tw - x1) / (nf + 1) * ttf * local_buckling_plate * (nlg - ttf / 2) ** 2 + (b_effective_web_tension ** 3) * tw * 2 / 12 +
2 * (b_effective_web_tension) * tw * (-b_effective_web_tension / 2 + (y1 - y4) - nlg) ** 2 + (b_e_1_web ** 3) * tw / 12 * 2 + (b_e_1_web) * tw * ((nlg - b_e_1_web / 2) ** 2) + (b_e_2_web ** 3) * tw / 12 * 2 + (b_e_2_web * tw
* 2) * ((b_effective_web_compression - b_e_2_web / 2) - nlg) ** 2
sumation = 0
for i in range(nw - 1):
    sumation = 2 * I_WEB_stiffeners + 2 * A_WEB_stiffeners * ((y1 - y4) / nw * (i + 1) - nlg) ** 2
le = le + sumation
We = min(le / nle, le / (y1 - nle))
Meff = fy * We / 10 ** 9
print('In iteration {i+1} we={We:0.4} mm3 ; Ae={Ae:0.4} mm2; le={le:0.4} mm4; neutral line from top = {nle:0.4} mm Meff={Meff:0.4}')
print('Tension stress={Meff/le*(y1-nle)*10**9:0.4} compression stress={Meff/le*(-nle)*10**9:0.4}')
sigma_E = np.abs(min(Meff * 10 ** 9 / le * nle, 355))
print(We)
print(Meff)
print('.....')
print('end iteration ', iteration + 1, 'in the whole section ', local_buckling_web)
print('.....')
#1 shear lag effect for sagging moment

if nf == 0:
    alfa_zero = 1
else:
    alfa_zero = (1 + A_flange_stiffeners * nf / ((x2 - x1 - 2 * tw) * ttf)) ** 0.5

kappa = alfa_zero * (x2 - x1 - 2 * tw) / Le

if kappa <= 0.02:
    beta = 1.0
elif 0.02 < kappa < 0.70:
    beta = 1 / (1 + 6.4 * kappa ** 2)
elif kappa > 0.7:
    beta = 1 / (8.6 * kappa)

Asl_p = A_flange_stiffeners * nf + (x2 - x1 - 2 * tw) * ttf
combi = beta

#combined effects of shear lag and of plate buckling = same as elastic if it is class 3

#Elastic-plastic shear lag effects allowing for limited plastic strains may be taken into account using Aeff as follows
ULS = max(beta ** kappa, beta)
print('reduction by elastic shear lag in SLS=', combi)
print('reduction by plastic shear lag in ULS=', ULS)
beta_a_p = (h_stf * t_stf * nf * combi + ((x2 - x1 - 2 * tw) * ttf * combi)) / Asl_p
#ttf = ttf * beta ** kappa
Asl_1 = h_stf * t_stf + (x2 - x1 - 2 * tw) / (nf + 1) * ttf
Asl_1_eff_local = combi * (x2 - x1 - 2 * tw) / (nf + 1) * ttf + h_stf * t_stf * combi
beta_a_c = Asl_1_eff_local / Asl_1

#Only panels
ULS = 1
A_lag = (x2 - 2 * tw - x1) * ttf * beta + (y1 - y4) * tw * 2 + (x3 - x4 - 2 * tw) * tbf * beta + nf * A_flange_stiffeners * beta + (nw - 1) * A_WEB_stiffeners * 2
di_lag = (x2 - 2 * tw - x1) * (ttf ** 2) * beta / 2 + ((y1 - y4) ** 2) / 2 * tw * 2 + (x3 - x4 - 2 * tw) * tbf * (y1 - y4 - tbf / 2) * beta + nf * A_flange_stiffeners * beta * (e_flange_stiffeners + ttf)
sumation = 0
for i in range(nw - 1):
    sumation = 2 * A_WEB_stiffeners * (y1 - y4) / nw * (i + 1)
di_lag = di_lag + sumation

nl_lag = di / A_lag
l_lag = (x2 - 2 * tw - x1) * beta * ttf ** 3 / 12 + (x2 - 2 * tw - x1) * ttf * (nl_lag - ttf / 2) ** 2 + ((y1 - y4) ** 3) * tw * 2 / 12 + 2 * (y1 - y4) * tw * ((y1 - y4) / 2 - nl_lag) ** 2 + (x3 - x4 - 2 * tw) * beta * (tbf ** 3) / 12 + (x3 - x4 - 2 * tw) * tbf * ((y1 - y4 - tbf / 2 - nl_lag) ** 2)
+ nf * A_flange_stiffeners * beta + nf * A_flange_stiffeners * beta * (h_stf / 2 + ttf - nl_lag) ** 2
sumation = 0
for i in range(nw - 1):
    sumation = 2 * I_WEB_stiffeners + 2 * A_WEB_stiffeners * ((y1 - y4) / nw * (i + 1) - nlg) ** 2
l_lag = l_lag + sumation
W_lag = np.abs(min(l_lag / nl_lag, l_lag / (y1 - nl_lag)))
print('elastic shearlag section properties')
print('f_w-shearlag={W_lag:0.4} mm3 A-shearlag={A_lag:0.4} mm2 l-shearlag,{l_lag:0.4} mm4 neutral line from top {nl_lag:0.4} mm')
print('f_w-elastic={W_lag*fy:0.4}')

```